# LOAN DOCUMENT

PHOTOGRAPH THIS SHEET

DTIC ACCESSION NUMBER

LEVEL

INVENTORY

DOCUMENT IDENTIFICATION

DISTRIBUTION STATEMENT

HANDLE WITH CARE

ACCESSION FOR
NTIS GRA&I
DTIC TRAC
UNANNOUNCED
JUSTIFICATION

BY

DISTRIBUTION/

AVAILABILITY CODES

| DISTRIBUTION | AVAILABILITY AND/OR SPECIAL | |
|---|---|---|
| A-1 | | |

DISTRIBUTION STAMP

DATE ACCESSIONED

DATE RETURNED

19981223 055

DATE RECEIVED IN DTIC

REGISTERED OR CERTIFIED NUMBER

PHOTOGRAPH THIS SHEET AND RETURN TO DTIC-FDAC

DTIC FORM 70A JUN 90

DOCUMENT PROCESSING SHEET

PREVIOUS EDITIONS MAY BE USED UNTIL STOCK IS EXHAUSTED.

LOAN DOCUMENT

VOUGHT CORPORATION

CONTRACT N62269-78-C-0177

# V/STOL AIRCRAFT DESIGN SENSITIVITY TO FLYING QUALITIES CRITERIA STUDY

MID-TERM REPORT

BILLY B. BRASSELL, JR.
V/STOL TECHNOLOGIES GROUP
VOUGHT CORPORATION

28 SEPTEMBER 1979



PREPARED FOR
NAVAL AIR DEVELOPMENT CENTER
WARMINSTER, PA 18974

VOUGHT CORPORATION

Post Office Box 225907 • Dallas, Texas 75265

TRANSMITTAL OF DATA 0-81202 R5

| TRANSMITTAL NUMBER | DATE |
|---|---|
| 2-32000/9L-1058 | 3 October 1979 |
| **TO**<br>Receiving Officer<br>Naval Air Development Center<br>Warminster, PA 18974 | **REFERENCE**<br>Contract N62269-78-C-0177, V/STOL Aircraft Design Sensitivity to Flying Qualities Criteria Study |
| **ATTENTION** | **VIA** |
| **THE MATERIAL BELOW IS:**<br>☒ TRANSMITTED FOR YOUR RETENTION<br>☐ TRANSMITTED FOR YOUR USE AND RETURN<br>☐ TRANSMITTED AS REQUESTED BY ABOVE REFERENCE<br>☐ TRANSMITTED AS REQUIRED BY CONTRACT<br>☐ NOT TRANSMITTED | **COPY TO:** |

| ITEM | COPIES | IDENTIFICATION AND DESCRIPTION OF MATERIAL | REV | CLASSIFICATION |
|---|---|---|---|---|
| 1 | 1 | Mid-Term Progress Report - V/STOL Aircraft Design Sensitivity to Flying Qualities Criteria Study | | Unclassified |

**REMARKS**

Documentation in support of contractural mid term oral briefing on 2 October 1979.

| SIGNATURE | TITLE |
|---|---|
| D.B. Schoelerman | Engineering Project Manager<br>Advanced V/STOL Projects |

☐ PLEASE SIGN AND RETURN ONE COPY

SIGNATURE _____ DATE _____ TITLE _____

# 1.0 INTRODUCTION

This report covers the work accomplished during the first half of the Design Sensitivity to Flying Qualities Criteria contract. The work to date is divided into two areas.

The first was the development of the design sensitivity results. Four aircraft were sized for typical VSTOL missions. Sensitivities were established for several parameters through which flying qualities criteria/requirements affect vehicle performance/design. These sensitivities are presented here in terms of vehicle size (TOGW) variation and mission degradation.

The second area of activity was directed at the extension of a scaling procedure for dynamic analysis of hovering vehicles. This technique allows the designer to assess the effect of mass and size variations on vehicle dynamics.

## 1.1 Flying Qualities Relationship to Design

Conventional aircraft are normally sized to mission/performance requirements. To carry a designated payload a specified distance requires a certain size aircraft. Flying qualities (stability and control) requirements may result in small design variations (e.g. tail size and location) but rarely significantly affect the design process. Granted, this is a somewhat simplistic view of the design process; but it is generally a true one. Flying qualities criteria merely lead to a fine tuning of the design. Increasing acceptance of artificial stability has further reduced flying qualities considerations in the preliminary design phase. For example, tail area does not necessarily need to grow to provide static stability as this stability can be provided by the control system.

On the other hand, VSTOL aircraft design is significantly affected by flying qualities criteria. In conventional flight, control forces and moments are provided aerodynamically for VSTOL and conventional aircraft. However, in low speed flight (transition and hover) the control forces and moments must be provided by the propulsion system. In effect, additional

"performance" is required of the propulsion system to handle the added demands of flying qualities criteria. While performance requirements still size the aircraft, certain of these requirements may be significantly altered or even established by flying qualities criteria.

Understanding the interaction between flying qualities and performance parameters can be enhanced by first looking at performance in a general sense. The performance of any given mission or task is affected by four fundamental quantities: lift, drag, weight, and thrust. This is shown schematically in Figure 1. Design variations affecting these four fundamental quantities affect performance. In the preceding paragraph, thrust required was affected by flying qualities criteria and thus provided the link between flying qualities and performance. Figure 2 presents another example showing how flying qualities and performance are tied together. One can visualize a flying qualities static stability criterion requiring a change in horizontal tail size and thus altering mission performance. It is important to grasp the concept that to affect performance a requirement/criterion must cause a change in one or more of the previously mentioned quantities (lift, drag, weight, and/or thrust).

A study of flying qualities effects on design can be separated into two parts. The first part is to define those design parameters where performance and flying qualities criteria interact (as in Figure 2). The second part is to evaluate the sensitivity of the aircraft design to the parameters identified in part one. This two part approach was used in this study.

Design parameters covering the majority of flying qualities/performance interaction are presented in Table 1. Four study aircraft (two Type A and two Type B) were selected for assessing design significance of these parameters. Each aircraft will be sized for a mission typical of its type. Mission definition is required to provide a basis for developing point design aircraft and for determining performance sensitivity about the design point.

TABLE 1 DESIGN PARAMETERS COVERING FLYING QUALITIES/PERFORMANCE INTERACTION

Thrust-to-Weight Ratio

Control Modulation Available

Horizontal Tail or Canard Area

Vertical Tail Area

Dead Weight

## 1.2 Mission Definitions

Vought studies have shown that the most demanding mission for the Type A aircraft is the VTO ASW mission which is shown in Figure 3. The mission definition consists of a 150nm radius of action and a 150 minutes loiter at 10,000 feet at mid mission. This mission definition was used for aircraft sizing purposes in this study while loiter time variation was used to determine performance sensitivities.

The Type B aircraft in the study were sized to the Deck Launched Intercept (DLI) mission definition and constraints as presented in Figure 4. This mission requires an outbound Mach 1.8 dash for 150nm at 45,000 feet with a subsonic return. A subsonic fighter escort mission with a radius of action of 400nm may also be demanding for this type of aircraft, but it was not considered for this study. Variation of radius of action for the DLI mission was used for performance sensitivities.

Engine out landing capability was not considered for either the Type A or Type B missions requirements.

## 1.3 Report Organization

This report is organized in the following manner. The airplanes selected for study are introduced in Section 2. Section 3 discusses the baseline sizing activity and presents the detailed weights breakdown for each aircraft. Results of the sensitivity analyses are presented in Section 4. A method for assessing the influence of configuration geometry, size, and mass on the dynamics of VSTOL aircraft is presented in Section 5. Section 6 summarizes the contract activity to date, presents preliminary conclusions, and reviews the remaining work to be accomplished in the study.

# 2.0 AIRCRAFT SELECTION

## 2.1 Selection of Aircraft for Sensitivity Analysis

A primary goal in the selection of aircraft configurations for analysis was that the sensitivity results obtained be applicable over a wide range of possible configurations. Highly detailed analysis of one or two configurations would not assure this generality. Time and cost constraints preclude analysis of a large number. So configuration selection requires careful consideration to ensure meeting the stated goal.

To aid the development of candidate configurations consider "generic aircraft systems." Each aircraft system includes:

(a) a propulsive lift system
(b) an aerodynamic system
(c) an external flight control system
(d) an internal flight control system (AFCS, SAS, etc.)

Each of the above systems embraces a range of system configurations as exemplified by the tables below.

PROPULSIVE LIFT SYSTEM CONFIGURATIONS

| DISC LOADING | | | NUMBER OF POSTS | NUMBER OF ENGINES |
|---|---|---|---|---|
| HIGH | MEDIUM | LOW | | |
| JET LIFT | FAN LIFT/ CRUISE | NOT OF INTEREST TO STUDY | TWO | TWO |
| LIFT + LIFT/ CRUISE | | | THREE | THREE |
| LIFT/CRUISE | | | FOUR | FOUR |

## AERODYNAMIC SYSTEM CONFIGURATIONS

| ARRANGEMENT OF THRUSTERS | FRONT LIFTING SURFACE SPAN ÷ AFT LIFTING SURFACE SPAN | | |
|---|---|---|---|
| | > 1 (CONVENTIONAL) | ≈ 1 (TANDEM WING) | < 1 (CANARD) |
| NO. OF POSTS AHEAD OF FRONT L.S.* | | | |
| NO. OF POSTS WITHIN FRONT L.S. | | | |
| NO. OF POSTS AFT OF FRONT L.S. | | | |
| NO. OF POSTS AHEAD OF AFT L.S. | | | |
| NO. OF POSTS WITHIN AFT L.S. | | | |
| NO. OF POSTS AFT OF AFT L.S. | | | |

*LIFTING SURFACE

## EXTERNAL FLIGHT CONTROL SYSTEMS

| FUSELAGE | WING | CANARD AND/OR HORIZONTAL TAIL | VERTICAL TAIL |
|---|---|---|---|
| THRUSTERS | THRUSTERS | ALL MOVING | RUDDER |
| VENTRALS | AILERONS | ELEVATORS | ALL MOVING |
| | SPOILERS | FLAPS | |

The Internal Flight Control System is of lesser priority than the other three aircraft systems (recognizing, of course, that any automatic system "moves" the aircraft through the external flight control systems) in its effect on preliminary design configuration selection.

One can readily visualize the tremendous number of configurations possible when all the permutations are considered. This number needs to be reduced in some acceptable way. One way is to first eliminate configurations not of interest: VATOL, helicopters, tilt-props, and deflected slipstream. Secondly, consider only those configurations that are "meaningful;" i.e., configurations that have a demonstrated or near term viability. Futuristic and/or high technological risk aircraft should not be considered for this initial study. (This conclusion stems from a similar one reached by the VSTOL Technology Assessment Committee in Reference 1).

Four example aircraft were selected for the study; two Type A and two Type B. Two of the more typical propulsive lift configurations for each Type were selected. The full range of aerodynamic lift configurations are covered, including canard, tandem wing, and conventional horizontal tail arrangements. All aircraft have digital fly-by-wire flight control systems and high pressure hydraulic systems. This selection attempts to cover a range of representative sensitivities within a given Type and between the different Types. A general description of the aircraft selected for analysis is presented in the next section.

## 2.2 Description of V-530 Tandem Fan

The Tandem Fan nacelle features two fans on a common shaft driven directly by the core engine with no reduction gear between engine and fans. The core engine exhaust is combined with the aft fan exhaust in order to make maximum use of all available thrust in the hover mode. All propulsion components except the cross shaft are housed within this nacelle.

A common fan size is used in all four fan applications. Fixed fan blades combined with variable inlet guide vanes provide the thrust modulation and quick response needed for hover control. Fan diameters are reduced by the selection of the four fan configuration instead of three or two.

The aircraft itself is a high wing monoplane with a moderate aspect ratio wing and a high "tee" tail. The wide stance landing gear provides excellent stability against tip-over and tip-back on a pitching deck. With the wings folded, the maximum aircraft width is 21 feet, well suited for stowage in the hangar of a DD-963 class ship.

The tandem fan V-530 flight control system uses magnitude and direction changes of the four fan thrust vectors for control during hover. Aerodynamic control is obtained with flaperons, rudder and horizontal tail. Individual fan thrust magnitude is modulated by variable inlet guide vanes (VIGV). Thrust direction is changed by fore and aft nacelle nozzles. Roll control in hover is accomplished by differentially modulating left and right fan thrust. Pitch control is provided by differentially modulating thrust between fore and aft fans. Yaw moment generation is achieved by differentially deflecting thrust between the left and right nacelles. Height control is achieved by collectively controlling the thrust of all four fans. Longitudinal translation is obtained by collectively deflecting thrust from both nacelles.

A general arrangement of the V-530 Tandem Fan is shown in Figure 5. Propulsion system parameters are defined in Figure 6. The drive system is shown schematically in Figure 7 with a listing of the main propulsion components.

## 2.3 Description of Tilt Nacelle Aircraft

This V/STOL aircraft uses two propulsive nacelles mounted such that total (or effective) thrust in the V-mode acts through the aircraft C.G. Each propulsive nacelle contains a turboshaft engine driving a high-by-pass ratio fan. The nacelles tilt through an arc of 100°.

The moderately high aspect ratio wing is mounted low on the fuselage with the inboard trailing edge section cut out for the tilting nacelle.

The conventional fuselage size and shape is determined by the requirements of crew, equipment, fuel volume, and support for wing, surfaces, nacelles, and alighting gear attachments.

The wide stance main gear is mounted in pods extending aft from the wing structural box to satisfy tip-over and tip-back considerations. The nose gear mounts and retracts into the fuselage.

In aerodynamic forward flight control is from conventional surfaces; ailerons for roll, elevators for pitch, and the rudder for directional. In thrust supported flight, control in all three axis is obtained as follows:

Roll - Variable inlet guide vanes on each fan allow modulating the thrust differentially between left and right fan thrust.

Pitch and Yaw - Fore and aft reaction nozzles whose thrust is provided by continuous bleed air from the two engines.

A general arrangement of this aircraft is shown in Figure 8. Propulsion system characteristics are presented in Figure 9 and the drive system is shown schematically in Figure 10 with a listing of the main propulsion components.

## 2.4 Description of Lift + Lift Cruise Aircraft

This aircraft is powered by two lift cruise engines and two lift engines. The inlets to all four engines are located on the upper surface of the aircraft to minimize hot gas ingestion. A forward facing door opens to provide high takeoff recovery for the lift engines. Both lift engines use a hooded ventral nozzle which deflects the exhaust from 15° forward to 65° aft from vertical. The lift cruise engines use a variable geometry inlet with by-pass to provide the necessary pressure recovery in all modes of flight. A deflecting nozzle at the aft end directs the exhaust flow down and aft or forward as required.

The aerodynamic configuration of this aircraft is a "blended-body" with a moderate aspect ratio mid wing. Full span leading edge flaps and full span trailing edge flaps and ailerons are used.

The tail surfaces consist of widely spaced twin vertical tails and twin all moving horizontal tails.

The vertical stroking main gear mounts on the trailing edge beam of the wing box and retracts aft into the body strake.

In aerodynamic flight, control is from conventional surfaces; ailerons for roll, all moving horizontal tails for pitch, and rudders for directional. In thrust supported flight, control is from reaction nozzles whose thrsut is provided by bleed air from the two lift jet engines.

A general arrangement of this aircraft is shown in Figure 11, propulsion system characteristics in Figure 12 and the drive system schematic in Figure 13 with a listing of the main propulsion components.

## 2.5 Description of Remote Auxiliary Lift System (RALS) Aircraft

This twin engine aircraft uses a combination of bleed and burn for forward vertical thrust and deflected engine nozzles for aft vertical thrust in the V-mode. For cruise and high speed flight, the engine bleed ducts are shut off and all the engine thrust is diverted aft in the conventional manner. Since the bleed ducts from the engine forward to the duct burners are comparatively large as are the burners themselves, the fuselage needs to be somewhat larger than usual to provide the volume required for fuel and equipments as well as for the propulsion system.

The aircraft is a delta-canard configuration. The canard is mounted forward and high on the nacelles and the moderate aspect ratio swept wing is mounted low and aft of the canard. The canard is an all moving surface and the wing uses full span leading edge flaps and full span trailing edge flaps/ailerons. Twin vertical tails consisting of fixed fins and rudders are mounted aft and outboard on the fuselage.

The wide stance, vertical stroking main gear is mounted to the wing and retracts forward and inward into the fuselage. The nose gear mounts and retracts into the fuselage.

In thrust supported flight, modulating the continuous engine bleed at each wing tip provides the roll control. Pitch is obtained by differential thrust between the forward burn nozzles and the aft engine thrust deflector nozzles. Swiveling the forward and aft nozzles provide the yaw control. In aerodynamic forward flight, control is from conventional surfaces; ailerons for roll, all moving canard surfaces for pitch, and rudders for directional.

A general arrangement of this aircraft is shown in Figure 14, propulsion system characteristics in Figure 15 and the drive system schematic in Figure 16 with a listing of the main propulsion components.

## 2.6 Propulsion System Usage for VTO Control

The propulsion system control provided in VTO for each of the airplane concepts is summarized in Figure 17. All aircraft except the tandem fan require reaction thrust from engine bleed to achieve control in one or more axes. For aircraft sizing in this study, reaction thrust is not included in the vertical thrust contribution. Studies have shown that the most desirable control system utilizes reaction jets that do not require gas transfer for control. Thus the design is such that in the neutral position the reaction thrust is both up and down, thus not contributing to actual thrust. When control is demanded, a couple is created with forces in one direction on one side of the C.G. and in the opposite direction on the other.

As shown in Figure 17 the tilt nacelle and L+L/C aircraft achieve pitch control from reaction jets, while the tandem fan uses VIGV and RALS uses differential thrust. Roll control is accomplished by VIGV for the Type A aircraft and reaction jets for the Type B. Reaction jets are used for yaw control for Tilt Nacelle and L+L/C aircraft while differential thrust deflection is used in the Tandem Fan and RALS concepts. All designs use thrust modulation for height control and nozzle deflection angle for fore and aft translation.

# 3.0 BASELINE SIZING

Vought's Aircraft Synthesis and Analysis Program (ASAP) was used to accomplish aircraft sizing and determine performance sensitivities. ASAP is a highly integrated digital computer routine designed using a modular approach. Aerodynamics, performance, weights, and propulsion are a few of the modules incorporated in the program.

## 3.1 Tandem Fan

Tandem Fan sizing was accomplished using relevant results from earlier Vought studies. Control requirement investigations indicated a fan control modulation ($\Delta F_G/F_G$) of 27% was required to meet VTO combined control demands. Also engine studies had shown that a fan pressure ratio of 1.5 was optimum for this design. Configuration studies had shown that wing area and aspect ratio have a small influence on TOGW, but are important for carrier spotting considerations. Therefore, a control margin of 27%, a fan pressure ratio (FPR) of 1.5, a wing area of 450 $ft^2$, and an aspect ratio of 7 were fixed for the sizing study. Figure 18 shows a parametric plot of TOGW as a function of relative core size (RCS) and engine size factor (ESF) with a VTO T/W = 1.05 constraint imposed. The break in the T/W line is due to the characteristic of VTO thrust available with relative core size as shown in Figure 19. At core sizes less than about 1.33 for 27% control margin the engine core horsepower is insufficient to power the fans and thus thrust decreases.

The baseline aircraft was sized at the break in the thrust available (relative core size for maximum thrust) and weighs about 45,100 lb. Point design characteristics of the aircraft are presented in Figure 20 and a design mission breakdown in Figure 21.

## 3.2 Tilt Nacelle

A propulsion system study was conducted to determine the optimum characteristics for the tilt nacelle concept. Figure 22 shows the effect of relative core size and FPR on TOGW for a T/W = 1.05 and a roll control thrust margin ($\Delta F_G/F_G$) of 21.5%, which was determined to be required for the concept since pitch control is provided by bleed.

Lines of constant percent pitch control are noted while the absolute levels of reaction thrust available for pitch control are presented in Figure 23. A FPR and a relative core size of about 1.4 result in the lightest aircraft. As with the tandem fan, wing area and aspect ratio were judged to be of secondary importance and were fixed for the engine screening studies. The baseline aircraft weighs about 48,000 pounds and has characteristics summarized in Figure 24. A breakdown for the ASW design mission is presented in Figure 25.

The VTO thrust characteristics of the tilt nacelle concept do not exhibit the same characteristics with relative core size as the tandem fan system as shown in Figure 26. This is due to the core having sufficient horsepower to drive the fans.

### 3.3 Lift + Lift/Cruise

Sizing of the L + L/C concept to the DLI mission and associated constraints was accomplished by varying cruise engine size factor (ESF) and wing area.

Geometrical separation for the design layout resulted in a 60%/40% thrust split between lift engines and cruise engines. Lift engines were sized to yield thrust balance up to intermediate thrust on the cruise engines. A 10% continuous bleed flow from the lift engine was utilized for sizing the baseline aircraft.

The L + L/C sizing results are shown in Figure 27. The critical performance requirements are sustained 6g turn at 10,000 feet and acceleration time at 35,000 feet. Ceiling is more constraining than acceleration time, but a reduction to 58,600 feet is judged to be acceptable for the reduced TOGW. The VTO thrust to weight of the parametric aircraft in Figure 28 shows that T/W is not critical to sizing. The point design aircraft weighs about 44,100 pounds and has characteristics presented in Figure 29. DLI mission breakdown is shown in Figure 30.

## 3.4 RALS

The baseline RALS aircraft is developed with an engine bleed flow of 36 lb/sec which is ducted to the front nozzle for thrust balance and is also used for the reaction control system. For the baseline system the optimum thrust split between the forward and aft nozzles is 61%/39%.

The RALS concept sizing to the DLI mission is shown in Figure 31. The aircraft is sized by the sustained 6g turn and the VTO T/W = 1.05 requirements. Other thrust-oriented constraints are noted on the figure, but are not critical. The baseline aircraft weighs about 45,400 pounds and has characteristics summarized in Figure 32. Figure 33 presents the mission breakdown.

## 3.5 Weight/Structure Design Data & Technology Groundrules

Summary group weight statements inertia data and technology groundrules are provided for each point design.

Table 2 provides group weight summaries and inertia data for each of the four point designs. The weight estimates were derived using Vought's Semi-Analytic weight estimation procedures with 1990 technology effects. The primary technology advances employed are:

- Level II Composite Application
- Gust Allevation/CCV
- Lightweight High SHP/lb. Core Engines
- Advanced Fan Materials
- Advanced Modularized Avionics
- High Pressure Hydraulics
- Advanced High Voltage DC Electrical System
- Advanced Air Conditioning System

Four factors regarding the weight estimates are emphasized:

- Weight penalties for reliability and maintainability (R&M) have been accounted for and are listed as a line item under Systems and Equipment.

- All composite material applications involve inspectable and/or replacable assemblies (i.e., there are no buried composites --- e.g. major fuselage bulkheads).
- Transmission system weight estimates are based on current technology thereby reducing development risks.
- Avionics weights are based on recent detailed estimates derived by Vought in conjunction with avionics industry study participants.

TABLE 2 POINT DESIGN WEIGHT SUMMARIES AND INERTIA DATA

| | TYPE A TANDEM FAN ASW (VTO) | TYPE A TILT NACELLE ASW (VTO) | TYPE B RALS | TYPE B LIFT + LIFT/CRUISE |
|---|---|---|---|---|
| STRUCTURE | (10,948) | (10,596) | (10,160) | (10,468) |
| Wing | 2,515 | 2,576 | 2,066 | 2,567 |
| Tail | 659 | 1,144 | 743 | 923 |
| Body | 3,404 | 4,087 | 3,558 | 3,706 |
| Landing Gear | 1,489 | 1,563 | 1,620 | 1,691 |
| Engine Section | 2,881 | 1,226 | 2,173 | 1,581 |
| PROPULSION | (10,065) | (12,860) | (11,864) | (10,347) |
| L/C Engines | 4,304 | 5,398 | 6,234 | 4,141 |
| Lift Engines | 0 | 0 | 0 | 2,048 |
| Fans | 2,014 | 3,382 | 0 | 0 |
| Transmission-Mechanical | 1,590 | 2,137 | 0 | 0 |
| Gas Duct System | 0 | 442 | 1,243 | 277 |
| Exhaust | 997 | 204 | 2,942 | 2,377 |
| Fuel System | 860 | 997 | 1,107 | 1,145 |
| Controls & Starting | 200 | 200 | 179 | 209 |
| Accessory Gearbox | 100 | 100 | 150 | 150 |
| SYSTEMS & EQUIPMENT | ( 7,382) | ( 7,230) | ( 4,801) | ( 4,842) |
| Flight Controls & Hyd. | 1,186 | 1,033 | 941 | 983 |
| Aux. Power Unit | 200 | 200 | 100 | 100 |
| Instruments | 170 | 170 | 130 | 130 |
| Electrical | 600 | 600 | 456 | 456 |
| Avionics | 3,000 | 3,000 | 1,888 | 1,888 |
| Armament | 310 | 310 | 412 | 412 |
| Furnishings | 700 | 700 | 260 | 260 |
| Air Cond. & Anti-Ice | 650 | 650 | 347 | 347 |
| Handling | 16 | 17 | 17 | 16 |
| Reliability & Maintainability Provisions | 550 | 550 | 250 | 250 |
| WEIGHT EMPTY | [28,395] | [30,686] | [26,825] | [25,657] |

TABLE 2. POINT DESIGN WEIGHT SUMMARIES AND INERTIA DATA (CONTINUED)

| | TYPE A TANDEM FAN ASW (VTO) | TYPE A TILT NACELLE ASW (VTO) | TYPE B RALS | TYPE B LIFT + LIFT/CRUISE |
|---|---|---|---|---|
| USEFUL LOAD | | | | |
| Crew | 600 | 600 | 200 | 200 |
| Fuel - Usable | 12,024 | 12,573 | 14,786 | 14,674 |
| Fuel - Unusable | 121 | 126 | 149 | 148 |
| Oil | 60 | 60 | 120 | 120 |
| Torpedoes | 2,120 | 2,120 | 0 | 0 |
| Sonobouys | 1,125 | 1,125 | 0 | 0 |
| Sonobouy Containers | 400 | 400 | 0 | 0 |
| Missiles | 0 | 0 | 2,228 | 2,228 |
| Weapon Suspension | 100 | 100 | 570 | 570 |
| Survival Equip. & Miscellaneous | 165 | 165 | 42 | 42 |
| Cannon (M61-A1) | 0 | 0 | 250 | 250 |
| Ammunition (400 Rnds., 20mm) | 0 | 0 | 208 | 208 |
| TAKEOFF GROSS WEIGHT - LBS. | [45,110] | [47,955] | [45,378] | [44,097] |
| FLIGHT DESIGN GROSS WEIGHT | 40,302 | 42,926 | 39,462 | 38,227 |
| DCPR WEIGHT | | | | |
| ULTIMATE MANEUVER LOAD FACTOR (NZ) | 5.25 | 5.25 | 11.25 | 11.25 |
| INERTIA (SLUG FT.$^2$) | | | | |
| Emergency Landing Condition | | | | |
| IXX | 45,866 | 65,620 | 19,861 | 22,377 |
| IYY | 83,509 | 94,549 | 138,385 | 134,297 |
| IZZ | 114,620 | 130,139 | 151,339 | 149,937 |
| Normal Landing Condition | | | | |
| IXX | 47,585 | 66,813 | 20,725 | 22,902 |
| IYY | 87,520 | 98,506 | 140,760 | 136,241 |
| IZZ | 117,485 | 133,679 | 152,382 | 151,364 |

TABLE 2. POINT DESIGN WEIGHT SUMMARIES AND INERTIA DATA (CONCLUDED)

| | TYPE A TANDEM FAN ASW (VTO) | TYPE A TILT NACELLE ASW (VTO) | TYPE B RALS | TYPE B LIFT + LIFT/CRUISE |
|---|---|---|---|---|
| INERTIAS (SLUG FT.$^2$) (CONTD.) | | | | |
| Flight Design Condition | | | | |
| IXX | 59,734 | 67,526 | 21,157 | 23,685 |
| IYY | 89,662 | 100,497 | 144,646 | 138,786 |
| IZZ | 121,348 | 135,674 | 156,736 | 154,141 |
| Normal Takeoff Condition | | | | |
| IXX | 64,991 | 76,008 | 24,180 | 27,168 |
| IYY | 92,993 | 103,316 | 149,396 | 139,700 |
| IZZ | 133,101 | 145,687 | 164,076 | 159,867 |

# 4.0 PERFORMANCE SENSITIVITIES

## 4.1 Approach to Sensitivities

Sensitivities were determined for the four baseline aircraft in two forms; TOGW variations and mission parameter variations. TOGW variations require resizing the aircraft while mission parameter variations use the baseline design and performance is the fallout. For the Type A aircraft ASW mission TOS is the mission parameter while DLI radius of action is used for the Type B designs.

The parameters used in the sensitivity analysis follow:

| | EVALUATION OF PARAMETER: | |
|---|---|---|
| PARAMETER | TOGW | MISSION PERFORMANCE |
| Thrust to Weight, T/W | X | X |
| Control Modulations, Bleed or $\Delta F_G/F_G$ | X | X |
| Horizontal Tail or Canard Area | | X |
| Vertical Tail Area | | X |
| Dead Weight | | X |

Dead weight covers penalties for add-ons such as maneuver flaps, larger computer for control laws, mechanical backup, vanes for side force control, etc.

The effect of T/W and control margin or bleed flow on TOGW is determined from the baseline parametric analysis with various levels of each parameter imposed on the carpet plot and TOGW sensitivity resulting.

Performance sensitivities are determined for the baseline point design. For these studies the aircraft geometry, propulsion system, and structure are frozen. When T/W and control margin or bleed flow are varied, fuel available is charged appropriately. Fuel system weight is scaled to match available fuel and aircraft geometry is assumed to have adequate volume for additional fuel. As the TOGW is increased beyond the design weight, the aircraft is operated in an overload condition.

The effect of perturbation in tail and wing area are determined by applying a structural weight increment to the baseline aircraft with an appropriate change in fuel available. Drag of the surface is adjusted to account for size variations.

The effect of dead weight variation is also a change to fuel available and the resulting effect on mission capability.

## 4.2 Tandem Fan Sensitivities

The sensitivity of the tandem fan to VTO T/W and control margin is presented in Figure 34. Near the design point, the aircraft shows slightly more sensitivity to T/W (480 lb. per % T/W) than to control margin (400 lb. per % $\Delta F_G/F_G$). In the low control margin region the sensitivity to T/W is much larger (150 lbs per % $\Delta F_G/F_G$ vs. 340 lb per % T/W). This is due to the variation of VTO thrust characteristics for different control modulation levels as shown in Figure 35. The break in the thrust available is due to insufficient horsepower to drive the fans at smaller relative core sizes. The impact on aircraft sizing is that for a given control power margin, the aircraft minimum TOGW occurs at the thrust break point and, therefore, at varying relative core sizes. At control margin levels below 20%, the relative core size at which the break occurs increases significantly. Since TOGW increases with increasing relative core size, TOGW tends to be less sensitive to levels of control margin below 20%.

The tandem fan mission sensitivity to T/W and control margin is presented in Figure 36. The variation in ASW time on station (TOS) with T/W is about 8 min per % T/W. The sensitivity to control margin is about 6 min per % $\Delta F_G/F_G$ for control power margin above 20% and about 3 min per % $\Delta F_G/F_G$ below 20%. The break in the ASW TOS is again due to the engine thrust characteristics as shown in Figure 35.

The sensitivity of tail size to ASW TOS is shown in Figure 37. Both absolute area and percent area change are presented. The horizontal tail shows a variation of 0.07 min per $ft^2$ or 0.09 min per % change in area from the baseline. The vertical tail is slightly more sensitive with a variation of 0.13 min per $ft^2$ and 0.10 min per % change in area.

Dead weight sensitivity is about 2.5 min per 100 lbs. as presented in Figure 38.

4.3 Tilt Nacelle Sensitivities

The tilt nacelle sensitivity to T/W and control margin is presented in Figure 39 for the optimum fan pressure ratio and RCS. In general T/W and control margin show near equal sensitivity. For example a 10% change in T/W has about the same effect as a 10% in control margin. Near the design point, the sensitivity to T/W and control margin is about 700 lb per % T/W or % $\Delta F_G/F_G$.

The effect of T/W and control margin on ASW TOS is presented in Figure 40 for the point design aircraft. The sensitivity to T/W and control margin is about 8 min per % T/W and about 7 min per % $\Delta F_G/F_G$. Thus there is nearly a 1 to 1 trade between T/W and control margin. The figure does not show the same break as the tandem fan due to core limitations. The tilt nacelle has ample power from the core for all control margins examined.

The ASW TOS sensitivity to both absolute tail area and percent area are presented in Figure 41. The horizontal tail, or rear wing, shows a variation of about 0.07 min per $Ft^2$ or 0.16 min per % change in area from the baseline. The vertical tail is slightly more sensitive and shows a variation of 0.13 min per $Ft^2$ and about 0.11 min per % change in baseline area.

The sensitivity to dead weight is about 2.5 min per 100 lbs and is shown in Figure 42.

4.4 Lift + Lift/Cruise Sensitivity Analysis

The effect of percent bleed flow and VTO T/W ratio on TOGW is presented in Figure 43. The plot is developed with all points meeting the 6g sustained turn requirement, but the ceiling constraint is disregarded. Since VTO T/W is not critical to aircraft sizing, the acceleration constraint is used to determine sensitivity. Near the design point the variation of TOGW with percent bleed flow is about 150 lb per % bleed flow and

also 150 lb per % T/W. In the low T/W region the sensitivity to T/W is less, due to the high power settings and, therefore, high fuel consumption required for the 1.8 Mach dash with smaller engines.

The sensitivity of DLI mission R/A to variations of percent bleed flow and thrust to weight is presented in Figure 44. Percent bleed flow affects R/A at the rate of about 16 NM per % bleed flow. Sensitivity to T/W ratio is approximately 6 NM per % T/W. Lift engine percent bleed flow below 10% does not increase DLI R/A since the cruise engines cannot balance the additional thrust.

The variation of DLI mission R/A with tail size is presented in Figure 45. The horizontal tail shows a sensitivity of about 0.28 nm per $ft^2$ or 0.19 nm per % change in area from the baseline. The vertical tails (twin) are more sensitive and show a variation of about 0.45 nm per $ft^2$ or 0.23 nm per % change in area when both vertical tail sizes are varied.

The sensitivity of the aircraft to dead weight is presented in Figure 46 and shows a variation of about 2.6 nm per 100 lbs.

## 4.5 RALS Sensitivity Analysis

The effect of T/W and bleed flow rate on TOGW for the RALS concept is shown in Figure 47. Bleed flow from the cruise engine is ducted to the forward nozzle for thrust balance and is also used for the reaction control system. The split of thrust available with bleed flow rate for the forward nozzle and reaction control system is presented in Figure 48. Note that the aft nozzle thrust is constant with bleed flow rate. The T/W and bleed flow analysis assumes that the RALS design is able to achieve thrust balance for all bleed flow rates examined.

As noted on Figure 47 certain performance contraints are critical at low values of T/W and/or bleed flow rate. The entire carpet is developed

for aircraft capable of meeting the 6g sustained load factor requirement. Nonlinearity in the low T/W and bleed flow region is due to the high thrust levels and thus SFC required to meet the 1.8 Mach dash condition. The sensitivity of the RAL's concept near the design point is about 300 lbs per % TW and 200 lbs per lb/sec of bleed flow.

The sensitivity of DLI R/A to variation in T/W and bleed flow rate of the point design aircraft is presented in Figure 49. DLI mission R/A is effected at the rate of approximately 10 nm per % T/W and 7 nm per lb/sec of bleed flow. Thus 1 % T/W is equivalent to 0.7 lb/sec bleed flow.

Figure 50 presents the sensitivity of DLI R/A to canard and vertical tail size. The canard shows a sensitivity of about 0.35 per $ft^2$ and 0.22 per % canard area change. The vertical tail is sensitive at the rate of about 0.30 nm per $ft^2$ and 0.18 nm per % area change.

Dead weight variation, presented in Figure 51, shows the sensitivity to be about 31 nm per 100 lbs.

## 4.6 Summary of Sensitivity Results

Sensitivity results are summarized in Table 3. Thrust-to-weight and incremental thrust available for control created the largest sensitivities for all four aircraft. The other study parameters produced smaller, significant results.

Type A aircraft sensitivities to T/W and $\Delta F_G/F_G$ were much larger than Type B sensitivities. One reason for this is that Type B aircraft have other demands for high thrust (T/W → 1.0 or greater) imposed on them; e.g., the 6g sustained turn and/or acceleration requirements.

The obvious conclusion here is that flying qualities criteria most affect vehicle design through their added demands on the propulsion system. These added demands are largest in the hover regime where all control forces and moments must be generated by the propulsion system.

TABLE 3 SUMMARY OF SENSITIVITY ANALYSIS

| SENSITIVITY TO: \ A/C | TANDEM FAN | TILT NACELLE | LIFT + LIFT/CRUISE | RALS |
|---|---|---|---|---|
| VTO T/W - | | | | |
| TOGW | 480 lb/% T/W | 740 lb/% T/W | 150 lb/% T/W | 300 lb/% T/W |
| ASW TOS | 8 min/% T/W | 8 min/% T/W | | |
| DLI R/A | --- | --- | 6nm/% T/W | 10nm/% T/W |
| Control Parameter - | | | | |
| TOGW | 400 lb/$\%\Delta F_G/F_G$ | 660 lb/$\%\Delta F_G/F_G$ | 150 lb/% Bleed Flow | 200 lb/PPS Bleed Flow |
| ASW TOS | 6 min/$\%\Delta F_G/F_G$ | 7 min/$\%\Delta F_G/F_G$ | | |
| DLI R/A | --- | --- | 16nm/% Bleed Flow | 7nm/PPS Bleed Flow |
| Horizontal/Rear Wing/ Canard Size - | | | | |
| ASW TOS | 0.07 min/$Ft^2$ | 0.07 min/$Ft^2$ | --- | --- |
| DLI R/A | --- | --- | 0.28 nm/$Ft^2$ | 0.35 nm/$Ft^2$ |
| Vertical Tail Size - | | | | |
| ASW TOS | 0.13 min/$Ft^2$ | 0.13 min/$Ft^2$ | --- | --- |
| DLI R/A | --- | --- | 0.45 nm/$Ft^2$ | 0.30 nm/$Ft^2$ |
| Empty Weight Variation - | | | | |
| ASW TOS | 2.5 min/100 lb | 2.5 min/100 lb | --- | --- |
| DLI R/A | --- | --- | 2.6 nm/100lb | 3.1 nm/100 lb |

# 5.0 CORRELATION PARAMETERS FOR DESIGN SENSITIVITY TO FLYING QUALITIES REQUIREMENTS

## 5.1 Introduction

An aircraft design may be characterized in terms of its external geometry ("shape") its size, its mass, and its internal geometry, i.e., the arrangement of its mass-elements, such as engines, structural components, payload, and fuel. Aspects of each of these four descriptors relating to flying qualities can be expressed in terms of quantitative parameters, as shown below.

| DESIGN DESCRIPTOR | EXAMPLES OF ASSOCIATED PARAMETERS |
|---|---|
| Shape | Tail-Volume Ratio $\overline{V} = \frac{S_T \, l_T}{S \, \overline{C}}$, |
| Size | Dihedral Angle<br>Wing Area,<br>Span,<br>Tail Moment Arm |
| Mass | Max. TOGW |
| Internal Geometry (Mass Distribution) | $I_X$, $I_Y$, $I_Z$, $I_{XZ}$ |

The parameters listed in the right-hand column of the above table represent a class of parameters which we shall denote as "design parameters". For a given flight condition, varying the aircraft's shape, size, mass, and internal geometry (as reflected in its inertias) will cause changes in flying qualities parameters, e.g. periods, damping ratios, etc.

For conventional (non VSTOL) flight flying qualities parameters can be related to design descriptors via the aircraft's stability derivatives. The separate influences of shape, size, mass and mass distribution are most clearly expressed through the use of partly-dimensional or non-dimensional stability derivatives (see below).

To explain the above terminology for stability derivatives, consider the roll equation of motion, written in "fully-dimensional" form.

$$I_X \frac{dp}{dt} - I_{XZ} \frac{dr}{dt} = L_p \cdot p + L_r \cdot r + L_v \cdot v + L_{\delta A} \cdot \delta_A + L_{\delta R} \cdot \delta_R \qquad (1)$$

In equation (1), the derivative $L_p$ has dimensions of moment-sec/rad, i.e., $ML^2/T$. In this form $L_p$ varies considerably with aircraft shape and size, but is unaffected by mass or internal geometry. It has been found to be convenient to employ an alternative form of derivative which we shall call the "partly-dimensional" form. In this form the roll equation of motion becomes:

$$\frac{dp}{dt} - \frac{I_{xz}}{I_x} \frac{dr}{dt} = L_p \cdot p + L_r + L_v \cdot v + L_{\delta A} \cdot \delta_A + L_{\delta R} \cdot \delta R \qquad (2)$$

In equation (2) $L_p$ has dimensions of moment-sec/slug $ft^2$ - rad, i.e., $\frac{1}{T}$. It is now a function of aircraft shape, size, mass, and mass distribution. However, compared to the equation (1) form, the equation (2) form of $L_p$ varies less with aircraft size. This is because the aerodynamic moment and the inertia both increase as size is increased. The same advantage applies for $L_r$, $L_v$, $N_p$, $N_r$, etc., and is a reason for the widespread use of the "partly dimensional" form.

A further step can be taken to express the airplane equations of motion in a form which allows complete seapration of the efforts of shape, size, mass, and internal geometry. This step originally due to Glauert involves writing the equations of motion in a fully nondimensional form. Several different systems are in use, but the differences between them are not significant for the present discussion. A typical derivative in one of the nondimensional forms is

$$1_p = \frac{\partial C_l}{\partial \frac{pb}{2U_o}} = C_{l_p}$$

Where $C_l$ = rolling moment/1/2 $\rho U_o^2 Sb$. Note that $1_p$ or $C_{l_p}$ does not depend

on the size, mass, or mass distribution of the aircraft, but only on its external geometry. (Aeroelastic effects are neglected for the present discussion) with this nondimensional system of derivatives the effects of each design descriptor on flying qualities parameters is accounted for by the following quantities:

| DESIGN DESCRIPTORS | AFFECTS FLYING QUALITIES PARAMETERS THROUGH: |
|---|---|
| Shape | Nondimensional Derivatives |
| Size | Unit of aerodynamic time |
| Mass | $t = \frac{m}{\rho S U_o}$ |
| Mass<br>Mass Distribution | Nondimensional inertia coefficients<br>$i_x, i_y, i_z, i_{xz}$ |

Although partly-dimensional derivatives are widely used for purposes of simulation and calculation, recourse is made to the fully nondimensional forms to explain how factors relating to aircraft shape influence flying qualities. The utility of nondimensional derivatives for conventional aircraft stems from the fact that they are equal to the force and moment coefficients derived by dimensional analysis. These coefficients are obtained by dividing aerodynamic forces and moments by quantities involving $\rho$, S, $\frac{b}{2}$, $\bar{c}$, and $U_o$. Unfortunately these divisors are not physically meaningful for thrust-supported aircraft. Furthermore, division by $U_o$ is unacceptable for aircraft capable of hovering flight.

For helicopters nondimensionalization schemes employing tip speed have been derived. However for non-rotor type VTOL aircraft tip speed is not as functional a parameter as jet efflux density, $\rho_j$, jet efflux velocity, $V_j$, jet efflux area, $A_e$, and the airplane mass, m. These parameters determine the dynamic response of hovering vehicles. Therefore, in References 2 and 3 a new nondimensionalization method was proposed. This involved dividing each of the quantities in the equations of motion by divisors of corresponding dimensions formed from the following fundamental units.

$$\text{Unit of length, } l = \sqrt{A_e} \tag{3}$$

$$\text{Unit of mass, } m = \text{mass of airplane} \tag{4}$$

$$\text{Unit of time, } t_c = \sqrt{\frac{m}{\rho g A_e}} = \sqrt{\frac{\mu l}{g}} \tag{5}$$

$$\text{where } \mu = \frac{m}{\rho l^3} \tag{6}$$

References 2 and 3 considered the longitudinal equations of motion for small perturbations from hovering flight at zero airspeed. The standard ("Partly Dimensional") form of these equations is given in Reference 4 as:

$$\begin{bmatrix} s - X_u & 0 & g \\ -Z_u & s - Z_w & 0 \\ -M_u & 0 & s(s - M_q) \end{bmatrix} \begin{Bmatrix} u \\ w \\ \theta \end{Bmatrix} = \begin{Bmatrix} X_\delta \\ Z_\delta \\ M_\delta \end{Bmatrix} \delta \tag{7}$$

To nondimensionalize these equations, in References 2 and 3 the X- and Z-equations were divided by the unit of linear acceleration,

$$\frac{1}{t_c^2} = \frac{g}{\mu} \tag{8}$$

and the M-equation by the unit of angular acceleration,

$$\frac{1}{t_c^2} = \frac{g}{\mu l} \tag{9}$$

with the nondimensional differential operator $\lambda$ defined by

$$\lambda = \frac{d}{dt/t_c} = t_c s = \sqrt{\frac{\mu l}{g}}\, s \tag{10}$$

For the pitch derivatives an additional parameter $i_y$ was introduced. This characterizes the mass distribution.

$$i_y = \left(\frac{k_y}{l}\right)^2 \tag{11}$$

The above divisions yield the following nondimensional equations of motion for small perturbations from hover.

$$\begin{bmatrix} \lambda - x_u & 0 & \mu \\ -z_u & \lambda - z_w & 0 \\ -\frac{m_u}{i_y} & 0 & \lambda\left(\lambda - \frac{m_q}{i_y}\right) \end{bmatrix} \begin{Bmatrix} \hat{u} \\ \hat{w} \\ \theta \end{Bmatrix} = \begin{Bmatrix} x_\delta \\ z_\delta \\ \frac{m_\delta}{i_y} \end{Bmatrix} \hat{\delta} \tag{12}$$

where

$$x_u = \sqrt{\frac{\mu l}{g}}\, X_u; \quad m_u = i_y \sqrt{\frac{\mu l^3}{g}}\, M_u; \quad \hat{u} = \sqrt{\frac{\mu}{gl}}\, u; \quad x_\delta = \frac{X_\delta}{g}; \quad \hat{\delta} = \mu\delta$$

$$z_u = \sqrt{\frac{\mu l}{g}}\, Z_u; \quad m_q = i_y \sqrt{\frac{\mu l}{g}}\, M_q; \quad \hat{w} = \sqrt{\frac{\mu}{gl}}\, w; \quad z_\delta = \frac{Z_\delta}{g} \tag{13}$$

$$z_w = \sqrt{\frac{\mu l}{g}}\, Z_w; \qquad m_\delta = i_y \frac{l M_\delta}{g}$$

It was shown in Reference 3 that for hovering vehicles the nondimensional derivatives $x_u$, $m_u$, $z_w$, $m_q$, $z_u$ are primarily functions of aircraft "shape" or configuration, and only secondary functions of mass and size. Hence $x_u$, $m_u$, $z_w$, $m_q$ and $z_u$ are useful parameters for correlating shape effects, while $\mu$, $i_y$ correlate the effects of mass and mass distribution.

Although the above system of nondimensional derivatives (or coefficients) was derived for hover, it is reasonable to suppose that it will be of value at all speeds where the aircraft is primarily supported by its power plants. Accordingly, in the following sub-sections we extend the analysis of References 2 and 3 to include non-hovering flight. The goal of the work presented below is to produce a series of parameters which will serve as a basis for correlating the effects, of size, shape, mass, and mass distribution on flying qualities parameters for VSTOL aircraft.

## 5.2 Nondimensional Equations of Motion at Non-Zero Airspeed

At a general airspeed, $U_o$, the standard "partly-dimensional" longitudinal equations of motion are (from Reference 4).

$$\begin{bmatrix} s - X_u & -X_w & g \\ -Z_u & s - Z_w & U_o s - Z_q s \\ -M_u & -M_w - M_{\dot{w}} s & s^2 - M_q s \end{bmatrix} \begin{Bmatrix} u \\ w \\ \theta \end{Bmatrix} = \begin{Bmatrix} X_\delta \\ Z_\delta \\ M_\delta \end{Bmatrix} \delta$$

with the same divisors as previously, the nondimensional equations become:

$$\begin{bmatrix} \lambda - x_u & -x_w & \mu \\ -z_u & \lambda - z_w & (\hat{u}_o - z_q)\lambda \\ -\frac{m_u}{iy} & -\frac{m_w}{iy} - \frac{m_{\dot{w}}}{iy}\lambda & \lambda^2 - \frac{m_q}{iy} \end{bmatrix} \begin{Bmatrix} \hat{u} \\ \hat{w} \\ \theta \end{Bmatrix} = \begin{Bmatrix} x_\delta \\ z_\delta \\ \frac{m_\delta}{iy} \end{Bmatrix} \delta$$

with the additional symbols $z_q$, $m_{\dot{w}}$, and $\hat{u}_o$ defined as follows:

$$m_{\dot{w}} = i_y \, l \, M_{\dot{w}}, \quad z_q = Z_q \frac{\mu}{gl}, \quad \hat{u}_o = U_o \frac{\mu}{gl}$$

## 5.3 Correlation of Derivatives Using Nondimensional Forms

To illustrate one application of the above nondimensional derivatives we shall use them to compare two aircraft which are dissimilar in configuration ("shape") and in mass. There aircraft are:

(1) The AV-8B 4-poster jet lift aircraft, W = 16,538.5 lb.

(2) The modified RTA 3-poster lift-fan aircraft, W = 30,000 lb.

Table 4 below from Reference 5, summarizes the partly-dimensional longitudinal stability derivatives for the modified RTA.

TABLE 4. RTA DERIVATIVES (Trimmed for Steady Level Flight)
$\alpha = o^0$ Throughout

| CASE NO. | 1 | 2 | 3 | 4 |
|---|---|---|---|---|
| $U_o$, FPS | 0.0 | 33.747 | 67.58 | 101.373 |
| $X_u$ | -0.08424 | -0.08529 | -0.08549 | -0.08554 |
| $Z_u$ | -0.00158 | -0.0254 | -0.04208 | -0.04908 |
| $M_u$ | 0.00139 | 0.00264 | 0.00276 | 0.00245 |
| $X_w$ | 0.00188 | 0.01384 | 0.02567 | 0.03358 |
| $Z_w$ | -0.08968 | -0.16605 | -0.25131 | -0.34210 |
| $M_w$ | 0.00727 | 0.00995 | 0.01067 | 0.00996 |
| $Z_q$ | 0.57262 | -0.16613 | -0.96749 | -1.71753 |
| $M_q$ | -0.20021 | -0.39654 | -0.60537 | -0.79943 |
| $M_{\dot{w}}$ | 0.0000 | -0.00281 | -0.00280 | -0.00238 |

AV-8B derivatives are taken from Reference 6, for a similar range of airspeeds, with the aircraft trimmed for a 5-degree decelerating approach. (A level flight trimmed condition would have been preferable, but the appropriate data were not available. The change in the derivatives is not of major significance for our present purposes, so it will be assumed here that these derivatives also apply for steady level flight.) In the conventional "partly-dimensional" form the derivatives are as listed in Table 5.

TABLE 5. AV-8B DERIVATIVES

| $U_o$, FPS | 0 | 50.67 | 84.45 | 109.79 |
|---|---|---|---|---|
| $X_u$ | -0.044 | -0.044 | -0.044 | -0.044 |
| $Z_u$ | 0.0 | -0.023 | -0.054 | -0.092 |
| $M_u$ | 0.0 | -0.0009 | -0.0020 | -0.0026 |
| $X_w$ | 0.0 | 0.0 | 0.0035 | 0.010 |
| $Z_w$ | -0.018 | -0.125 | -0.195 | -0.240 |
| $M_w$ | 0.0042 | 0.0047 | 0.0040 | 0.0021 |
| $Z_q$ | -0.05 | -0.29 | -0.40 | -0.47 |
| $M_q$ | -0.036 | -0.118 | -0.160 | -0.191 |
| $M_{\dot{w}}$ | 0.0 | 0.0 | 0.0 | 0.0 |

Comparing corresponding derivatives for the RTA and the AV-8B indicates relatively large differences. For example, at hover the ratio $\left(\frac{\text{RTA Derivatives}}{\text{AV-8B Derivatives}}\right)$ is as follows:

$$\frac{X_{u_{RTA}}}{X_{u_{AV\text{-}8B}}} = 1.91, \quad \frac{Z_{w_{RTA}}}{Z_{w_{AV\text{-}8B}}} = 4.98, \quad \frac{M_{z_{RTA}}}{M_{z_{AV\text{-}8B}}} = 3.575$$

It is not apparent how much of this difference can be accounted for by the different configurations of the aircraft, and how much is due to their differing masses and sizes. A meaningful correlation of the two sets of data is therefore difficult.

The difficulty can be eliminated by employing nondimensional derivatives. The nondimensionalizing parameters employed are as follows:

| | AV-8B | RTA |
|---|---|---|
| l, FT | 3.605 | 9.948 |
| w, LB | 16,538.5 | 30,000 |
| m, SLUGS | 513.6 | 931.68 |
| $\rho$, SLUG/FT$^2$ | 0.002378 | 0.002378 |
| | 4,609.96 | 397.97 |
| $t_c = \frac{\mu l}{g}$, SEC | 22.72 | 11.09 |

The resulting nondimensional derivatives are given on Tables 6 and 7 below.

TABLE 6

RTA NONDIMENSIONAL DERIVATIVES

| CASE NO. | 1 | 2 | 3 | 4 |
|---|---|---|---|---|
| $TAS_1$ KN | 0.0 | 20.01 | 40.01 | 60.02 |
| $U_o$, FPS | 0.0 | 33.797 | 67.58 | 101.373 |
| $u_o$ | 0.0 | 37.671 | 75.326 | 112.99 |

Table Continued Overleaf

TABLE 6

RTA NONDIMENSIONAL DERIVATIVES (Continued)

| CASE NO. | 1 | 2 | 3 | 4 |
|---|---|---|---|---|
| $x_u$ | -0.934 | - 0.945 | - 0.948 | - 0.9486 |
| $z_u$ | -0.0175 | - 0.281 | - 0.4667 | - 0.5443 |
| $\frac{m_u}{i_y}$ | 0.153 | 0.2912 | 0.3044 | 0.270 |
| $x_w$ | 0.0208 | 0.1534 | 0.2846 | 0.3724 |
| $z_w$ | -0.995 | -1.84 | - 2.78 | -3.793 |
| $\frac{m_w}{i_y}$ | 0.80 | 1.0975 | 1.177 | 1.092 |
| $z_q$ | 0.6382 | -0.185 | -1.078 | -1.914 |
| $\frac{m_q}{i_y}$ | 2.22 | 4.397 | 6.713 | 8.866 |
| $\frac{m_{\dot{w}}}{i_y}$ | 0.0 | -0.0280 | -0.0278 | -0.0237 |

TABLE 7

AV-8B NONDIMENSIONAL DERIVATIVES

| $U_o$ (KN) | 0 | 30 | 50 | 65 |
|---|---|---|---|---|
| $U_o$ (FPS) | 0 | 50.67 | 84.45 | 109.79 |
| $\hat{u}_o$ | 0.0 | 319.22 | 532.03 | 691.67 |
| $x_u$ | -1.0 | - 1.0 | - 1.0 | - 1.0 |
| $z_u$ | 0.0 | -0.5226 | - 1.226 | - 2.09 |
| $\frac{M_u}{i_y}$ | 0.0 | -0.0737 | -0.1638 | - 0.21296 |
| $x_w$ | 0.0 | 0.0 | 0.0795 | 0.227 |
| $z_w$ | -0.407 | -2.84 | -4.43 | - 5.45 |
| $\frac{m_w}{i_y}$ | +0.344 | 0.385 | +0.3276 | - 0.172 |
| $z_q$ | -0.315 | -1.827 | -2.52 | - 2.961 |
| $\frac{m_q}{i_y}$ | 1.27 | 2.68 | 3.63 | 4.34 |
| $\frac{m_{\dot{w}}}{i_y}$ | 0.0 | 0.0 | 0.0 | 0.0 |

It is interesting to compare the ratios of the nondimensional derivatives calculated above.

$$\frac{X_{u_{RTA}}}{X_{u_{AV\text{-}8B}}} = 0.934\ , \qquad \frac{Z_{w_{RTA}}}{Z_{w_{AV\text{-}8B}}} = 2.432, \qquad \frac{(\frac{m_q}{i_y})RTA}{(\frac{m_q}{i_y})\ AV\text{-}8B} = 1.748$$

The compression that has been achieved can be seen by listing the "ratios of ratios," which are

$$\frac{X_{u\ RATIO}}{X_{u}\ RATIO} = 0.489 \qquad \frac{Z_{w}\ RATIO}{Z_{w}\ RATIO} = 0.488 \qquad \frac{(mq/iy)_{RATIO}}{M_{q}\ RATIO} = 0.489$$

Thus approximately 50% of the difference between the AV-8B derivatives of Table 5 and the RTA derivatives of Table 4 is due to size and mass effects rather than configuration effects.

## 5.4 Use of Nondimensional Derivatives for Extrapolation

In the analysis of flying qualities one frequently is required to extrapolate from results obtained on an aircraft of a certain size and mass to predict the dynamics of another aircraft of generally similar configuration but of different mass and magnitude. Thus for example, we might be interested in how a tilt-duct aircraft of the general configuration of the Doak VZ-4, (weight = 3,100 lb.) would fly if the design were scaled up to yield an aircraft of 31,000 lb.

Approximate answers to such questions can be obtained by the use of nondimensional equations of motion. The approximation results from the neglect of aerodynamic scale effects such as Reynolds number, and blade tip Mach number. However this is not a serious defect for purposes of preliminary analysis.

Reference 4 presents data on the Doak VZ-4, including derivatives and transfer functions. Those data have been validated against flight test results as described in Reference 7.

From page 726 of Reference 4 the transfer function relating pitch attitude to pitch control at $U_o$ = 58.8 FPS is of the form:

$$\frac{\theta}{\delta_e} = \frac{0.775\ (S + 0.0757)(S + 0.539)}{[S^2 + 2\ (0.464)(1.49)\ S + 1.49^2][S^2 + 2\ (0.378)(0.457)S + 0.457^2]}$$

For the Doak VZ-4 1 is estimated at 4.858 feet, giving a disc loading of $3{,}100/4.858^2 = 131.36$ lb/ft$^2$. At sea level standard conditions the mass parameter $\mu = 3{,}100/32.2 \times 0.002378 \times 4858^3 = 1{,}715.45$. The nondimensional speed $\hat{u}_o$ corresponding to $U_o$ = 58.8 FPS is 58.8 $\sqrt{1{,}715.45/32.2 \times 4.858}$ = 194.72.

Suppose that the scaled-up Doak has a gross weight of 31,000 lb. to keep this example simple we shall assume that it has the same $\mu$ as the original VZ-4. Thus the linear dimensions increase by $(31{,}000/3{,}100)^{1/3}$ = 2.154. Hence now $l = 4.858 \times 10^{1/3} = 10.466$ feet, and the disc loading has increased to $31{,}000/10.466^2 = 283.1$ lb/ft$^2$. The actual airspeed corresponding to $\hat{u}_o$ = 194.72 is

$$U_o = \hat{u}_o \sqrt{\frac{gl}{\mu}} = 194.72 \sqrt{\frac{32.2 \times 10.466}{1{,}715.45}} = 86.306 \text{ FPS}$$

Thus the <u>nondimensional</u> equations of motion for the Doak VZ-4 at $U_o$ = 58.8 FPS are identical to the nondimensional equations of motion for the scaled-up aircraft at $U_o$ = 86.306 FPS. It follows that the transfer functions are simply related. The damping ratios are unchanged by the scaling, but the frequencies and inverse time constraints must be ratioed by the time parameter $t_c$

$$\frac{t_c\ 31{,}000}{t_c\ 3{,}100} = \frac{\left(\frac{\mu l}{g}\right)^{1/2} 31{,}000}{\left(\frac{\mu l}{g}\right)^{1/2} 3{,}100} = (10^{1/3})^{1/2} = 1.4678$$

the lead coefficient $M_{\delta_e}$ has dimensions of $\frac{1}{T^2}$ and therefore scales by the ratio $1.4678^{-2} = 2.145^{-1}$.

Applying these scaling factors to the $\theta/\delta_e$ transfer function quoted above yields:

$$\left(\frac{\theta}{\delta_e}\right)_{\substack{W = 31{,}000 \text{ Lb.} \\ U_0 = 86.306 \text{ FPS}}} = \frac{0.3613\ (S + 0.0515)\ (S + 0.3672)}{[S^2+2(0.464)(1.015)S+1.015^2][S^2+2(0.378)(0.311)S+0.311^2]}$$

It should be noted that the assumption of constant $\mu$ was convenient in that it enabled the transfer function previously obtained to be scaled with no change in the relative pole-zero geometry, e.g. constant damping ratios. Another benefit of this assumption is that it maintains constant $C_L$ for both the original and the scaled-up aircraft, since

$$\frac{C_{L\ 3{,}100}}{C_{L\ 31{,}000}} = \frac{3{,}100}{31{,}000} \times \left(\frac{86.306 \times 2.154}{58.8}\right)^2 = 1.00$$

If $\mu$ is changed in scaling at forward speed conditions the accuracy of the scaling will decrease, because the "$1/2\rho\ U_o^2$" lift forces are not accounted for by this nondimensionalization procedure. Accordingly, at sufficiently high forward speeds, where the aircraft is mainly supported by aerodynamic lift (rather than by thrust) this particular nondimensionalization method should be replaced by one of the standard methods that have been developed for non V/STOL type aircraft (see Reference 8, for a summary of these methods).

The preceding sections have discussed only longitudinal dynamics, however there is no difficulty in applying the nondimensionalization technique to the lateral equations of motion.

# 6.0 CONCLUDING REMARKS

## 6.1 Summary of Activity to Date

This report covers the work accomplished during the first half of the Design Sensitivity to Flying Qualities Criteria contract. The work to date is divided into two areas.

The first was the development of the design sensitivity results. Four aircraft were sized for typical VSTOL missions. Sensitivities were established for several parameters through which flying qualities criteria/requirements affect vehicle performance/design. These sensitivities are presented here in terms of vehicle size (TOGW) variation and mission degradation.

The second area of activity was directed at the extension of a scaling procedure for dynamic analysis of hovering vehicles. This technique allows the designer to assess the effect of mass and size variations on vehicle dynamics.

## 6.2 Activity Remaining

The development of design sensitivities consumed the majority of time spent until now. As such, little effort has gone into the analysis of the results obtained to date. Further analysis is in order. In addition an attempt will be made to develop non-dimensional parameters which will correlate the sensitivities thereby generalizing these results.

The specific requirements of MIL-F-83300 need to be related to the parameters varied in the sensitivity studies. This will reinforce their selection as the key parameters where flying qualities and performance interact.

Additionally, time needs to be spent in evaluating the T/W and control power required for each study airplane to meet the requirements of MIL-F-83300. Based on the results of section 4, these requirements have a large impact on VSTOL design, especially Type A.

To date, no significant problems have been encountered and none are anticipated.

## REFERENCES


1. U. S. Navy VSTOL Technology Assessment: Volume I Executive Summary, prepared by the VSTOL Technology Assessment Committee (VTAC), June 1975.

2. Stapleford, R. L., J. Wolkovtich et al, An Analytical Study of V/STOL Handling Qualities in Hover and Transition, AFFDL-TR-65-73, 1965.

3. Wolkovitch, J., An Introduction to Hover Dynamics, S.A.E. Paper 660576, 1966,

4. McRuer, D. T., I. L. Ashkenas, and F. D. Graham, Aircraft Dynamics and Automatic Control, Princeton University Press, Princeton, N.J., 1973.

5. Flight Control/Flying Qualities Investigation for Lift/Cruise Fan V/STOL, Volume I Analytical Development, Contract No. N62269-78-C-0129, In Publication.

6. Lebasqz, J. W., Summary Documentation of AV-8A Model Development and X-22A Simulation of AV-8B, Calspan Corp., Buffalo, N.Y., X-22A TM No. 98, W/A P63-054, 1977.

7. Wolkovitch, J., and R. P. Walton, VTOL and Helicopter Approximate Transfer Functions and Closed-Loop Handling Qualities, S.T.I. TR 128-1, 1963.

8. Etkin, B., Dynamics of Flight, Wiley, New York, 1959.

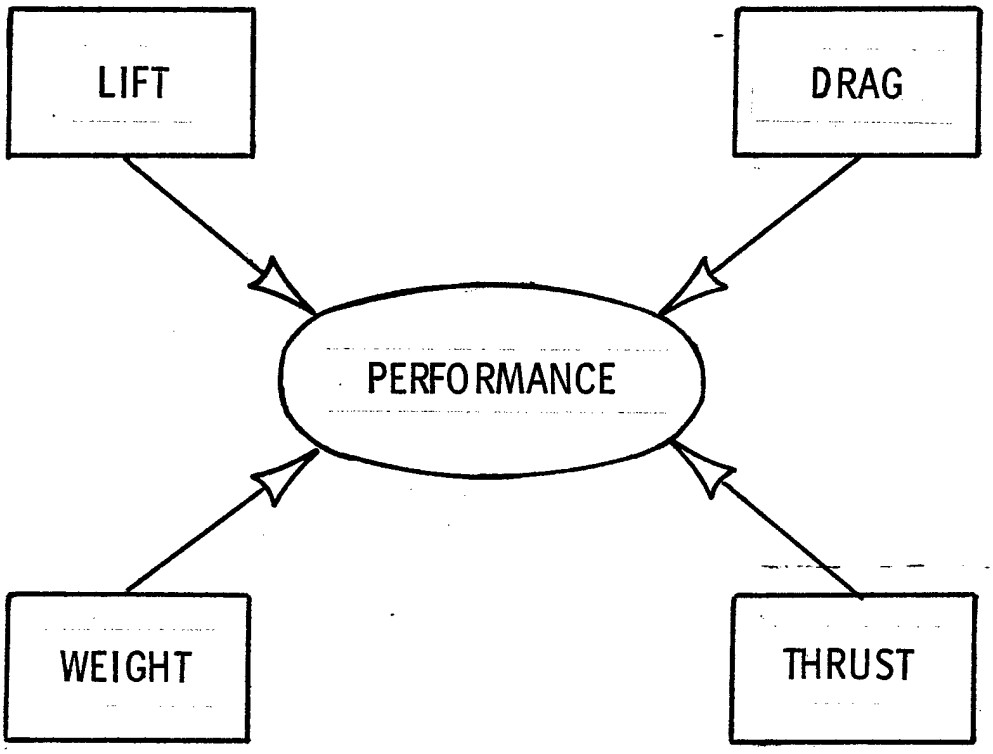


Figure 1 Four Factors Affect Performance

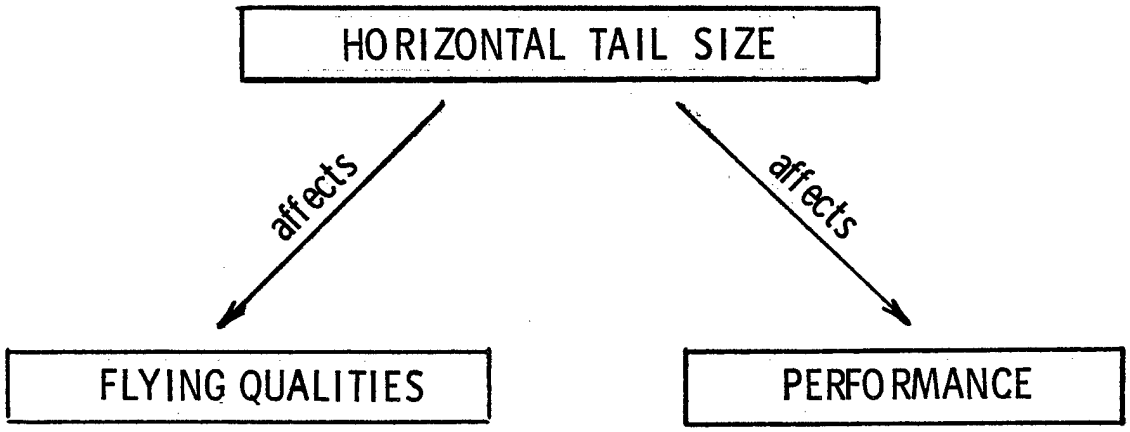


Figure 2 Horizontal Tail Size Provides An Example of Flying Qualities/Performance Interaction

ASW MISSION

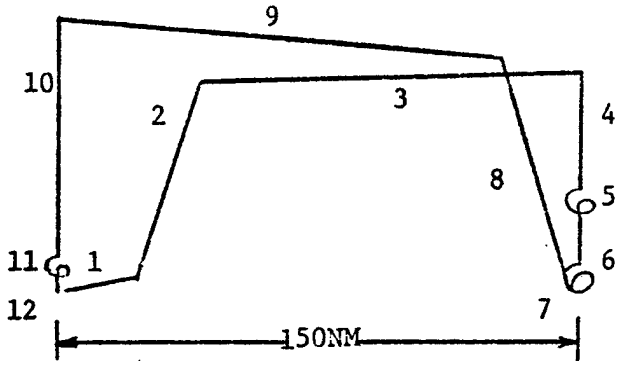


Loading: (4) MK-46 Torpedoes (2120 lbs.), 1125 lbs. mixed sonobuoys, 3000 lbs. ASW avionics.

1. Warm up, Takeoff and Acceleration to climb speed - 2.5 minutes at Intermediate Thrust at sea level.
2. Climb to Best Cruise Altitude.
3. Cruise out to 150 NM at BCAV.
4. Descend to 10,000 Ft. with no time, distance on fuel credit.
5. Loiter 150 minutes at 10,000 Ft.
6. Descend to S.L. with no time, distance or fuel credit.
7. Loiter 30 minutes at sea level.
8. Climb to best cruise altitude.
9. Cruise back to 150 NM at BCAV.
10. Descend to sea level with no time, distance or fuel credit.
11. Loiter 10 minutes at sea level.
12. Reserves: 5% of initial fuel.

Figure 3. VTO ASW Design Mission

DLI MISSION

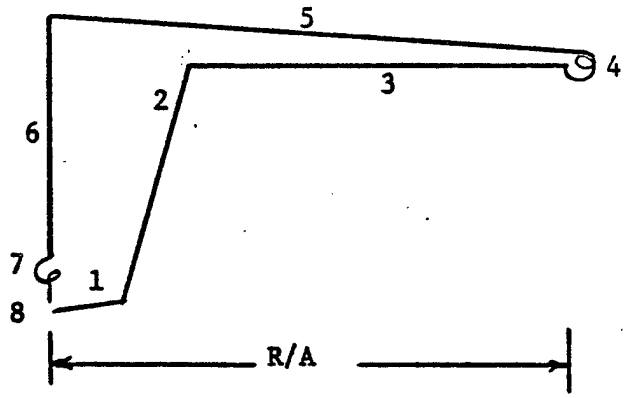


Loading: (2) HAPT plus (2) MRM, 1888 lbs. avionics

1. Takeoff Allowance - 2.0 minutes at intermediate thrust plus 0.5 minutes at takeoff thrust on all cruise engines; plus 1 minute at 80% maximum thrust plus 0.5 minute at takeoff thrust on all additional propulsive devices used for takeoff and landing.
2. Climb/Accelerate from sea level to dash altitude and Mach number at maximum thrust in minimum time.
3. Dash to total radius.
4. Combat for 2 minutes at maximum thrust.
5. Return cruise at BCAV.
6. Descend to sea level with no time, distance, or fuel credits.
7. Loiter 10 minutes at sea level with cruise engines plus 0.75 minutes at maximum thrust on all additional propulsive devices.
8. Reserves: 5% of initial fuel.

Performance Objectives/Requirements at Combat Weights :

- o Specific Excess Power
- o Sustained $N_Z$
- o Acceleration Time
- o Maximum Speed
- o A/B Combat Ceiling
- o Intermediate Thrust Combat Ceiling

Figure 4. DLI Design Mission

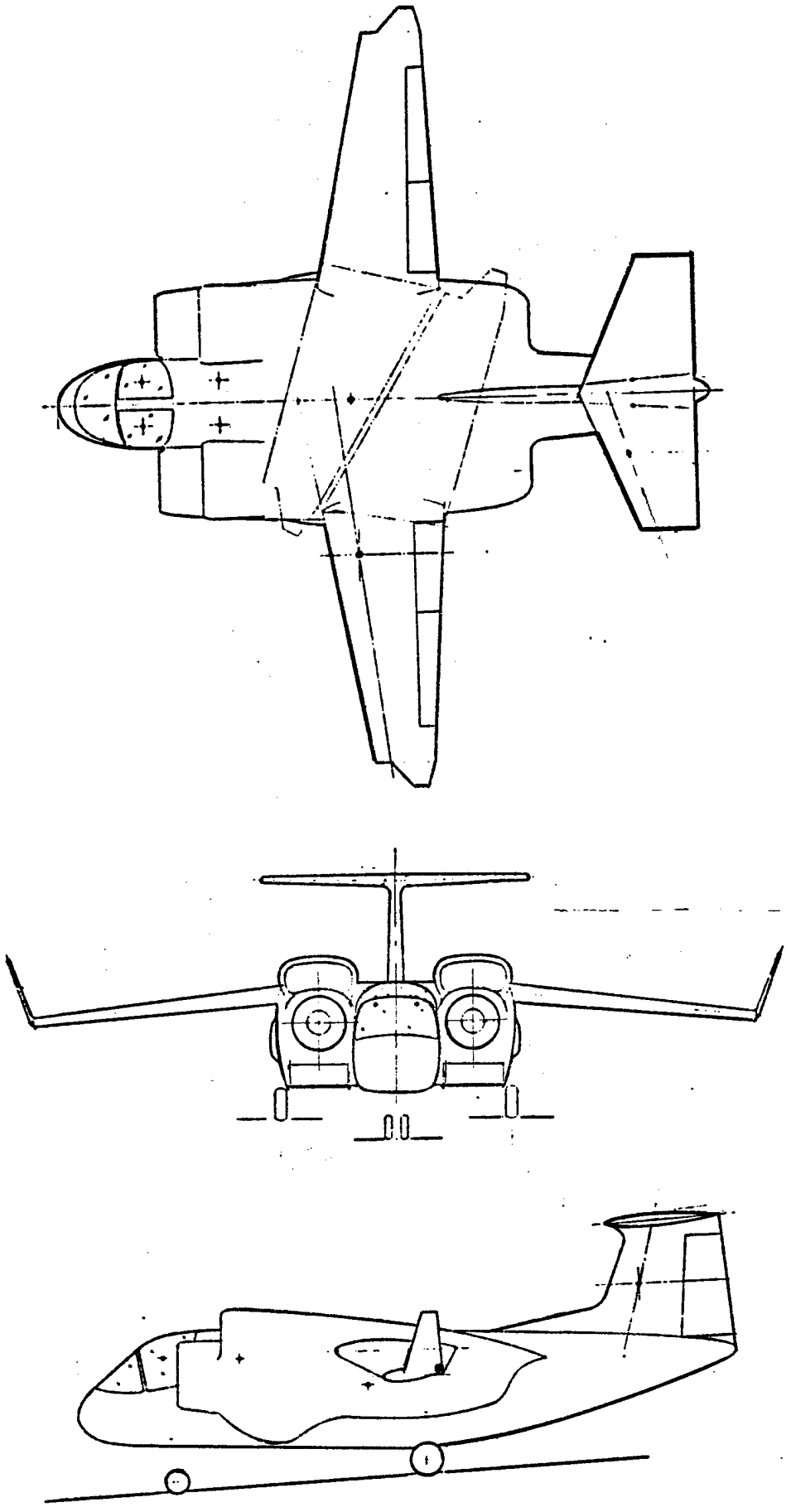

Figure 5 Tandem Fan V-530

# TANDEM FAN

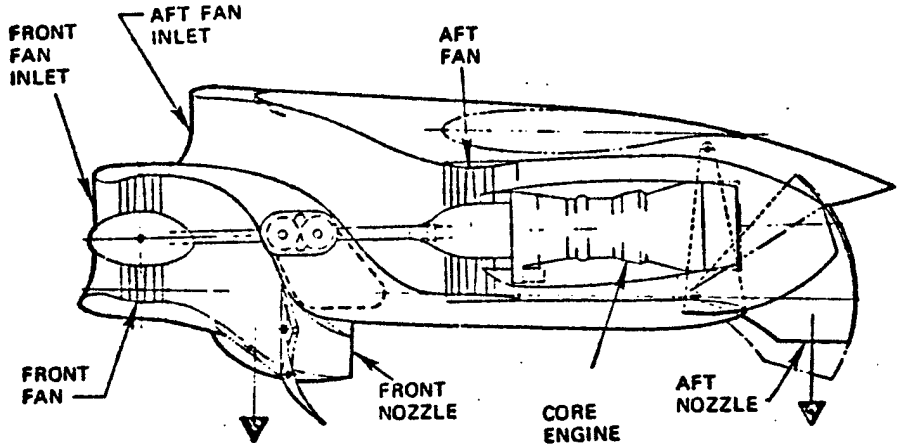


| | Front / Rear | |
|---|---|---|
| | VTO | E/O |
| FPR | 1.53 | 1.36 |
| BPR | 5.7 | 10 |
| CPR | 16 | 18 |
| BΘT, °F | 2640 | 2800 |
| Texit, °F | 170/415 | 145/475 |
| Thrust Split | 48/52 | 48/52 |
| %Control (roll or pitch) | ±27 | ±25 |

Figure 6 Tandem Fan Propulsion System Characteristics

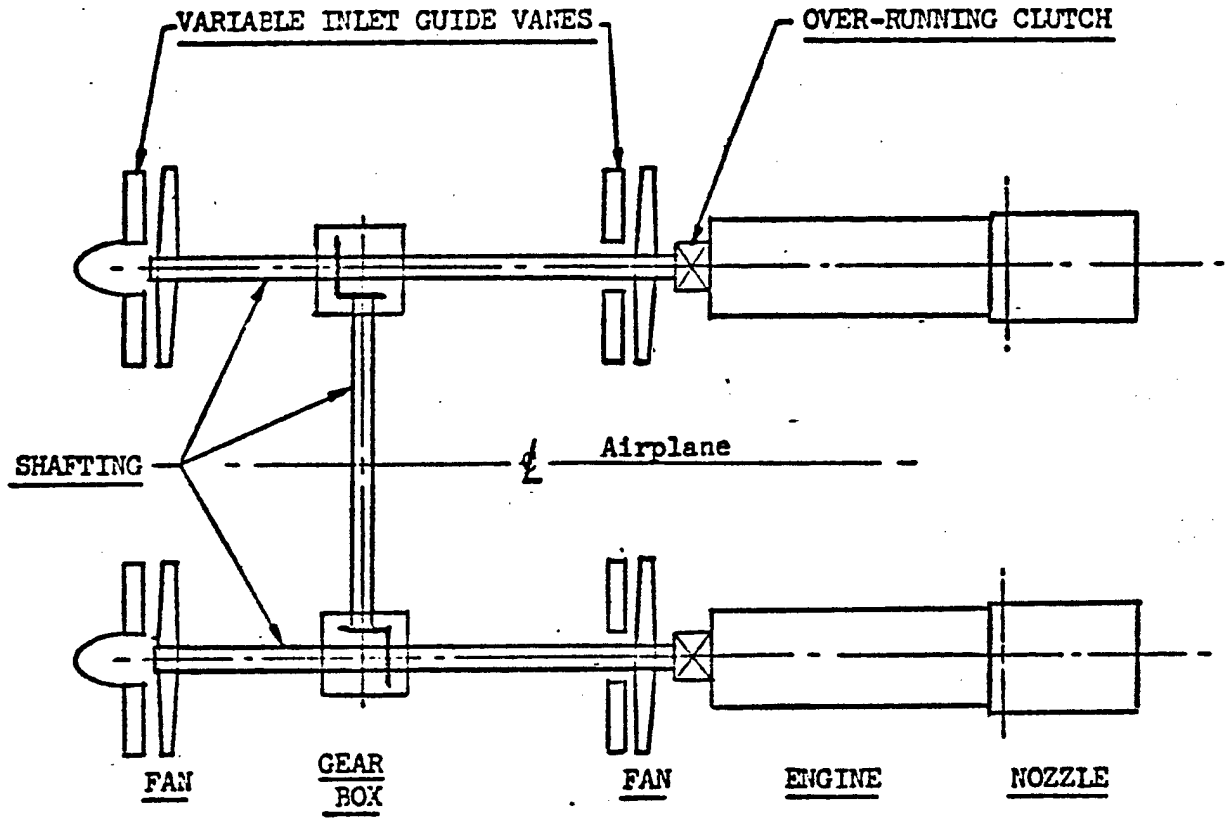


| Number | Main Propulsion Components |
|---|---|
| 2 | Turboshaft engines |
| 4 | Fans |
| 4 sets | Variable inlet guide vanes |
| 2 | Over-running clutches |
| 2 | Controllable deflector exhaust nozzle |
| 2 | Vane type front nozzles |
| 2 | Gear boxes (Fan drive and accessories) |
| 2 | Transmission oil coolers (one for each gearbox) |
| 22 ft. | Shafting plus shafting couplings, bearing supports, etc. |

Figure 7 Tandem Fan V-530 Drive System Schematic

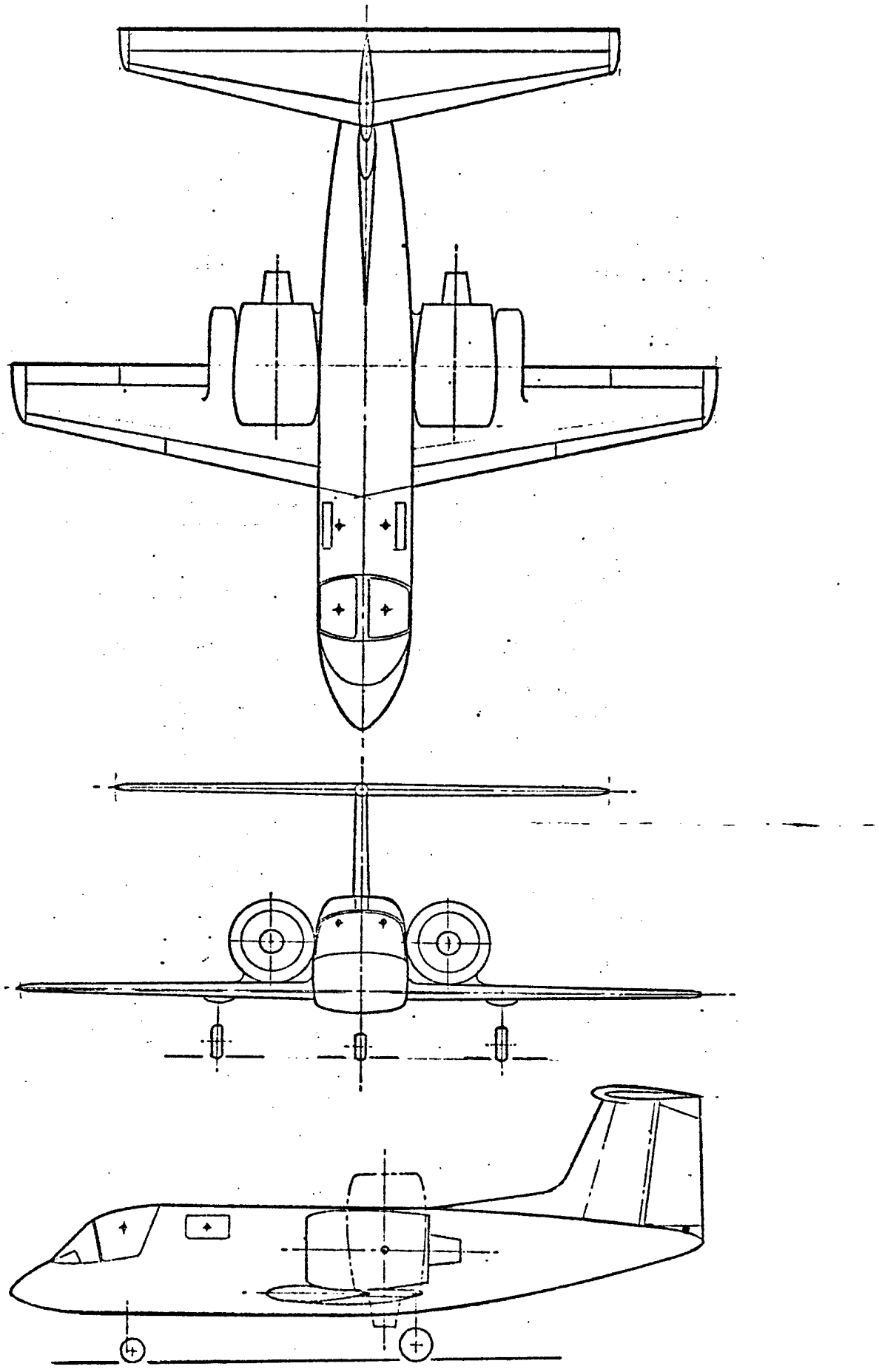

Figure 8 Tilt Nacelle

# TILT NACELLE

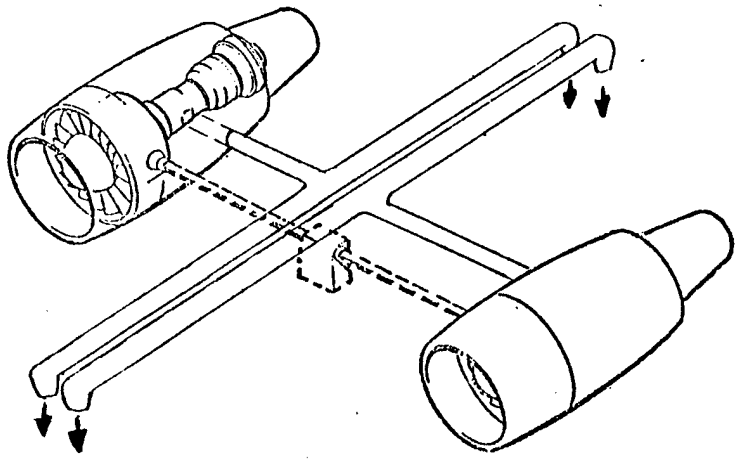

| Remote Bleed | |
|---|---|
| Wexit, pps | 9.7X2 |
| Pexit, psia | 135 |
| Texit, °F | 715 |
| %Thrust | 3.5 |

| Turbofan | Fan/Core | |
|---|---|---|
| | Cruise | VTO |
| FPR | 1.58 | 1.47 |
| BPR | 6.7 | 6.8 |
| CPR | 18 | 15.5 |
| BOT, °F | 2800 | 2800 |
| Texit, °F | 180/1150 | 165/1155 |
| %Bleed | 0 | 9.5 |
| %Thrust | 100 | 96.5 |
| %Roll | 0 | ±21 |

Figure 9 Tilt Nacelle Propulsion System Characteristics

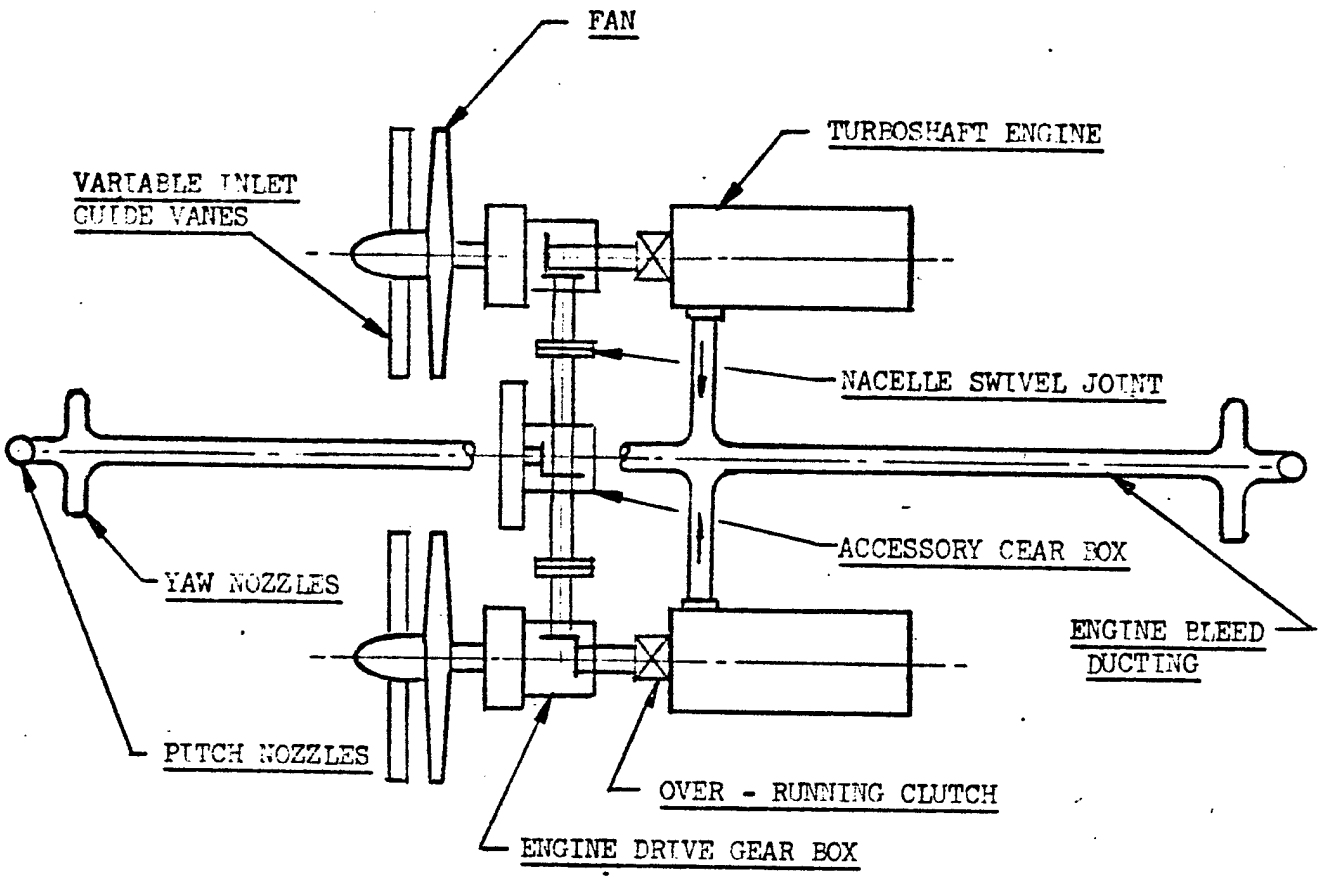


| NUMBER | MAIN PROPULSION COMPONENTS |
|---|---|
| 2 | Turboshaft engines |
| 2 | Fans |
| 2 sets | Variable inlet guide vanes |
| 2 | Engine/reduction gear box |
| 1 | Accessory drive gear box |
| 2 | Engine over-running clutch |
| 2 | Nacelle tilt swivels |
| 2 | Transmission oil coolers (one per gear box) |
| 4 | Pitch nozzles |
| 4 | Yaw nozzles |
| 8 ft. | Shafting (plus couplings, bearings, etc.) |
| 50 ft. | Compressor bleed hot gas ducting |
| | plus: shutoff valves, check valves, expansion joints, fittings, supports, insulation, clamps, etc. |

Figure 10 Tilt Nacelle Drive System Schematic

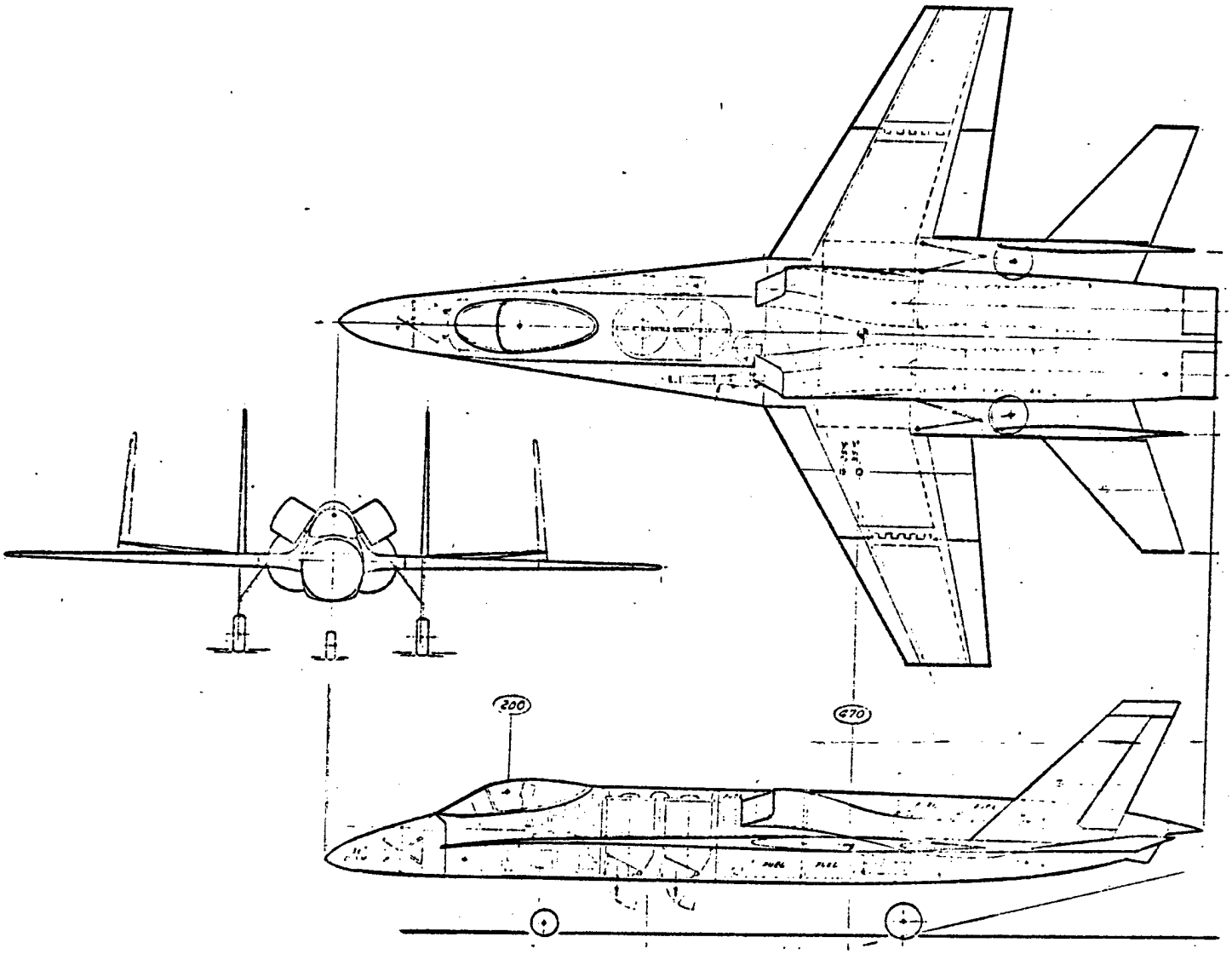


Figure 11 Lift + Lift/Cruise

## LIFT PLUS LIFT/CRUISE

### LIFT ENGINE

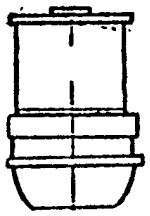

10% CONTINUOUS BLEED

12.5% INTERMITTANT BLEED

T/W - 20:1

EXHAUST TEMP ~2000°F

### LIFT/CRUISE ENGINE

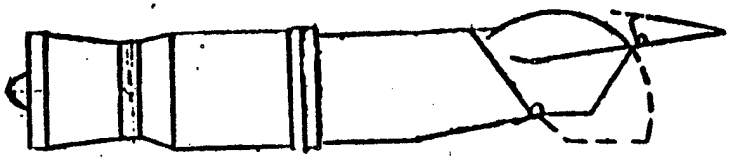

$FPR_{DES}$ - 3.2

$BPR_{DES}$ - 1.0

$CPR_{DES}$ - 7.8

$BOT_{DES}$ - 2800°F

EXHAUST TEMP - 1000°F

Figure 12 Lift + Lift / Cruise Propulsion System Characteristics

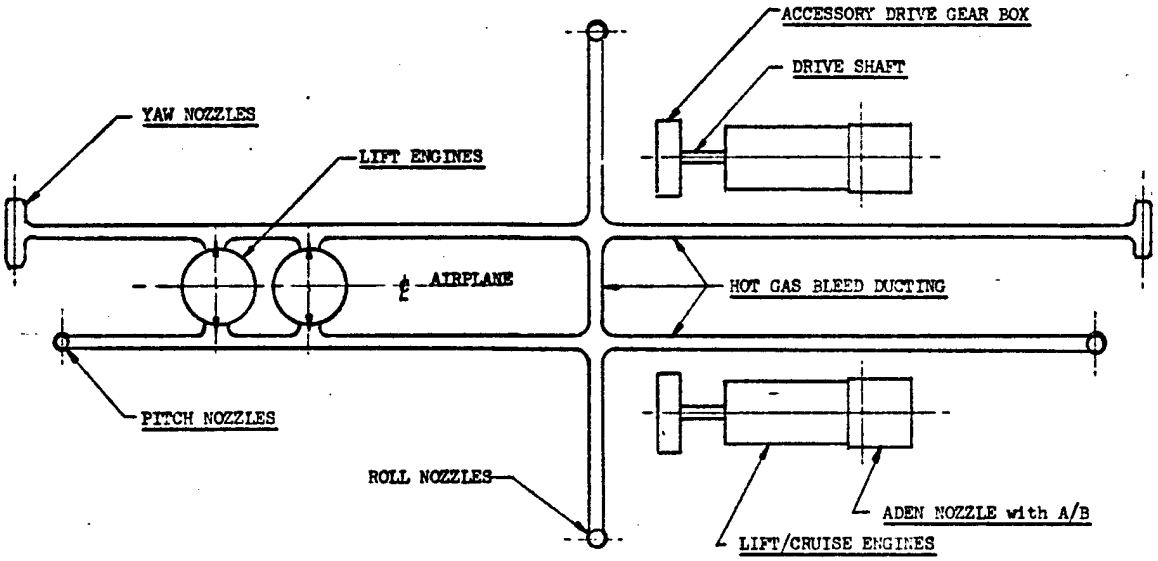


| NUMBER | MAIN PROPULSION COMPONENTS |
|---|---|
| 2 | Lift/cruise engines |
| 2 | Lift engines |
| 2 | Aden exhaust deflector nozzles with A/B |
| 2 | "Visor" type exhaust deflector nozzles |
| 1 | Top inlet door |
| 2 | Variable geometry inlets |
| 2 | Accessory drive gear boxes |
| 2 | Accessory gear box drive shafts |
| 2 | Gear box oil coolers (one per gear box) |
| 4 | Pitch nozzles |
| 4 | Roll nozzles |
| 4 | Yaw nozzles |
| 75 ft. | Compressor bleed hot gas ducting |
| | plus: shut-off valves, check valves, expansion joints, fittings, supports, insulation, clamps, etc. |

Figure 13 Lift + Lift/Cruise Drive System Schematic

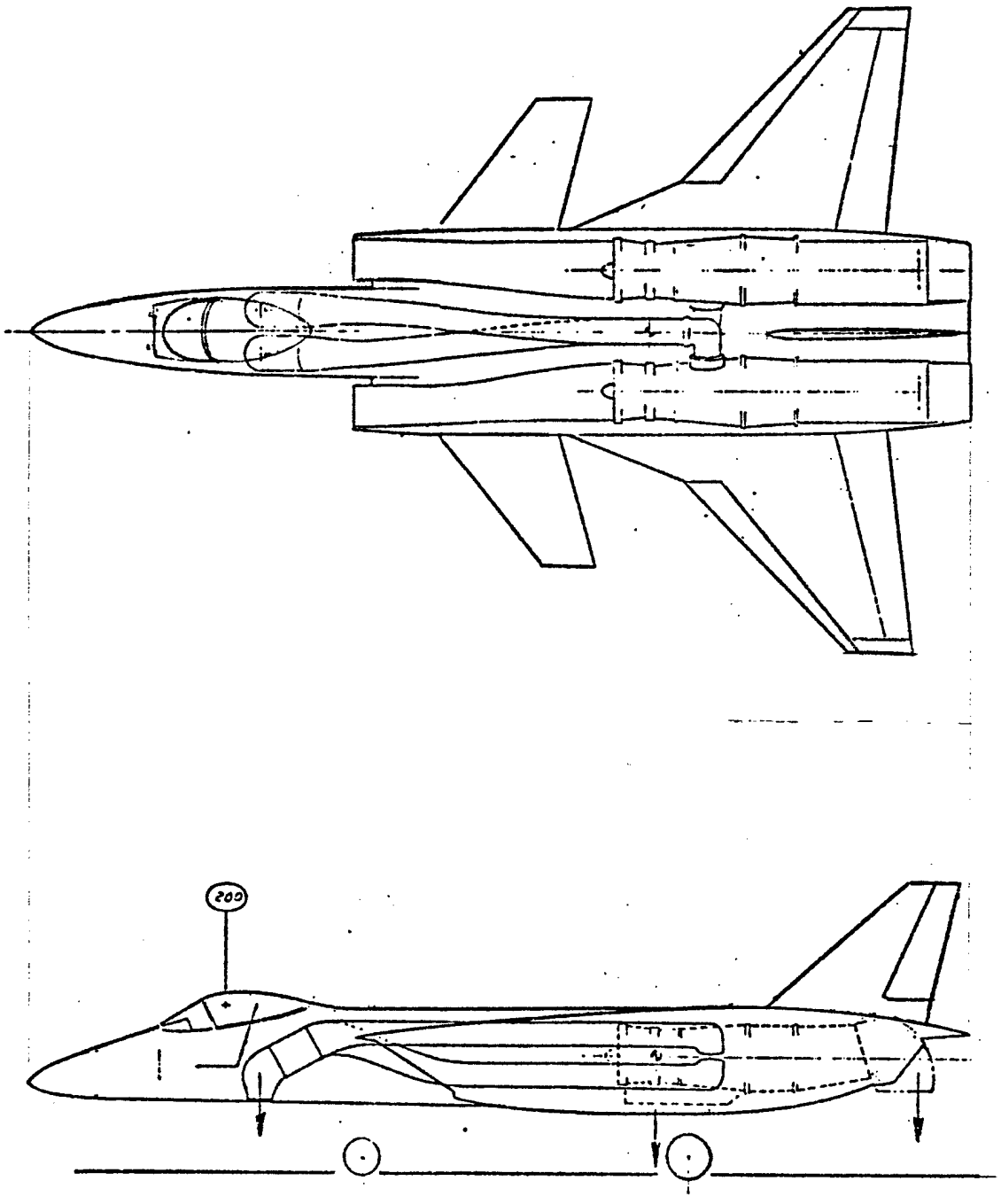


Figure 14 RALS

RALS

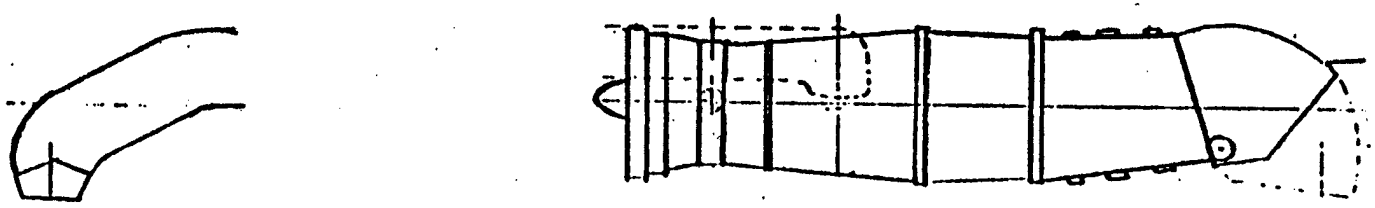

SYS-GE16/VF19-C1(M)

$FPR_{DES}$ - 3.4

$BPR_{DES}$ - 1.25

$CPR_{DES}$ - 5.9

| | | ADEN | RALS | RCS |
|---|---|---|---|---|
| THRUST SPLIT | % | 55.0 | 35.0 | 10.0 |
| FLOW | #/SEC. | 99.5 | 61.1 | 36.0 |
| EXHAUST TEMP | °F | 2800 | 2800 | 370 |

Figure 15 R A L S Propulsion System Characteristics

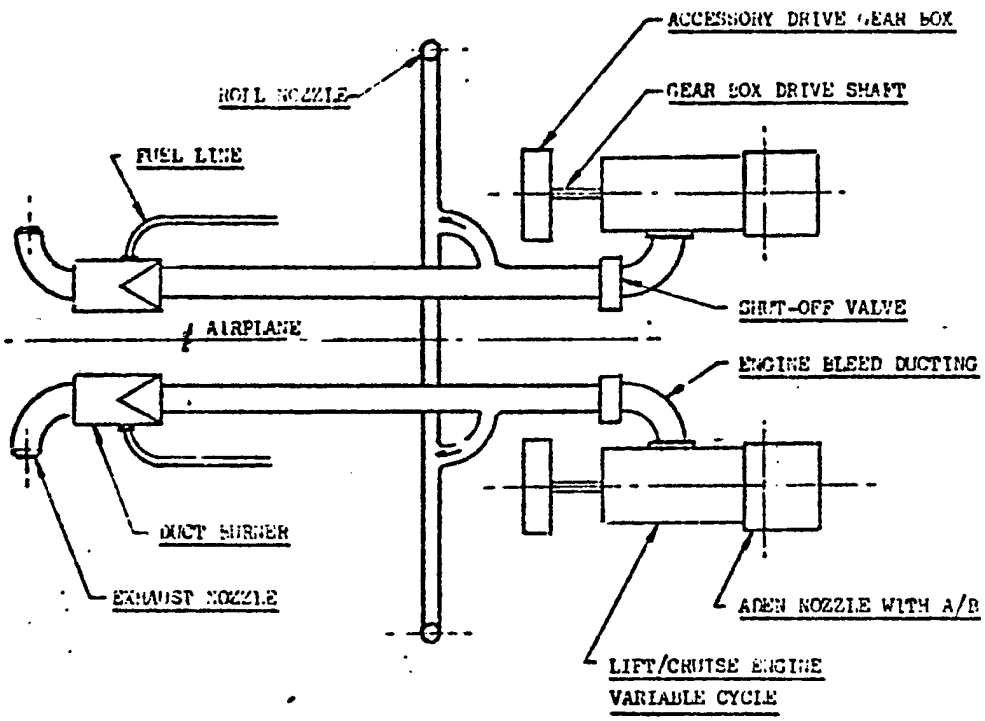


| NUMBER | MAIN PROPULSION COMPONENTS |
|---|---|
| 2 | Lift/cruise engines - Variable cycle |
| 2 | Duct burners |
| 2 | Front exhaust nozzles |
| 2 | Aden deflector nozzles with A/B |
| 2 | Variable geometry inlets |
| 2 | Accessory drive gear boxes |
| 2 | Gear box drive shafts |
| 2 | Gear box oil coolers (one per gear box) |
| 2 | Front exhaust closure doors |
| 2 | Roll nozzles |
| 50 ft. | Roll control engine bleed ducting (3" dia. approx.) |
| 48 ft. | Forward nozzles engine bleed ducting (18" dia. approx.) |
| | plus: shutoff valves, expansion joints, insulation, check valves, supports, clamps, etc. |

Figure 16 RALS Drive System Schematic

| A/P / CONTROL FUNCTION | TANDEM FAN | TILT NACELLE | LIFT + LIFT/CRUISE (LIFT ENGINE BLEED) | RALS |
|---|---|---|---|---|
| PITCH | IGV | REACTION JETS* | REACTION JETS* | DIFFERENTIAL THRUST |
| ROLL | IGV | IGV | REACTION JETS* | REACTION JETS* |
| YAW | DIFFERENTIAL NOZZLE DEFLECTION ANGLE | REACTION JETS | REACTION JETS | SWIVELING FORE AND AFT NOZZLES |
| HEIGHT | IGV + THRUST MODULATION | IGV + THRUST MODULATION | THRUST MODULATION | THRUST MODULATION |
| FORE & AFT TRANSLATION | NOZZLE DEFLECTION ANGLE | NOZZLE DEFLECTION ANGLE | NOZZLE DEFLECTION ANGLE | NOZZLE DEFLECTION ANGLE |

* REACTION THRUST BOTH UP AND DOWN IN NEUTRAL POSITION

Figure 17. Summary Control System Description

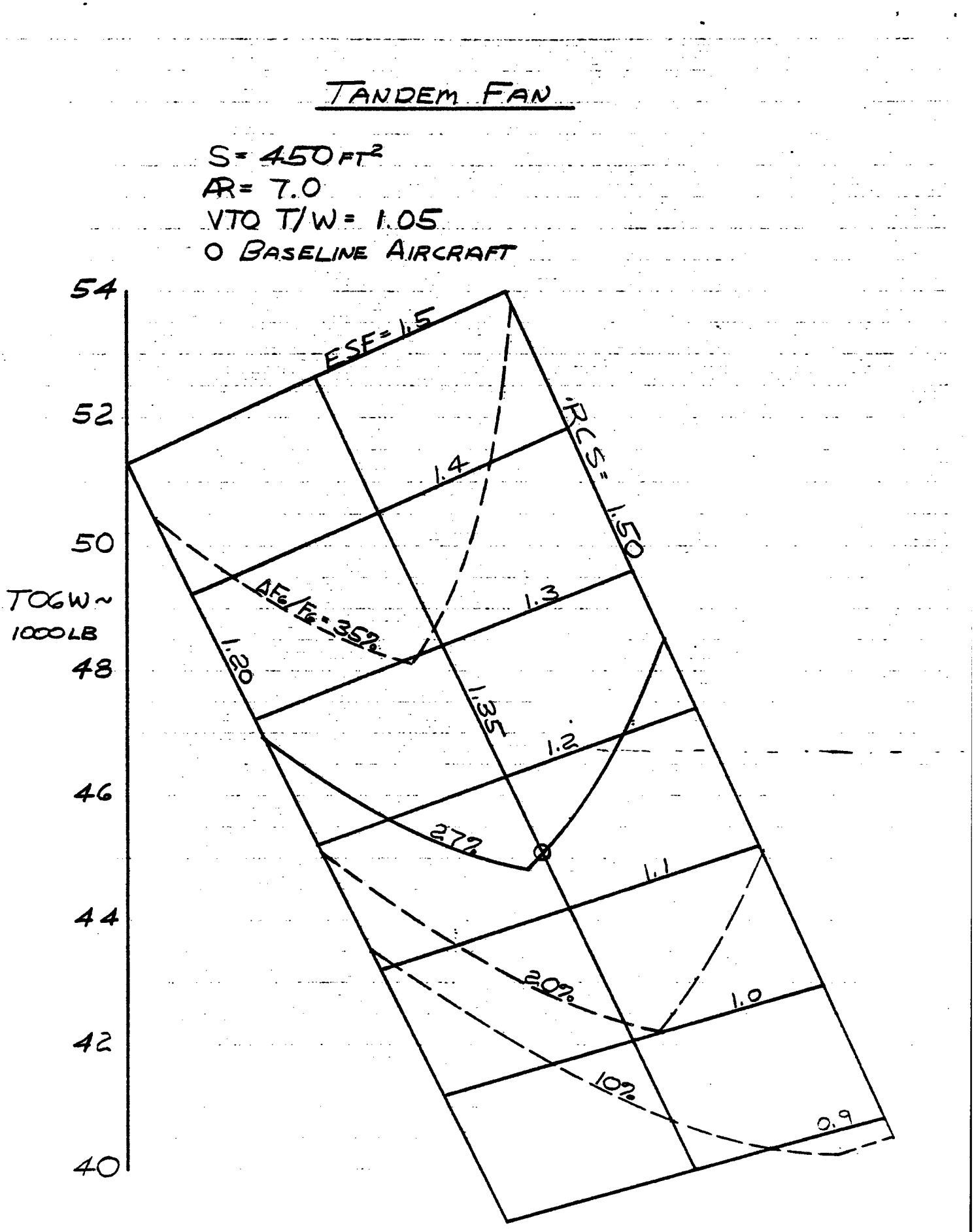


Figure 18. Tandem Fan Sizing Parametric

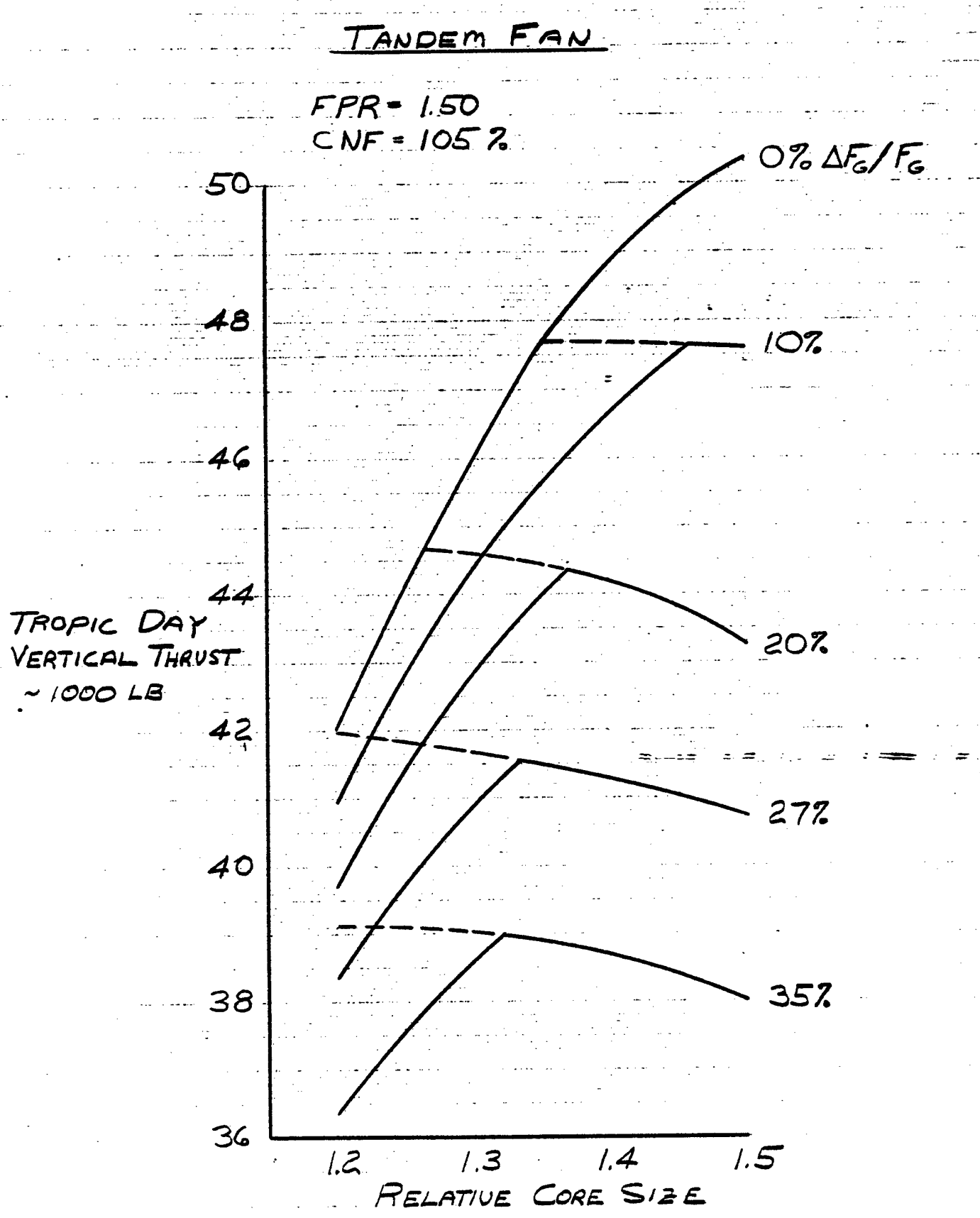


Figure 19. Tandem Fan VTO Thrust Characteristics

| | |
|---|---|
| TOGW - LB. | 45,111 |
| Wing Area - $Ft^2$ | 450 |
| Wing Loading - $Lb/Ft^2$ | 100 |
| Aspect Ratio | 7.0 |
| Engine Scale Factor | 1.14 |
| Relative Core Size/FPR | 1.35/1.5 |
| Fan Diameter - In | 52.1 |
| Number of Engines | 2 |
| Fuel Weight - Lb. | 12,024 |
| Structural Weight - Lb. | 10,948 |
| Systems and Equipment - Lb. | 7,382 |
| Propulsion System Weight - Lb. | 10,065 |
| Weight Empty - Lb. | 28,395 |
| Takeoff T/W | 1.05 |
| Design Control Margin - % $\Delta F_G/F_G$ | 27% |

Figure 20. Tandem Fan Point Design Characteristics

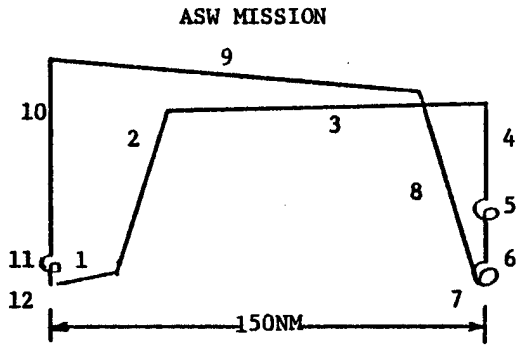


| MISSION SEGMENT | END WEIGHT (LBS.) | END ALTITUDE (FT.) | RANGE (N.Mi.) | TIME (MINUTES) | END SPEED (KNOTS) | END SPEED MACH | FUEL (POUNDS) |
|---|---|---|---|---|---|---|---|
| 1. Warmup, Takeoff and Accel. to Climb Speed | 46,939 | 0 | 0 | 2.5 | 495 | .748 | 1016 |
| 2. Climb | 46,342 | 37,776 | 19.7 | 2.8 | 415 | .724 | 593 |
| 3. Cruise Out | 45,428 | 38,346 | 130.3 | 19.1 | 410 | .715 | 918 |
| 4. Descent | 45,428 | 10,000 | 0 | 0 | - | - | 0 |
| 5. Loiter | 39,027 | 10,000 | 0 | 150.0 | 177 | .276 | 6401 |
| 6. Descent | 39,027 | SL | 0 | 0 | - | - | 0 |
| 7. Loiter | 37,715 | SL | 0 | 30.0 | 149 | .225 | 1312 |
| 8. Climb | 37,178 | 42,227 | 20.1 | 3.0 | 415 | .723 | 537 |
| 9. Cruise Back | 36,432 | 42,674 | 129.9 | 19.0 | 409 | .713 | 746 |
| 10. Descent | 36,432 | SL | 0 | 0 | - | - | 0 |
| 11. Reserve Loiter | 36,011 | SL | 0 | 10.0 | 146 | .22 | 421 |
| 12. 5% Initial Fuel | 35,382 | - | - | - | - | - | 629 |

TOTALS:

TOGW = 47,955 Lb.;Time on Station = 150 Min.

Fuel = 12,573 Lb.;Mission Radius = 150 Min.

LOADING: (4) MK-46 Torpedoes (2120 Lb.), 1125 Lb. Mixed Sonobuoys, 3000 Lbs. ASW Avionics

Figure 21. Tandem Fan Design Mission Breakdown

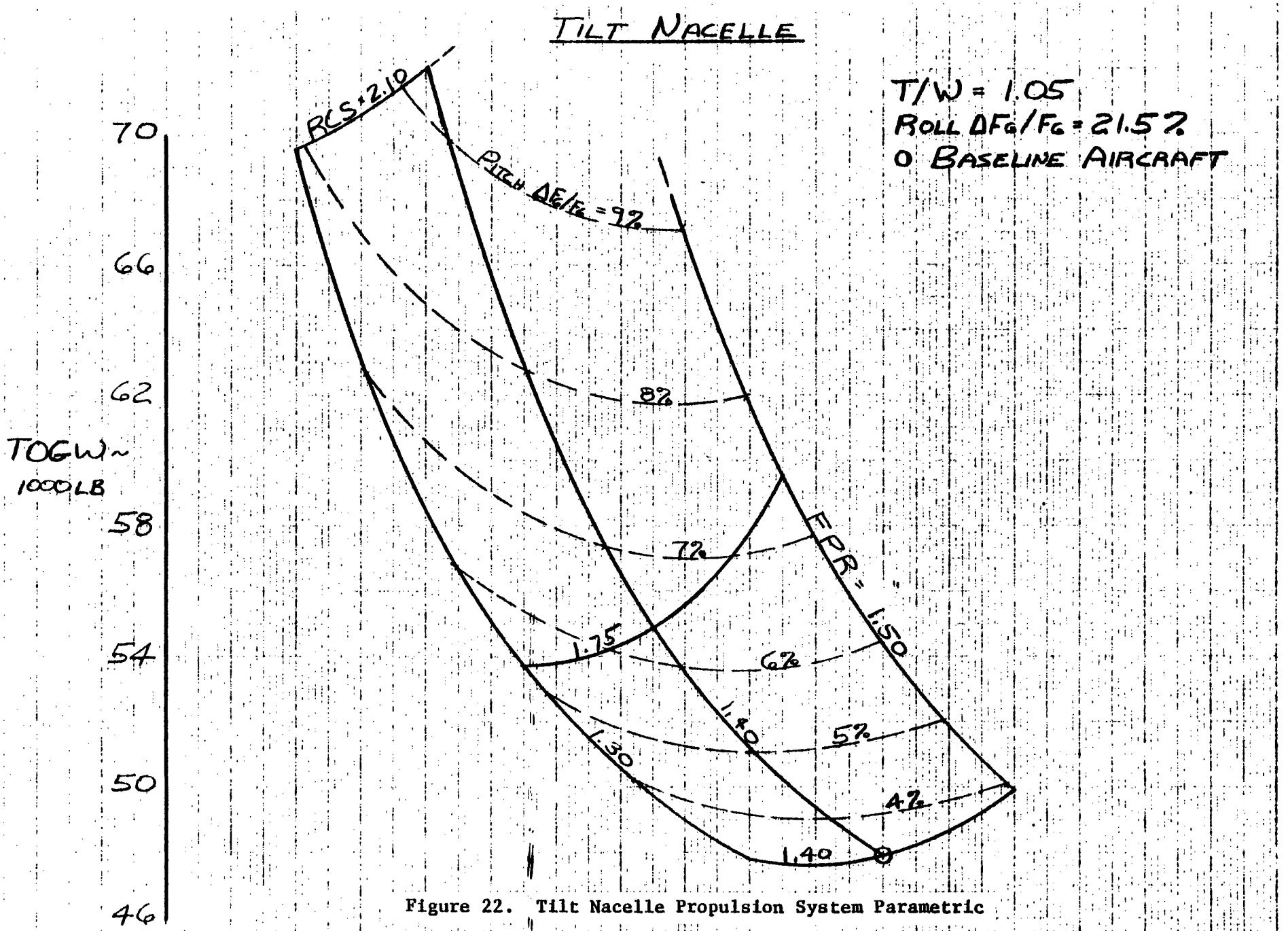


Figure 22. Tilt Nacelle Propulsion System Parametric

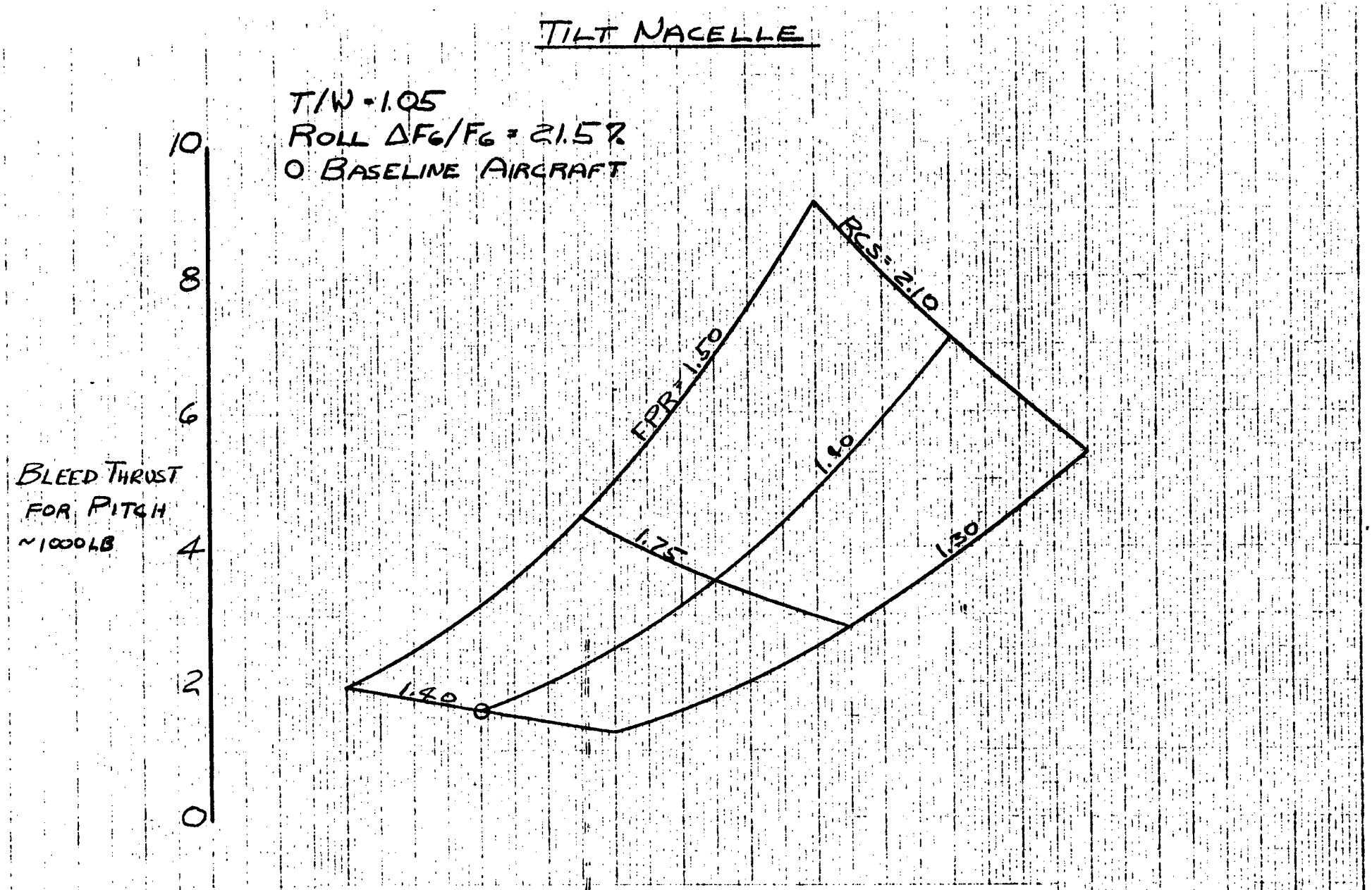


Figure 23. Tilt Nacelle Thrust Available for Pitch Control

| | |
|---|---|
| TOGW - LB. | 47,955 |
| Forward/Rear Wing Areas - $Ft^2$ | 358/219 |
| Wing Loading - $Lb/Ft^2$ | 83 |
| Aspect Ratio | 7.0 |
| Engine Scale Factor | 1.275 |
| Relative Core Size/FPR | 1.4/1.4 |
| Fan Diameter - In. | 76.0 |
| Number of Engines | 2 |
| Fuel Weight - Lb. | 12,573 |
| Structural Weight - Lb. | 10,596 |
| Systems and Equipment - Lb. | 7,230 |
| Propulsion System Weight - Lb. | 12,860 |
| Weight Empty - Lb. | 30,686 |
| Takeoff T/W | 1.05 |
| Design Control Margin, % $\Delta F_G/F_G$ | 21.5% |

Figure 24. Tilt Nacelle Point Design Characteristics

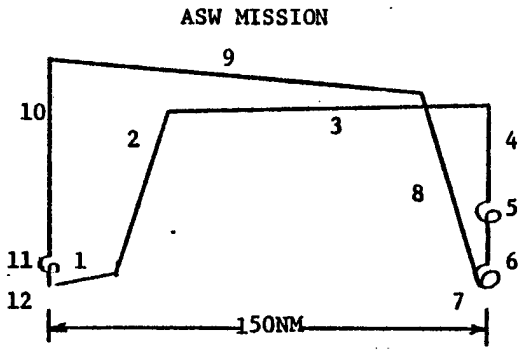


| MISSION SEGMENT | END WEIGHT (LBS.) | END ALTITUDE (FT.) | RANGE (N.Mi.) | TIME (MINUTES) | END SPEED (KNOTS) | END SPEED MACH | FUEL (POUNDS) |
|---|---|---|---|---|---|---|---|
| 1. Warmup, Takeoff and Accel. to Climb Speed | 44,430 | 0 | 0 | 2.5 | 401 | .606 | 681 |
| 2. Climb | 43,752 | 41,162 | 24.7 | 3.5 | 416 | .726 | 678 |
| 3. Cruise Out | 42,984 | 41,616 | 125.3 | 18.5 | 407 | .709 | 768 |
| 4. Descent | 42,984 | 10,000 | 0 | 0 | - | - | 0 |
| 5. Loiter | 36,727 | 10,000 | 0 | 150.0 | 162 | .253 | 6257 |
| 6. Descent | 36,727 | SL | 0 | 0 | - | - | 0 |
| 7. Loiter | 35,355 | SL | 0 | 30.0 | 141 | .214 | 1371 |
| 8. Climb | 34,753 | 46,034 | 25.4 | 3.7 | 416 | .726 | 603 |
| 9. Cruise Back | 34,131 | 46,500 | 124.6 | 18.4 | 407 | .709 | 621 |
| 10. Descent | 34,131 | SL | 0 | 0 | - | - | 0 |
| 11. Reserve Loiter | 33,688 | SL | 0 | 10.0 | 137 | .207 | 444 |
| 12. 5% Initial Fuel | 33,086 | - | - | - | - | - | 601 |

TOTALS:
TOGW = 45,111 Lb.;Time on Station = 150 Min.
Fuel = 12,024 Lb.;Mission Radius = 150 N.Mi.

LOADING: (4) MK-46 Torpedoes (2120 Lb.), 1125 Lb. Mixed Sonobuoys, 3000 Lb. ASW Avionics

Figure 25. TiltNacelle Design Mission Breakdown

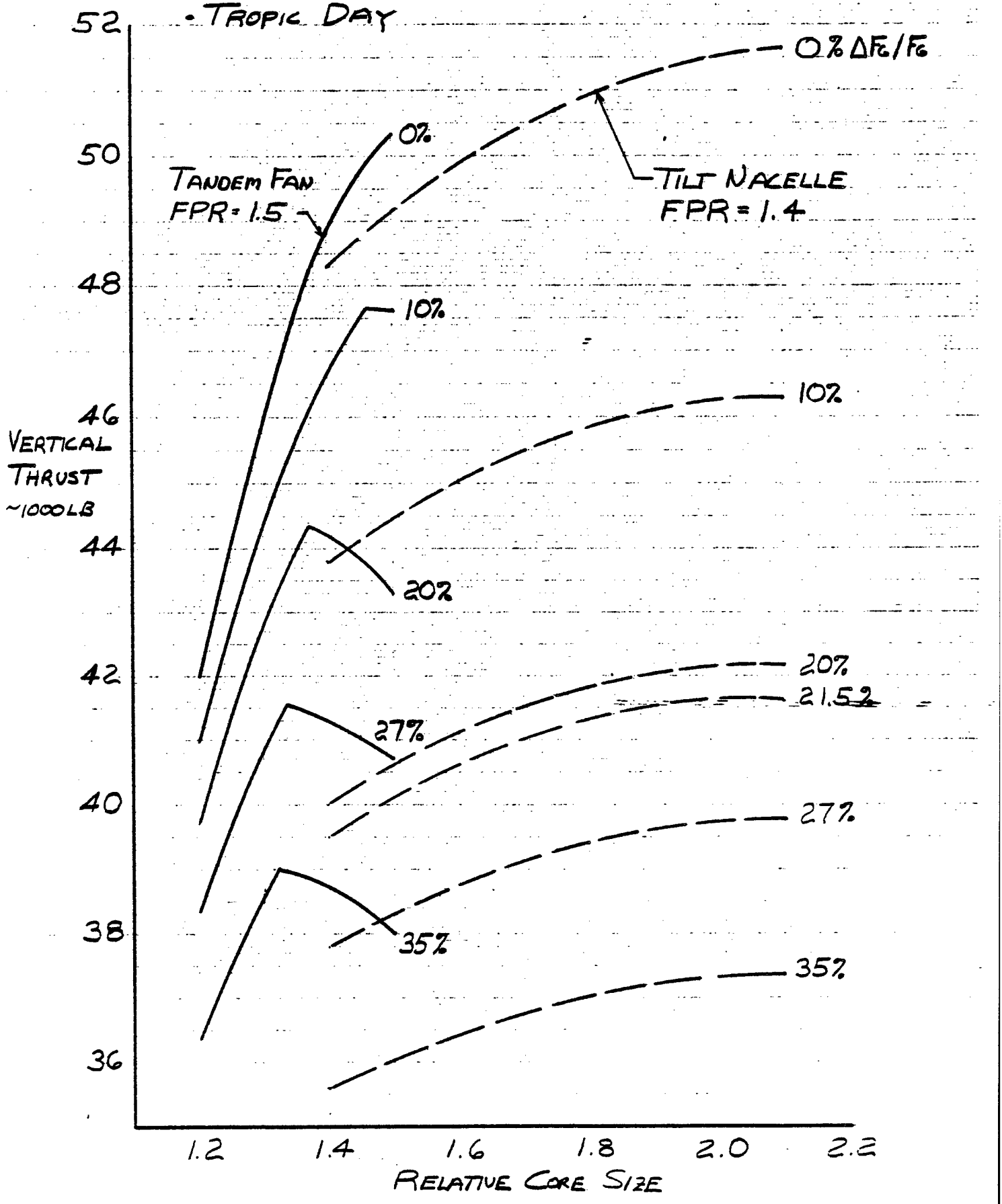


Figure 26. Comparison of Tandem Fan and Tilt Nacelle VTO Thrust Characteristics

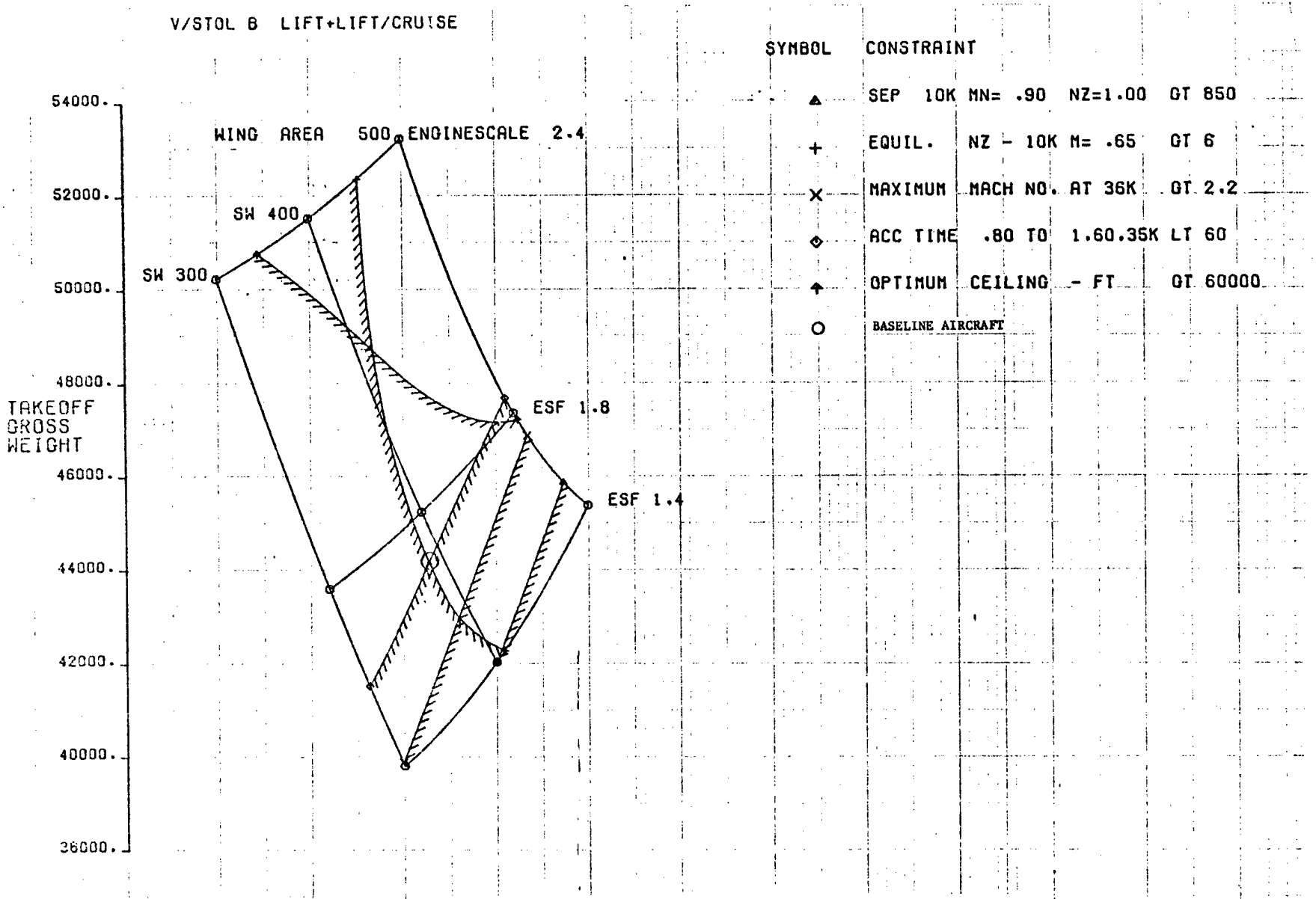


Figure 27. Lift + Lift/Cruise Sizing Parametric

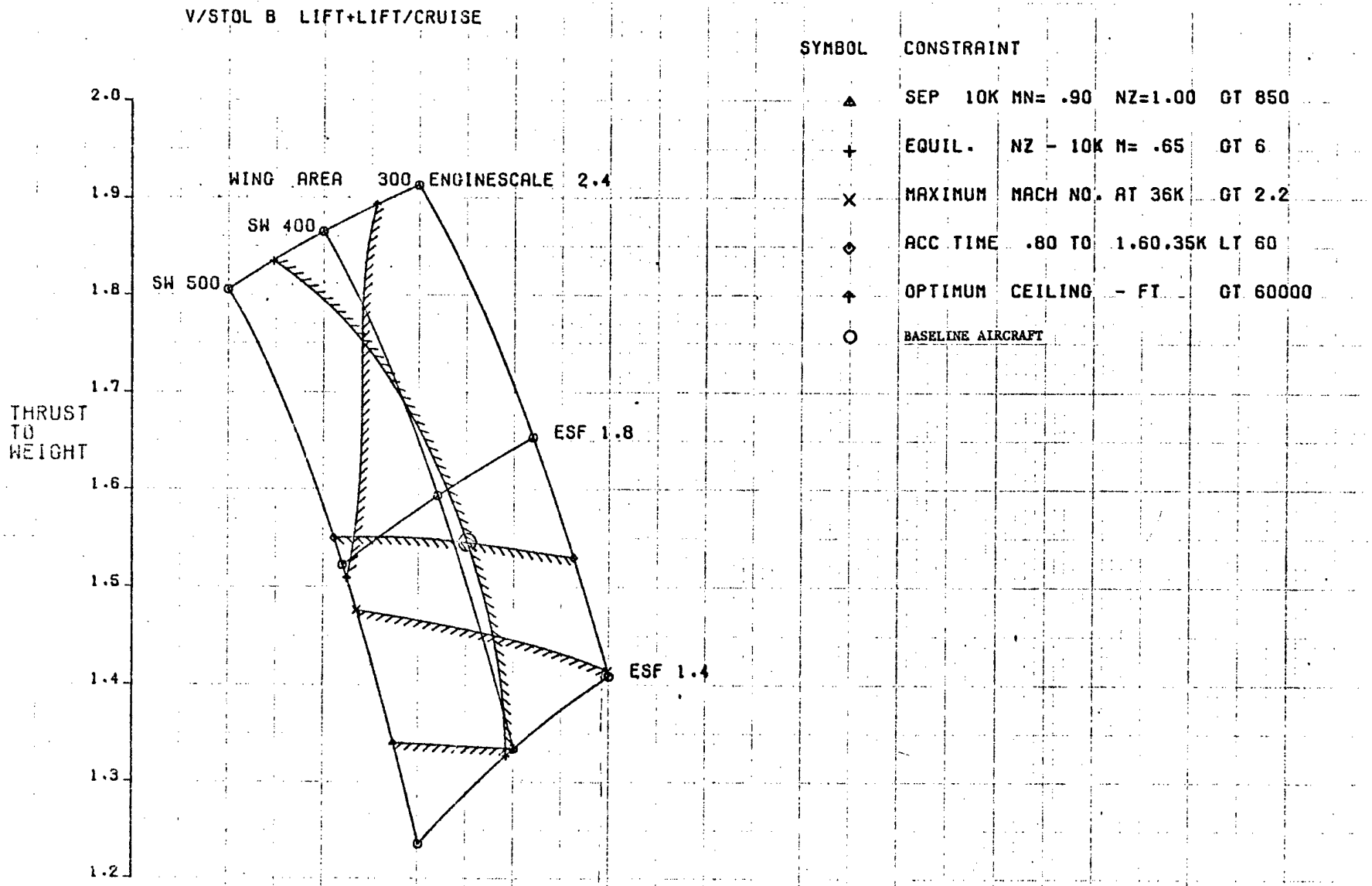


Figure 28. Lift + Lift/Cruise Thrust to Weight Parametric

| | |
|---|---|
| TOGW - Lb. | 44,098 |
| Wing Area - $Ft^2$ | 388 |
| Wing Loading - $Lb/Ft^2$ | 144 |
| Aspect Ratio | 4.0 |
| Cruise Engine Scale Factor | 1.70 |
| Lift Engine Scale Factor | 1.28 |
| Number of Lift/Cruise Engines | 2/2 |
| Fuel Weight - Lb. | 14,674 |
| Structural Weight - Lb. | 10,468 |
| Systems and Equipment - Lb. | 4,842 |
| Propulsion System Weight - Lb. | 10,347 |
| Weight Empty - Lb. | 25,657 |
| Takeoff T/W | 1.545 |
| Design Lift Engine Bleed | 10% |

Figure 29. Lift + Lift/Cruise Point Design Characteristics

DLI MISSION

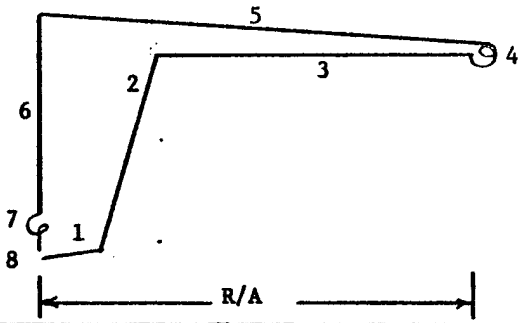


| MISSION SEGMENT | END WEIGHT (LBS.) | END ALTITUDE (FT.) | RANGE (N.Mi.) | TIME (MINUTES) | END SPEED (KNOTS) | END SPEED MACH | FUEL (POUNDS) |
|---|---|---|---|---|---|---|---|
| 1. Takeoff Allowance | 42,017 | 0 | 0 | 2.5 | - | - | 2080 |
| 2. Climb/Accelerate | 38,052 | - | - | 2.2 | - | - | 3965 |
| 3. Dash | 34,272 | - | - | - | - | - | 3780 |
| 4. Combat | 32,461 | - | 0 | 2.0 | - | - | 1811 |
| 5. Return Cruise | 31,470 | 42,155 | - | 19.2 | 469 | .818 | 992 |
| 6. Descent | 31,470 | SL | 0 | 0 | - | - | 0 |
| 7. Reserve Loitor | 30,851 | SL | 0 | 10.0 | 196 | .297 | 619 |
| Lift Engine Allowance | 30,157 | SL | 0 | 0.75 | 0 | 0 | 694 |
| 8. 5% Initial Fuel | 29,424 | - | - | - | - | - | 734 |

TOTALS:

TOGW = 44,098 Lb.

Fuel = 14,674 Lb.

LOADING: (2) HAPI plus (2) MRM, 1888 Lb. Avionics

Figure 30. Lift + Lift/Cruise Design Mission Breakdown

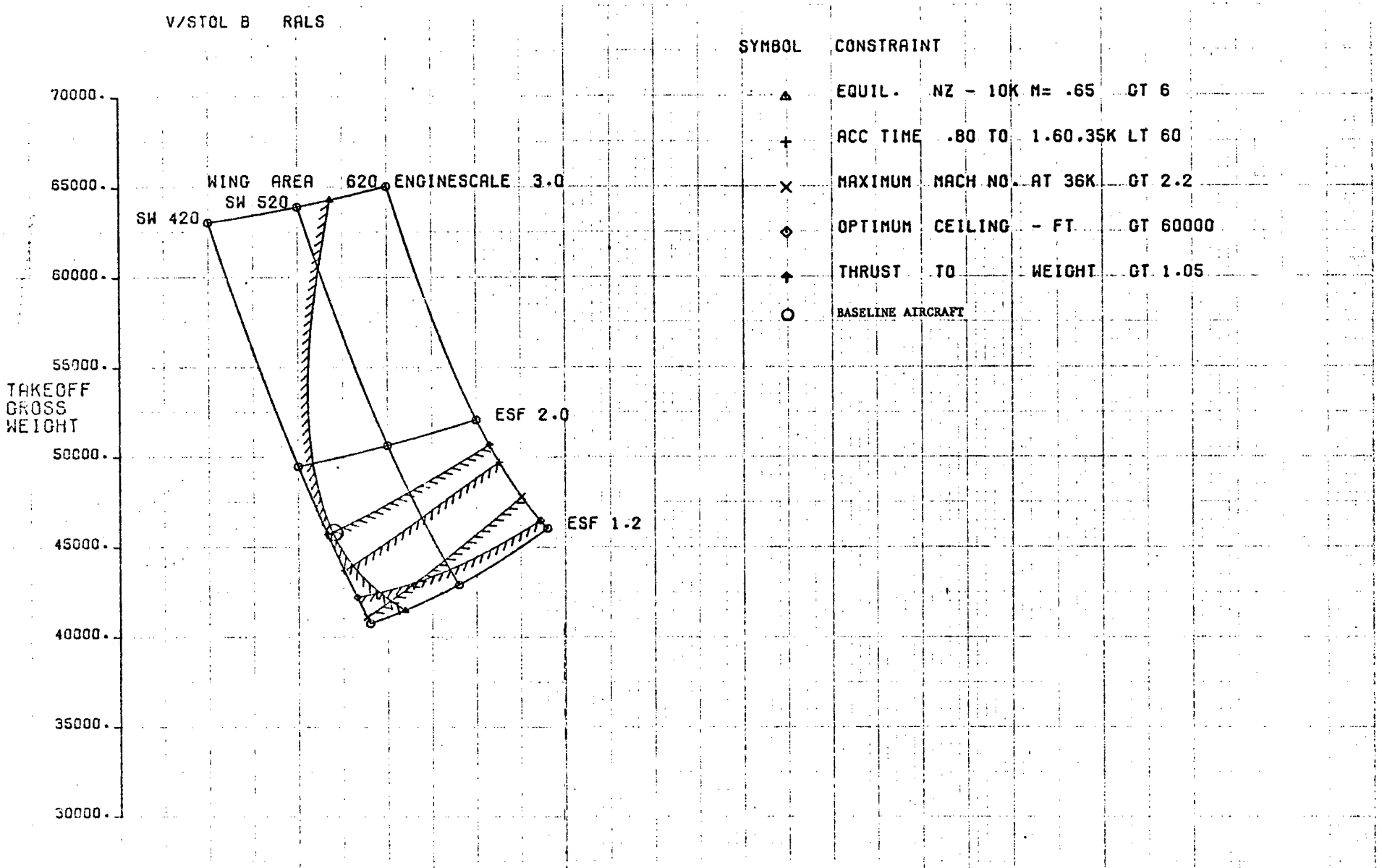


Figure 31 RALS Sizing Parametric

| | |
|---|---|
| TOGW - Lb. | 45,378 |
| Wing Area - $Ft^2$ | 426 |
| Wing Loading - $Lb/Ft^2$ | 107 |
| Aspect Ratio | 2.8 |
| Engine Scale Factor | 1.66 |
| Number of Engines | 2 |
| Fuel Weight - Lb. | 14,786 |
| Structural Weight - Lb. | 10,160 |
| Systems and Equipment - Lb. | 4,801 |
| Propulsion System Weight - Lb. | 11,864 |
| Weight Empty - Lb. | 26,825 |
| Takeoff T/W | 1.05 |
| Design Bleed Flow Rate - Lb/Sec | 36 |

Figure 32. RALS Point Design Characteristics

DLI MISSION

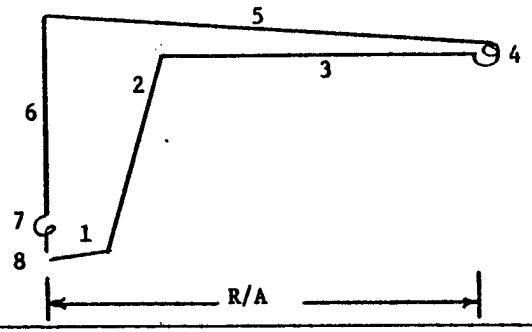


| MISSION SEGMENT | END WEIGHT (LBS.) | END ALTITUDE (FT.) | RANGE (N.Mi.) | TIME (MINUTES) | END SPEED (KNOTS) | END SPEED MACH | FUEL (POUNDS) |
|---|---|---|---|---|---|---|---|
| 1. Takeoff Allowance | 43,019 | 0 | 0 | 2.5 | - | - | 2359 |
| 2. Climb/Accelerate | 39, 278 | - | - | 1.5 | - | - | 3741 |
| 3. Dash | 35,555 | - | - | - | - | - | 3723 |
| 4. Combat | 33,029 | - | 0 | 2.0 | - | - | 2526 |
| 5. Return Cruise | 32,019 | 45,428 | - | 17.7 | 508 | .886 | 1010 |
| 6. Descent | 32,019 | SL | 0 | 0 | - | - | 0 |
| 7. Reserve Loitor | 31,331 | SL | 0 | 10.0 | 214 | .323 | 688 |
| 8. 5% Inital Fuel | 30,591 | - | - | - | - | - | 729 |

TOTALS:

TOGW = 45,378 Lbs.

Fuel = 14,786 Lbs.

LOADING: (2) HAPI plus (2) MRM, 1888 Lbs. Avionics

Figure 33. RALS Design Mission Breakdown

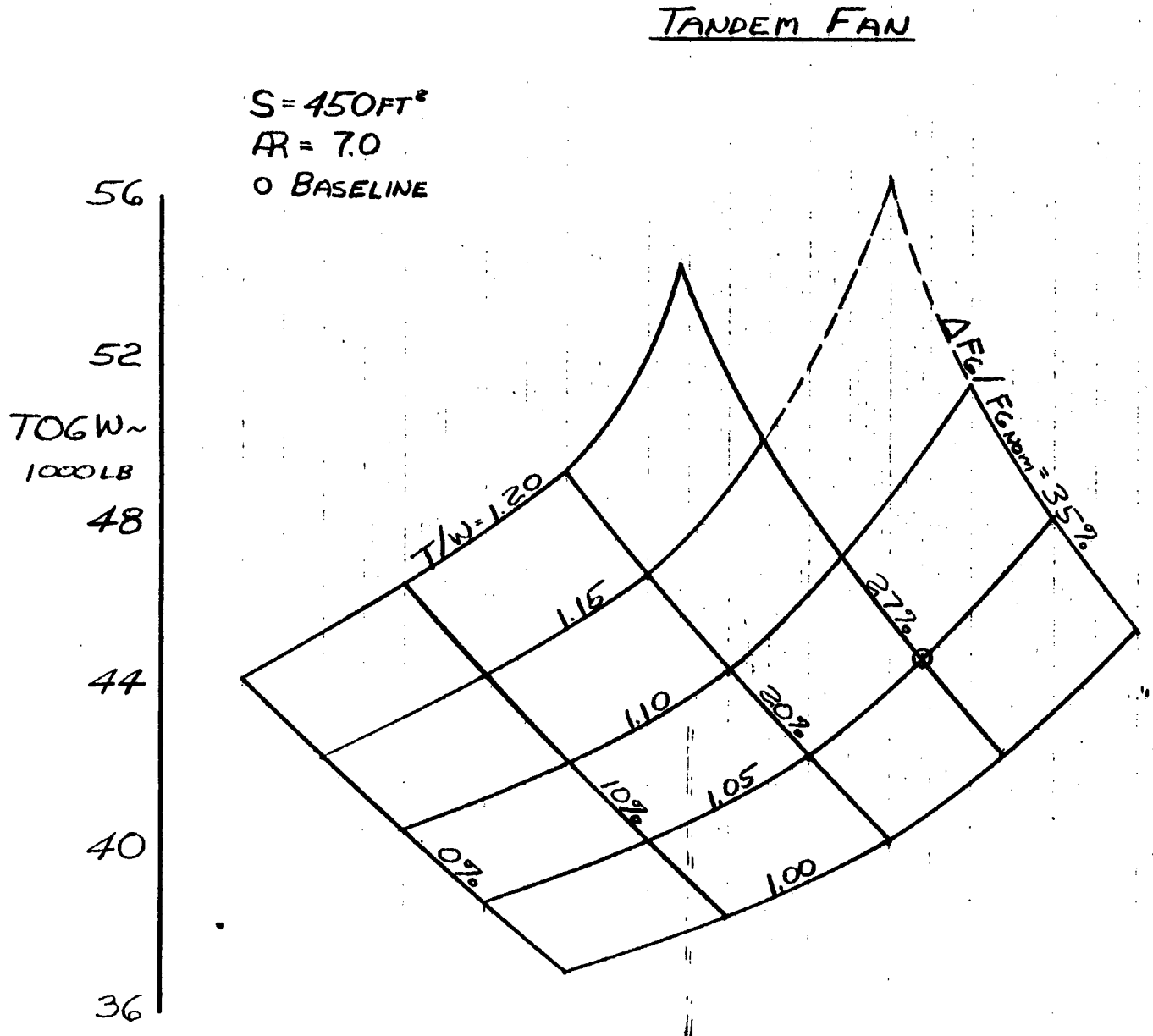


Figure 34. Tandem Fan TOGW Sensitivity to VTO Thrust to Weight and Control Margin

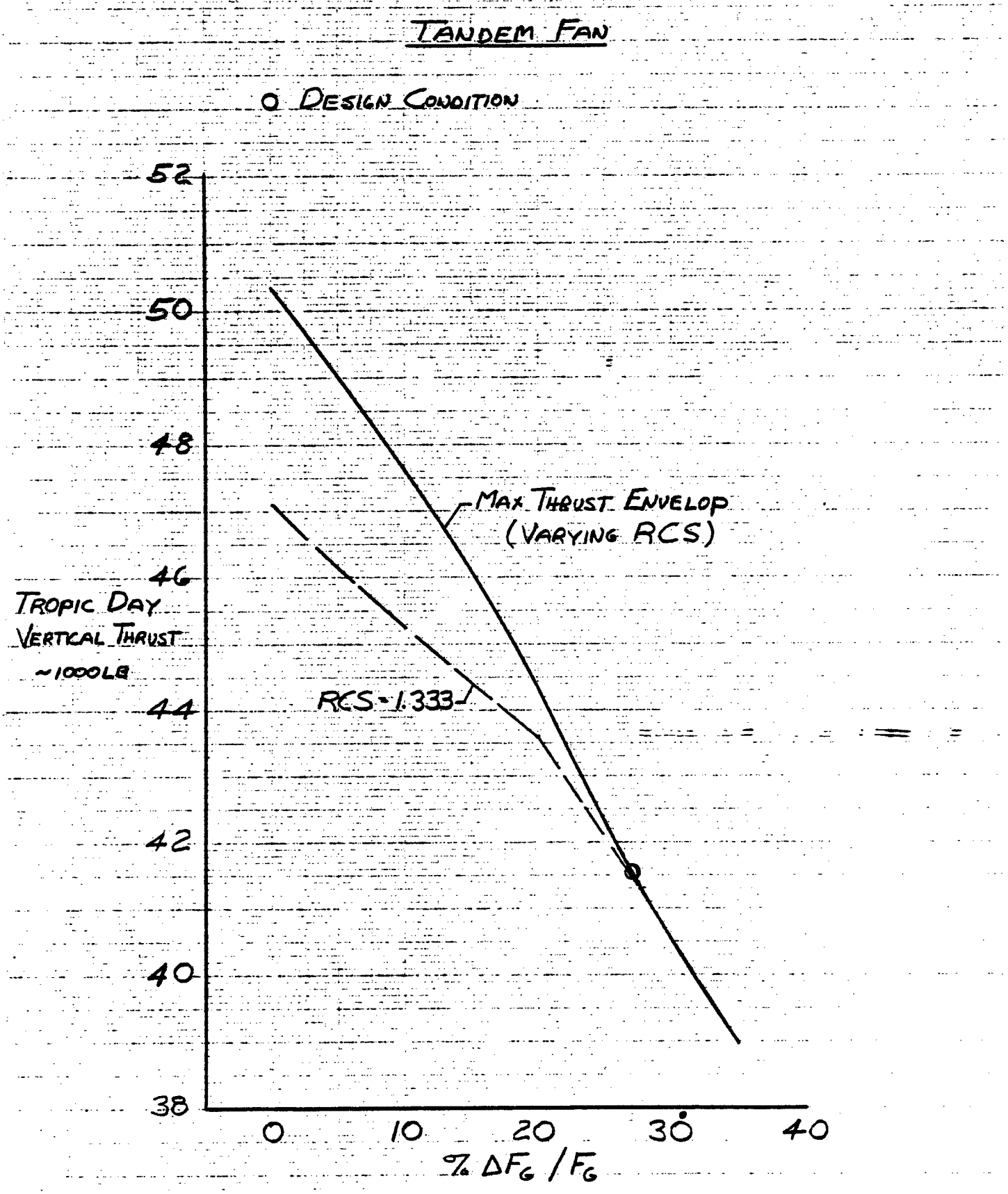


Figure 35. Design Point Thrust Characteristics

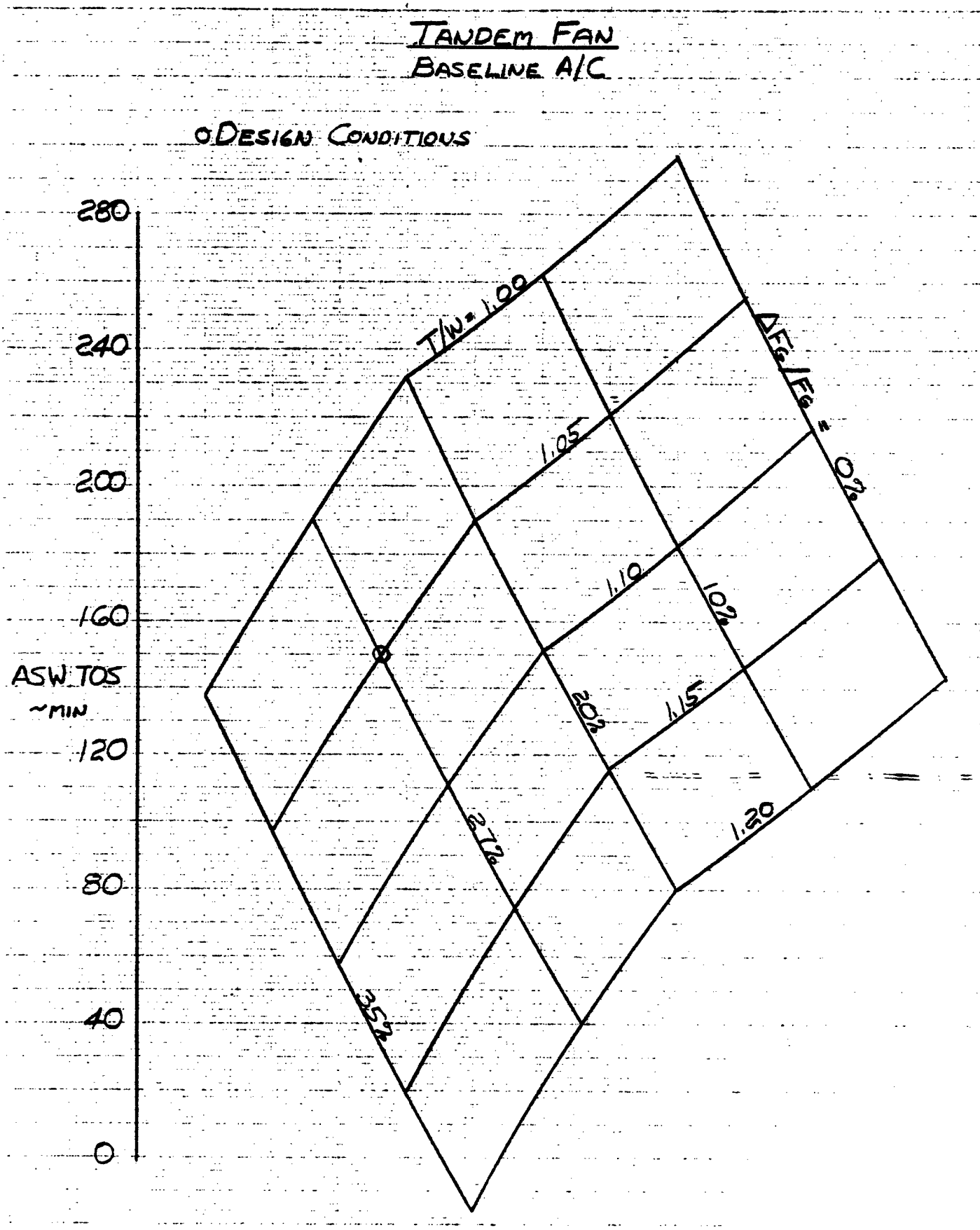


Figure 36. Tandem Fan ASW Time on Station Sensitivity to VTO Thrust to Weight and Control Margin

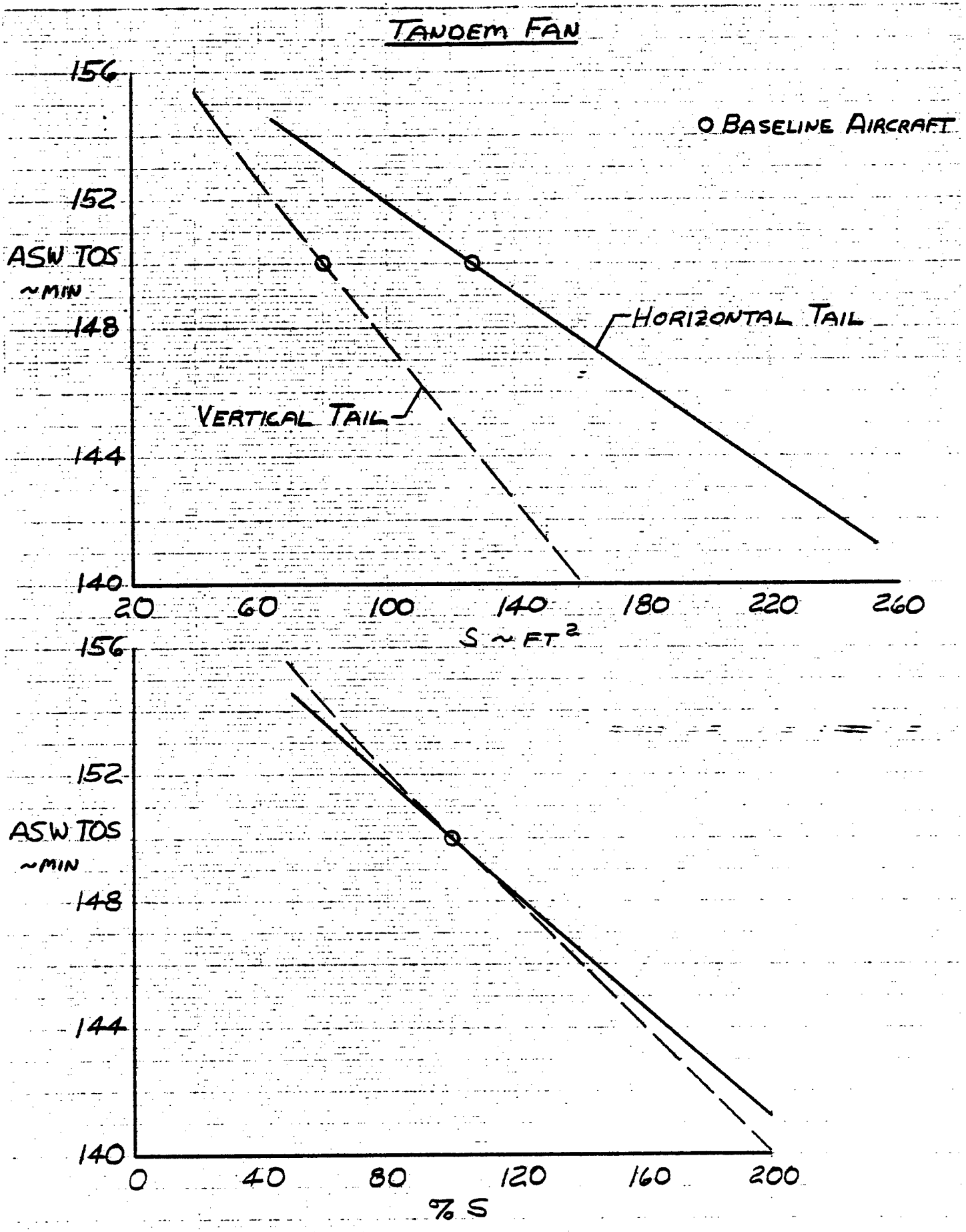


Figure 37. Tandem Fan ASW Time on Station Sensitivity to Tail Size Variation

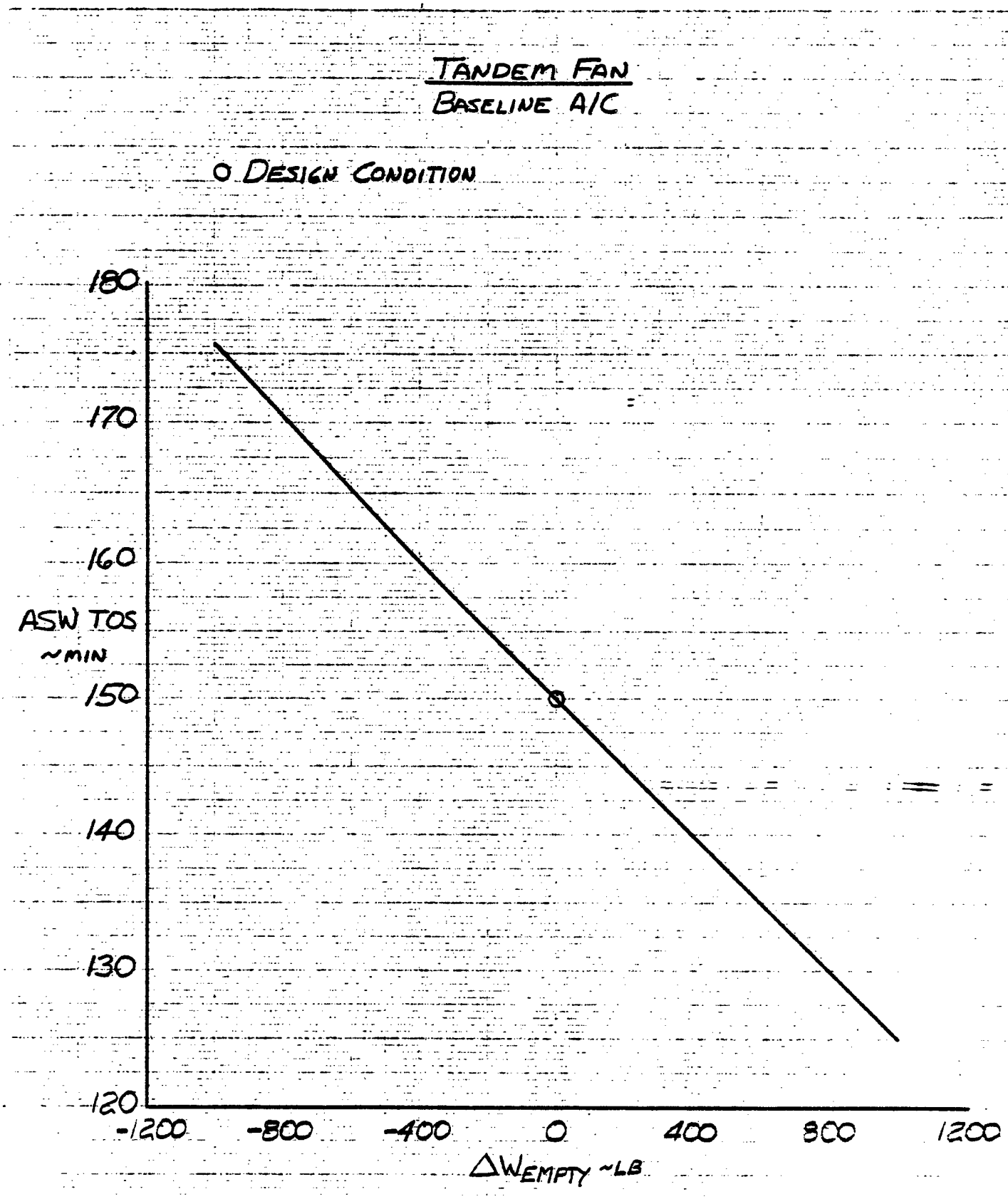


Figure 38. Tandem Fan ASW Time on Station Sensitivity to Empty Weight

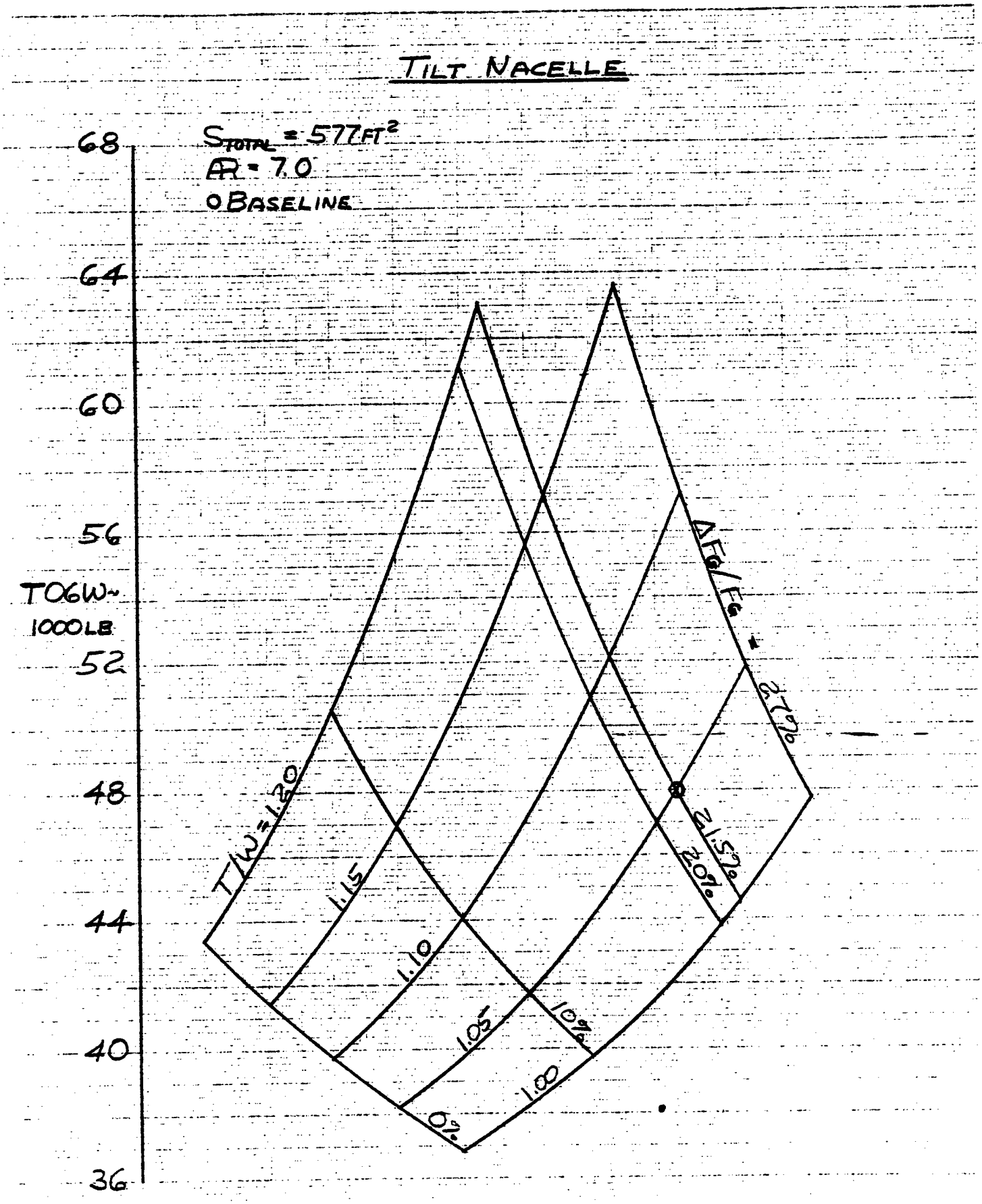


Figure 39. Tilt Nacelle TOGW Sensitivity to VTO Thrust to Weight and Control Margin

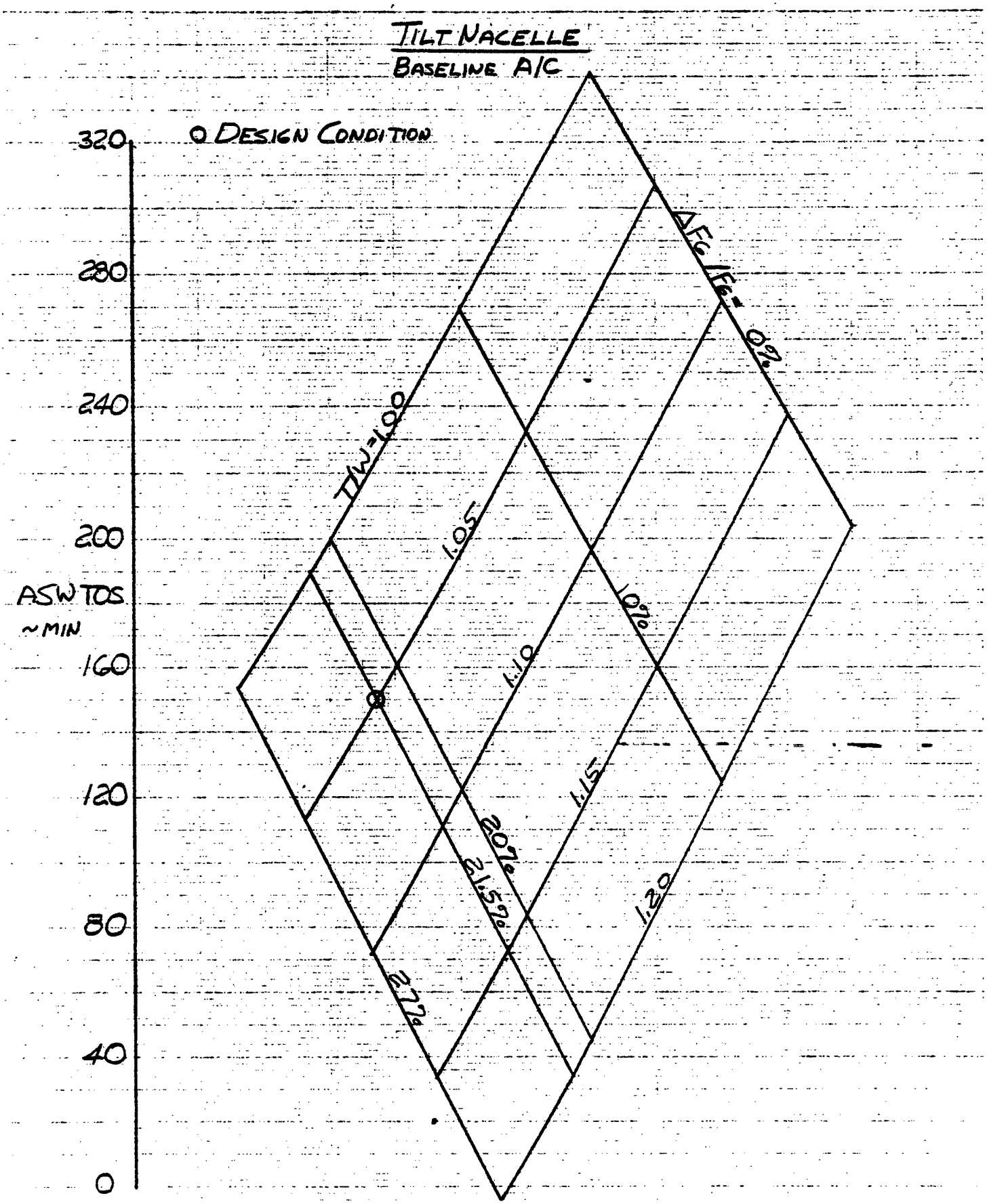


Figure 40. Tilt Nacelle ASW Time on Station Sensitivity to VTO Thrust to Weight and Control Margin

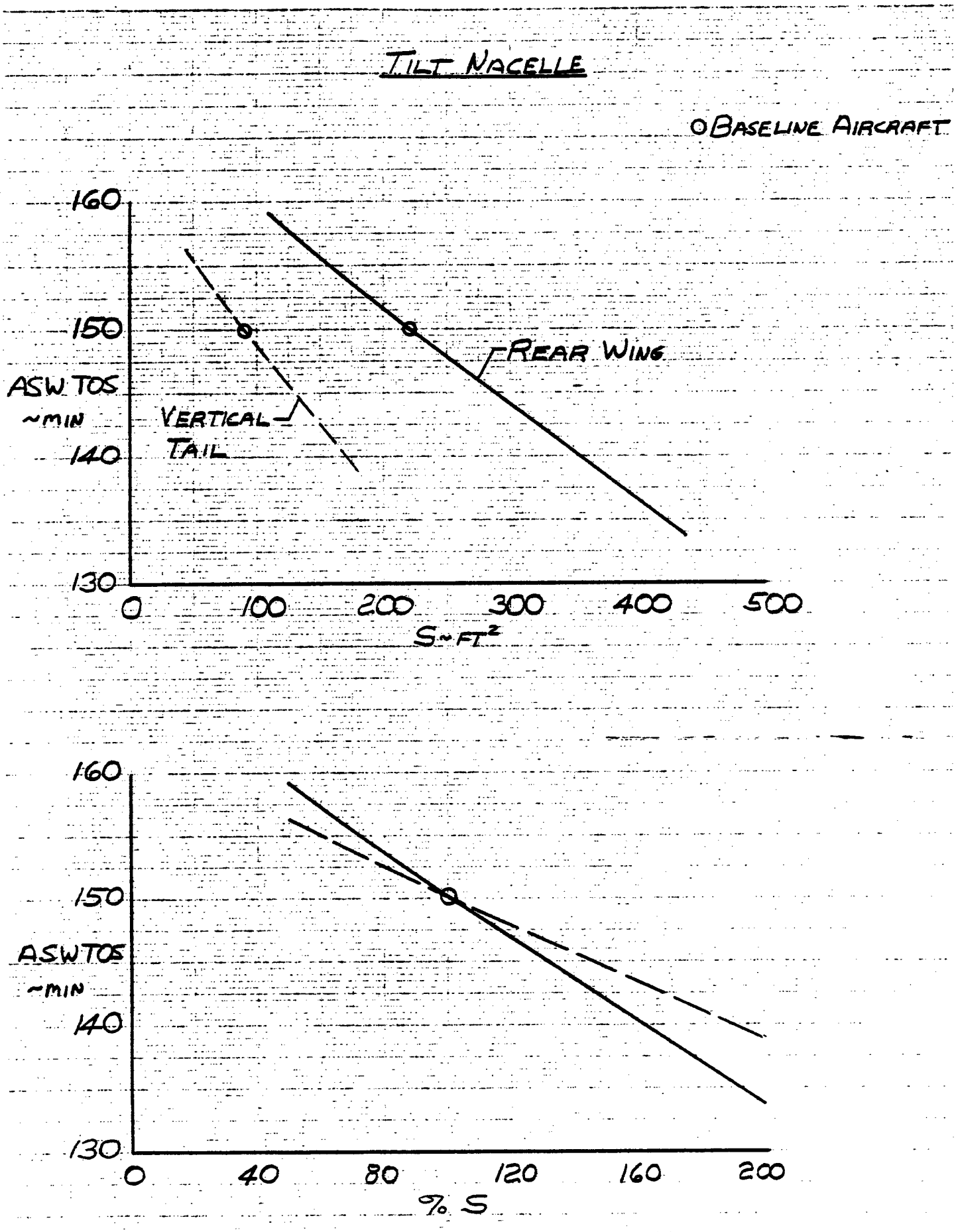


Figure 41. Tilt Nacelle ASW Time on Station Sensitivity to Tail Size Variation

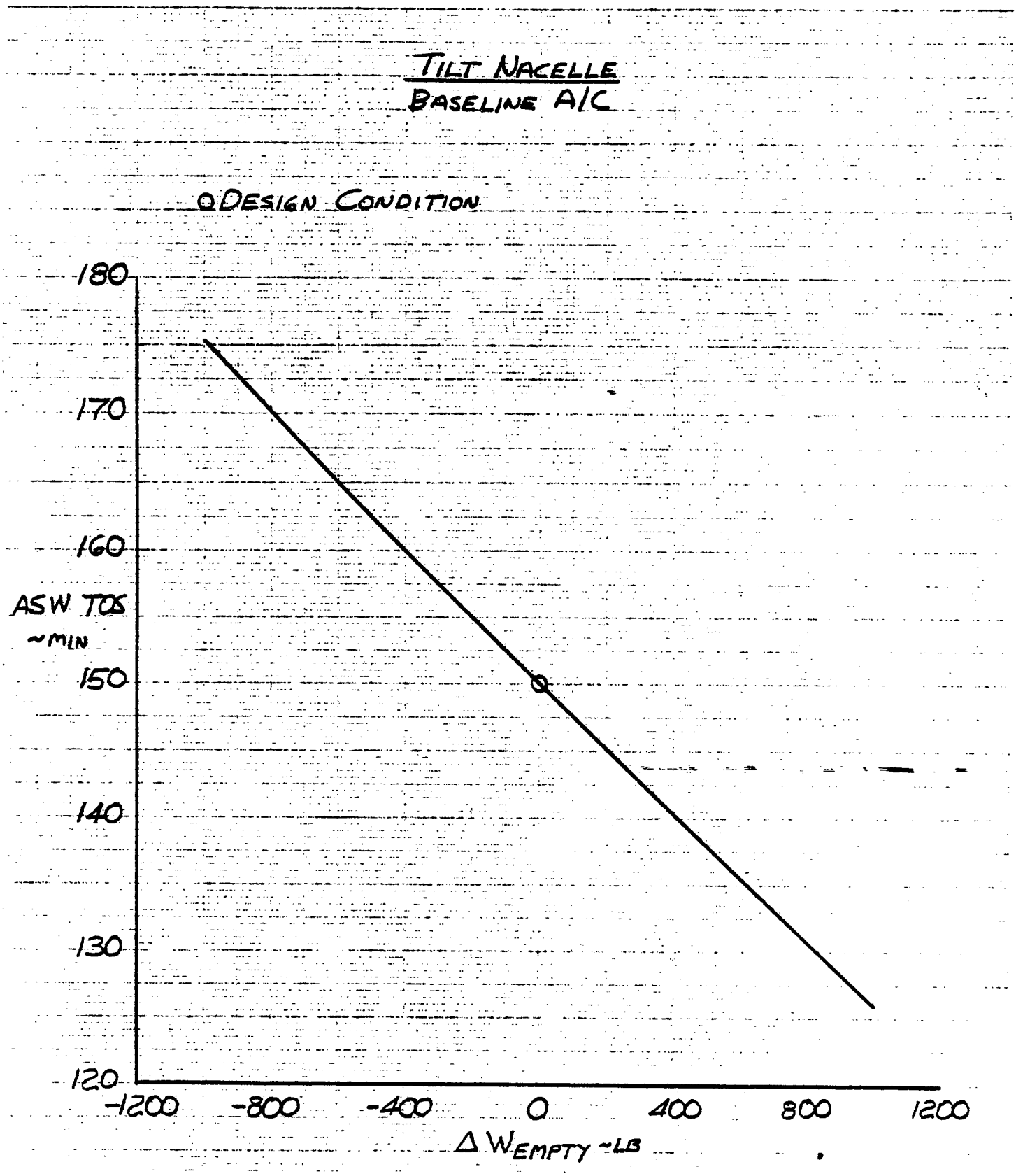


Figure 42. Tilt Nacelle ASW Time on Station Sensitivity to Empty Weight

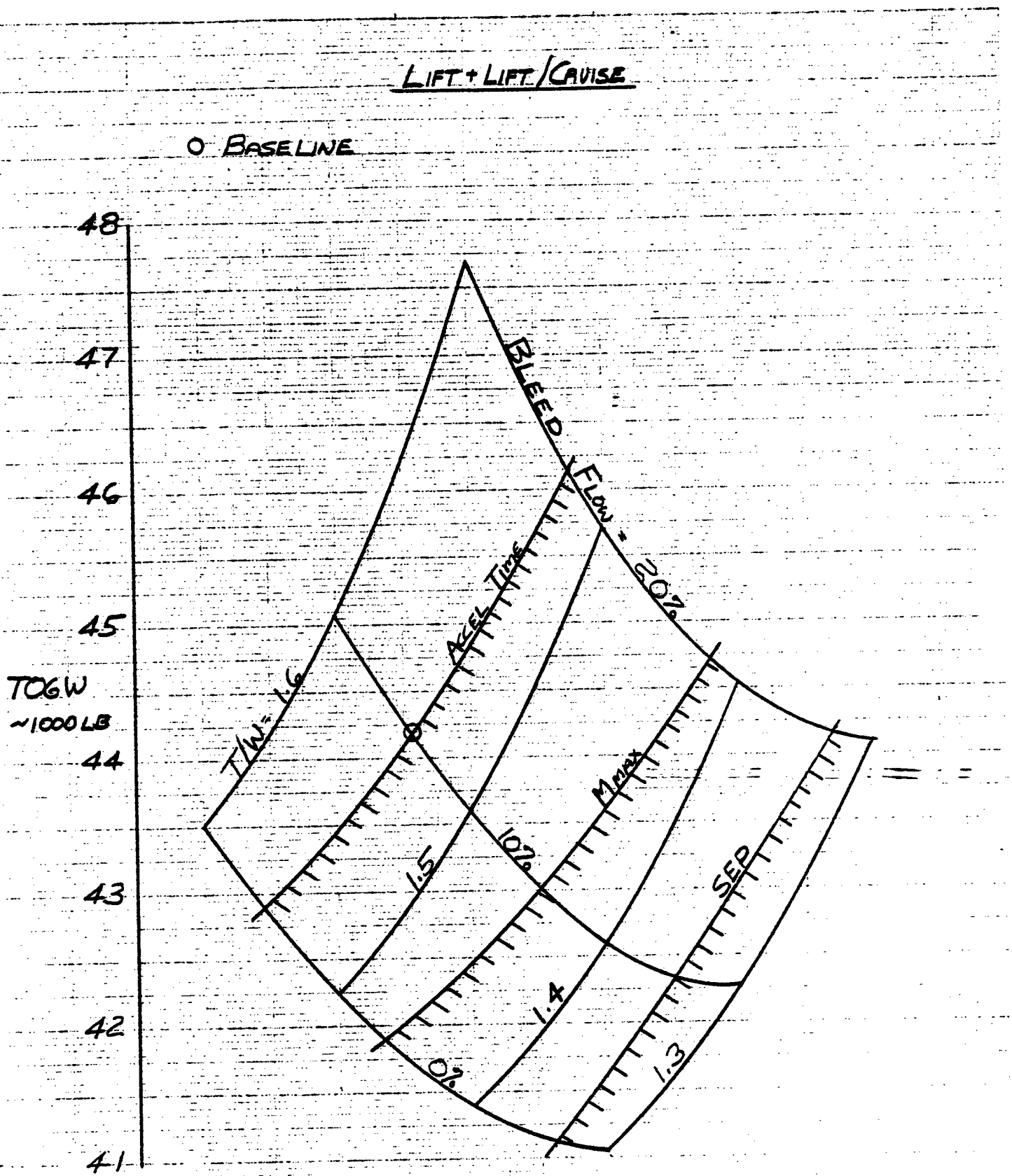


Figure 43. Lift + Lift/Cruise TOGW Sensitivity to VTO Thrust to Weight and Percent Bleed Flow

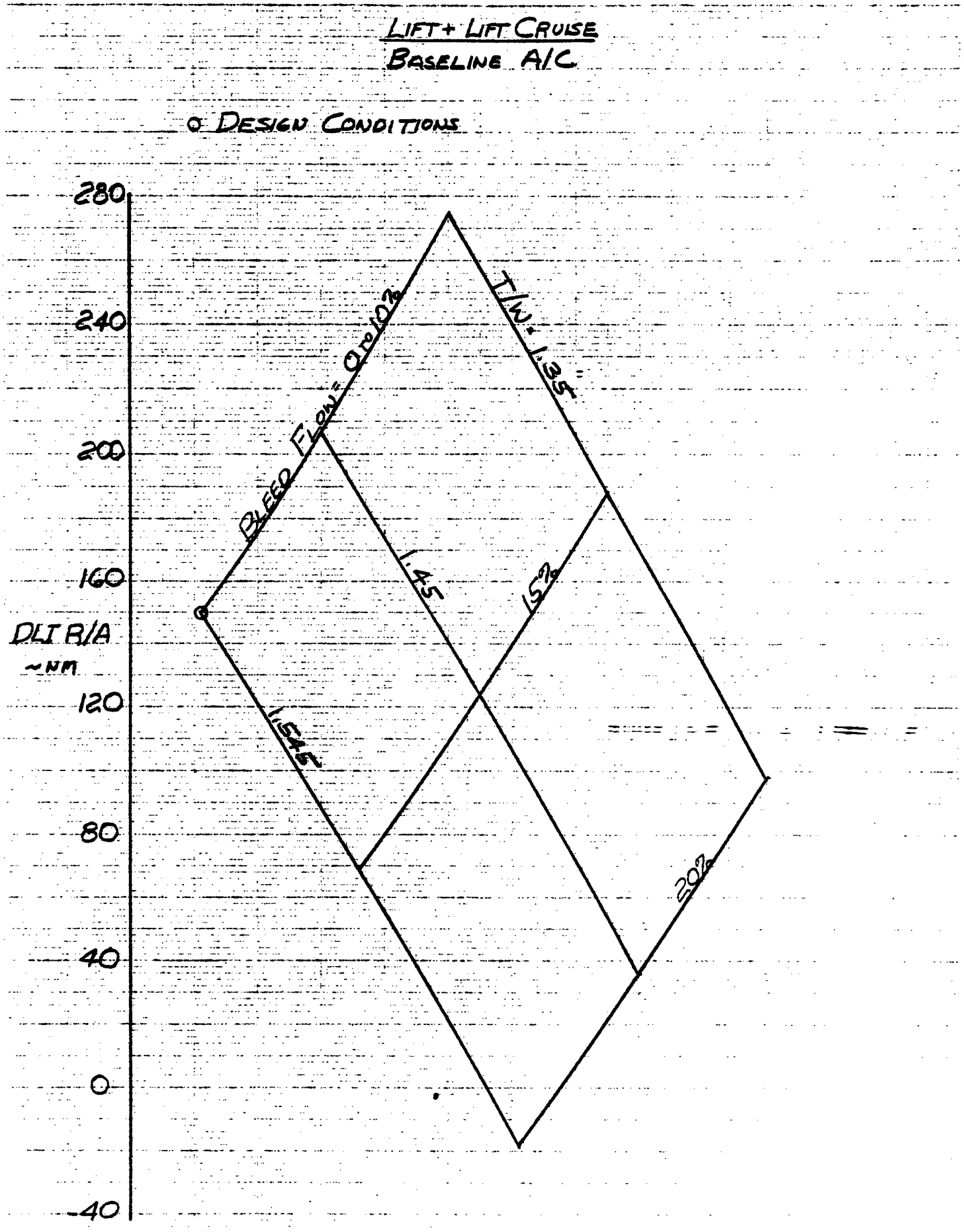


Figure 44. Lift + Lift/Cruise DLI Radius of Action Sensitivity to VTO Thrust to Weight and Percent Bleed Flow

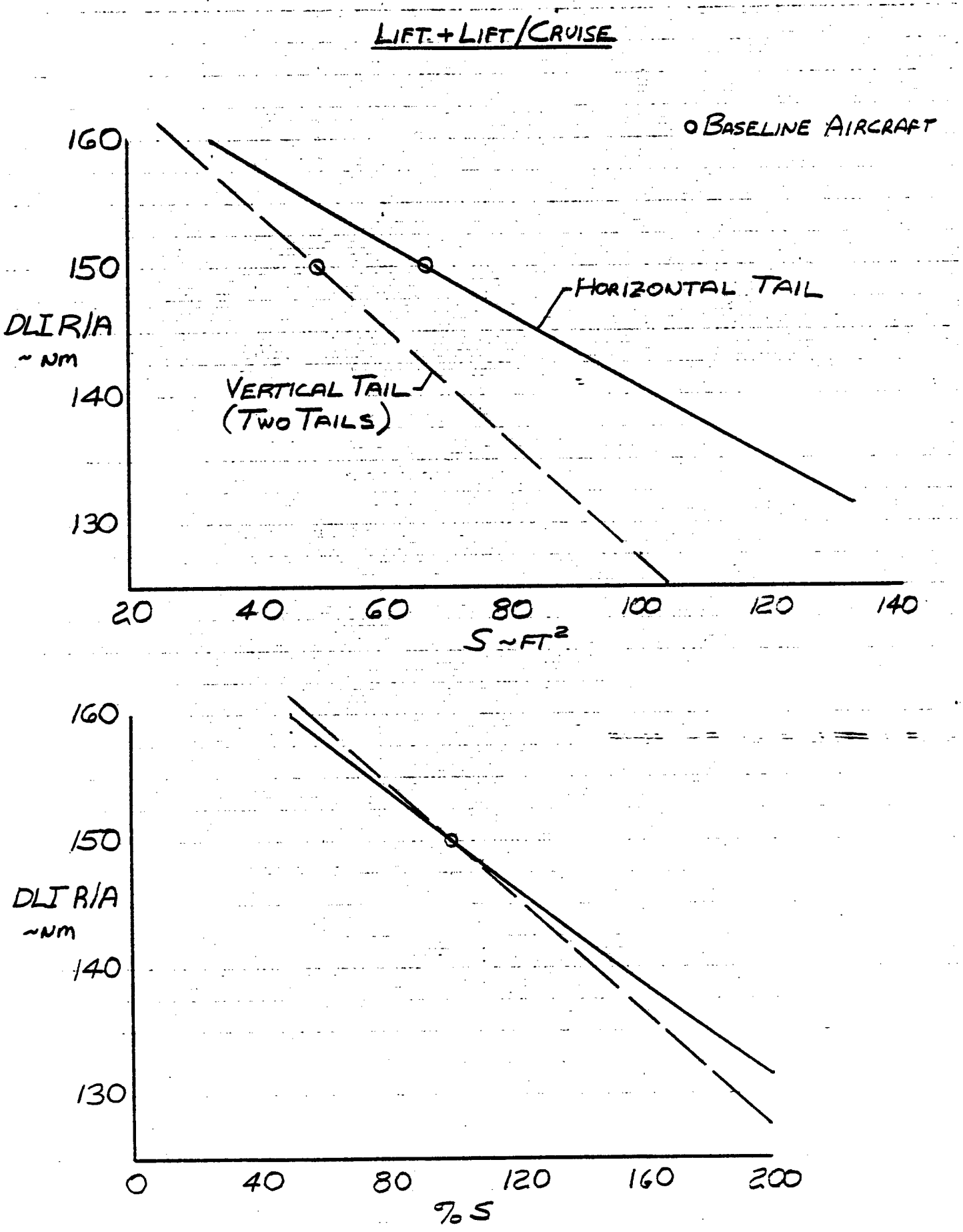


Figure 45. Lift + Lift/Cruise DLI Radius of Action Sensitivity to Tail Size Variation

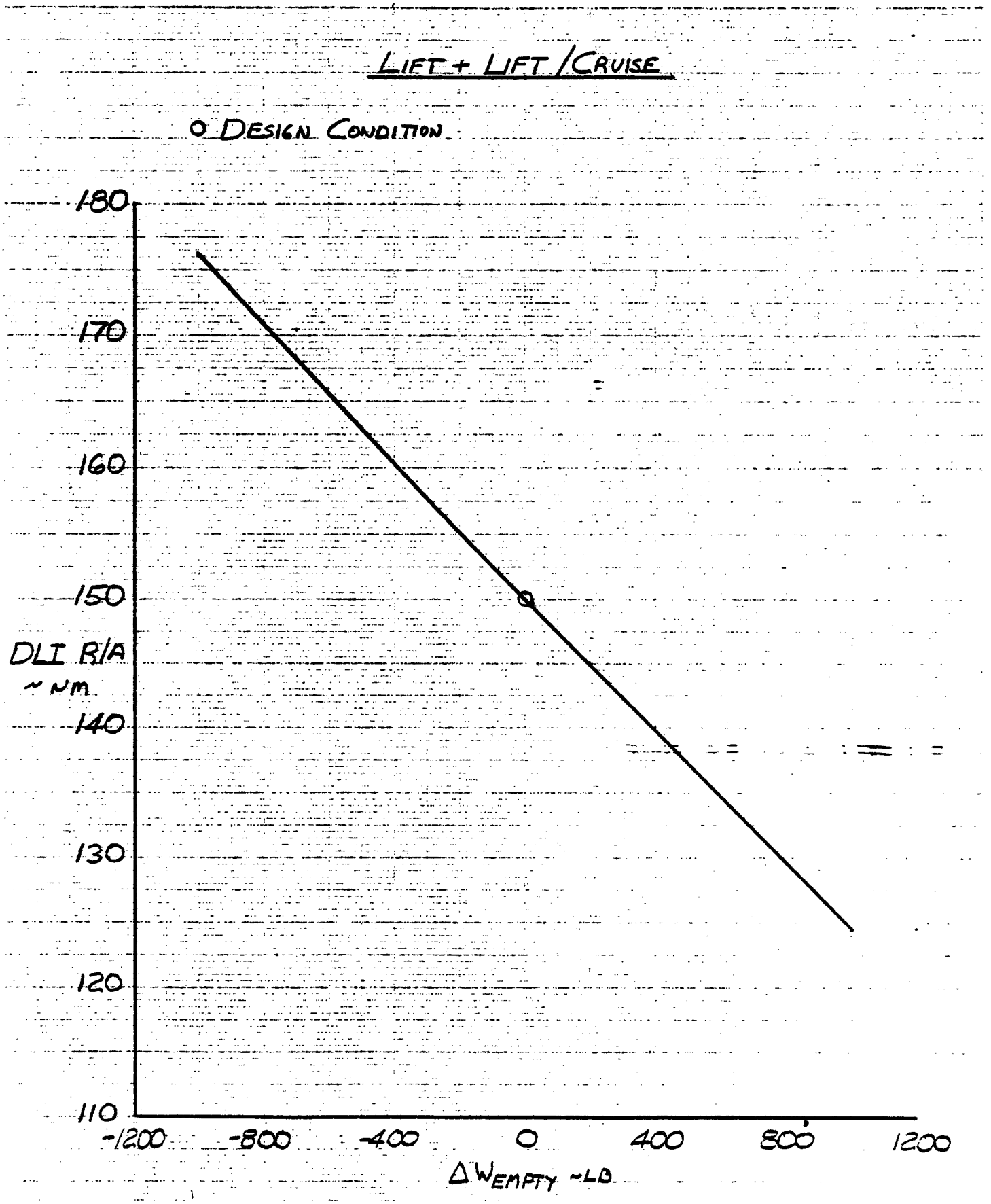


Figure 46. Lift + Lift/Cruise DLI Radius of Action Sensitivity to Empty Weight

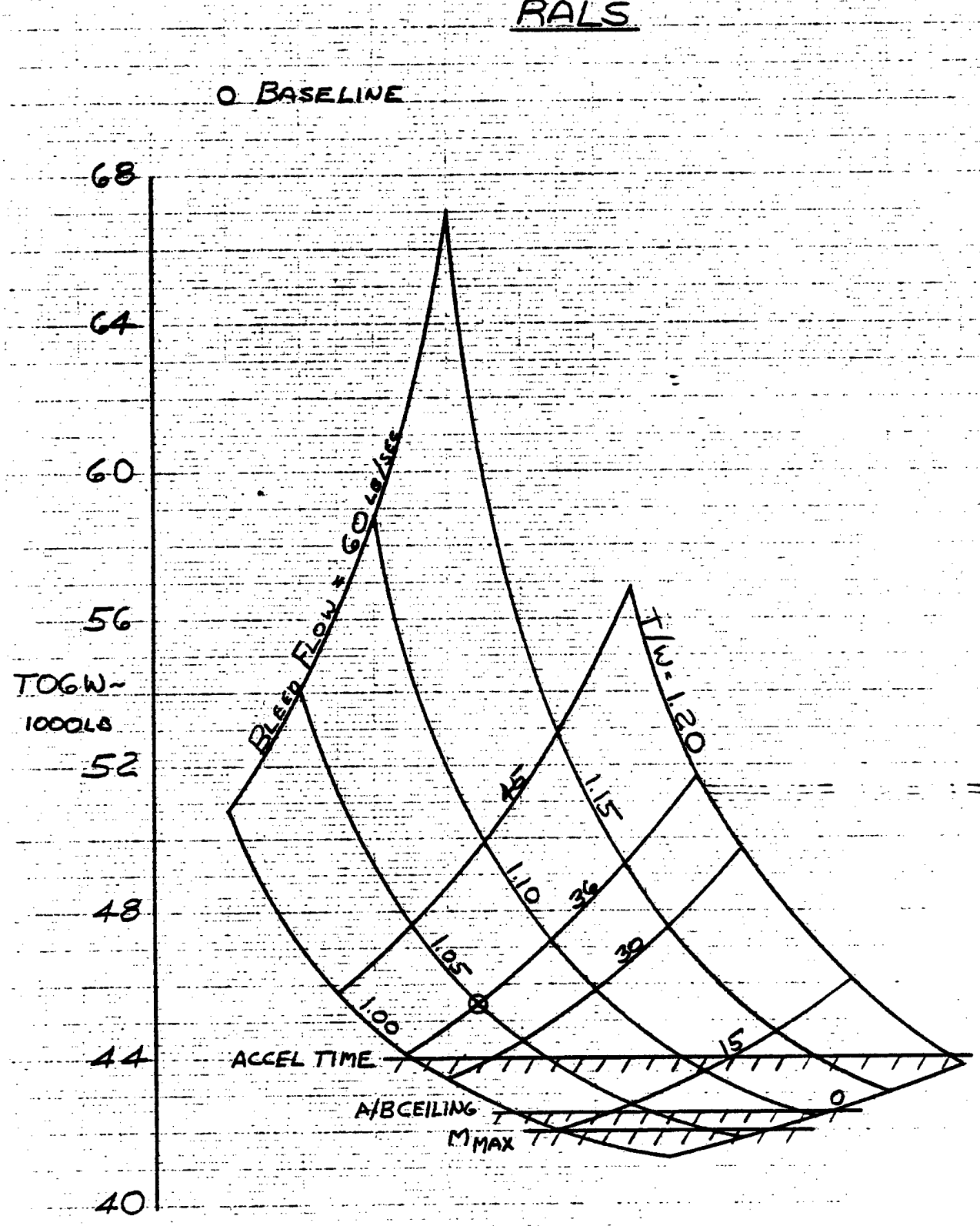


Figure 47. RALS TOGW Sensitivity to VTO Thrust to Weight and Bleed Flow Rate

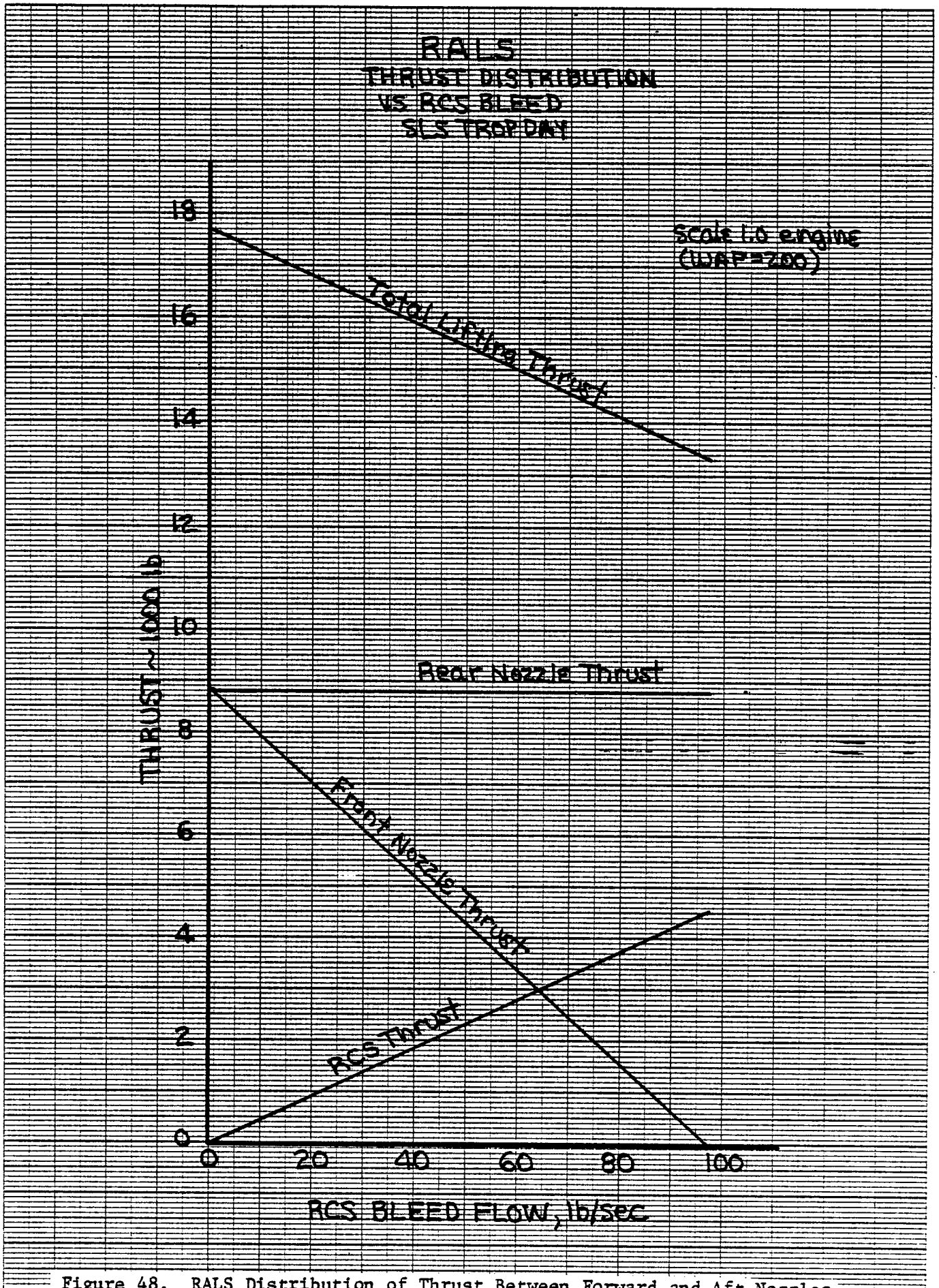


Figure 48. RALS Distribution of Thrust Between Forward and Aft Nozzles and the RCS for Varying Bleed Flow Rates

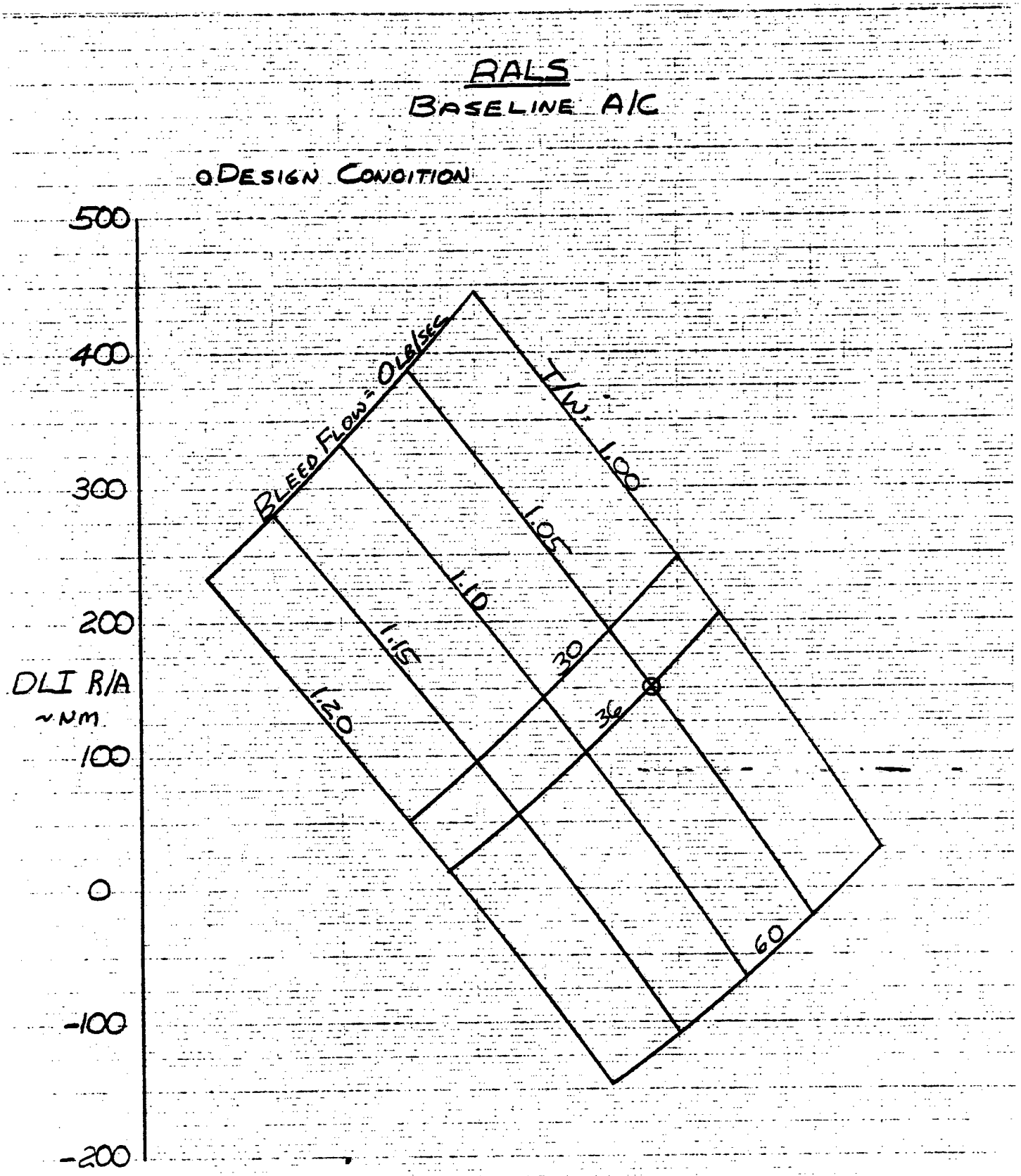


Figure 49. RALS DLI Radius of Action Sensitivity to VTO Thrust to Weight and Bleed Flow Rate

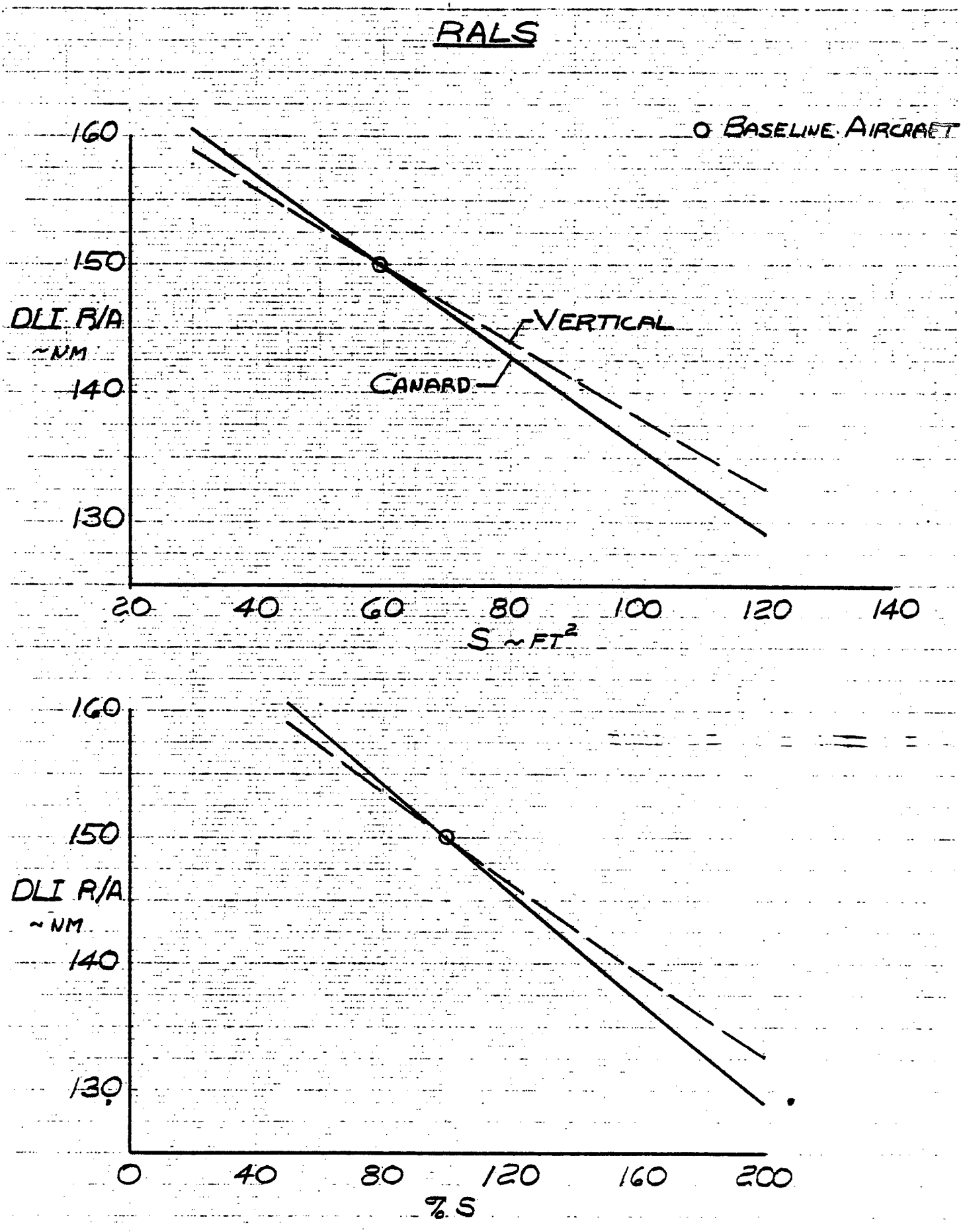


Figure 50. RALS DLI Radius of Action Sensitivity to Tail Size Variation

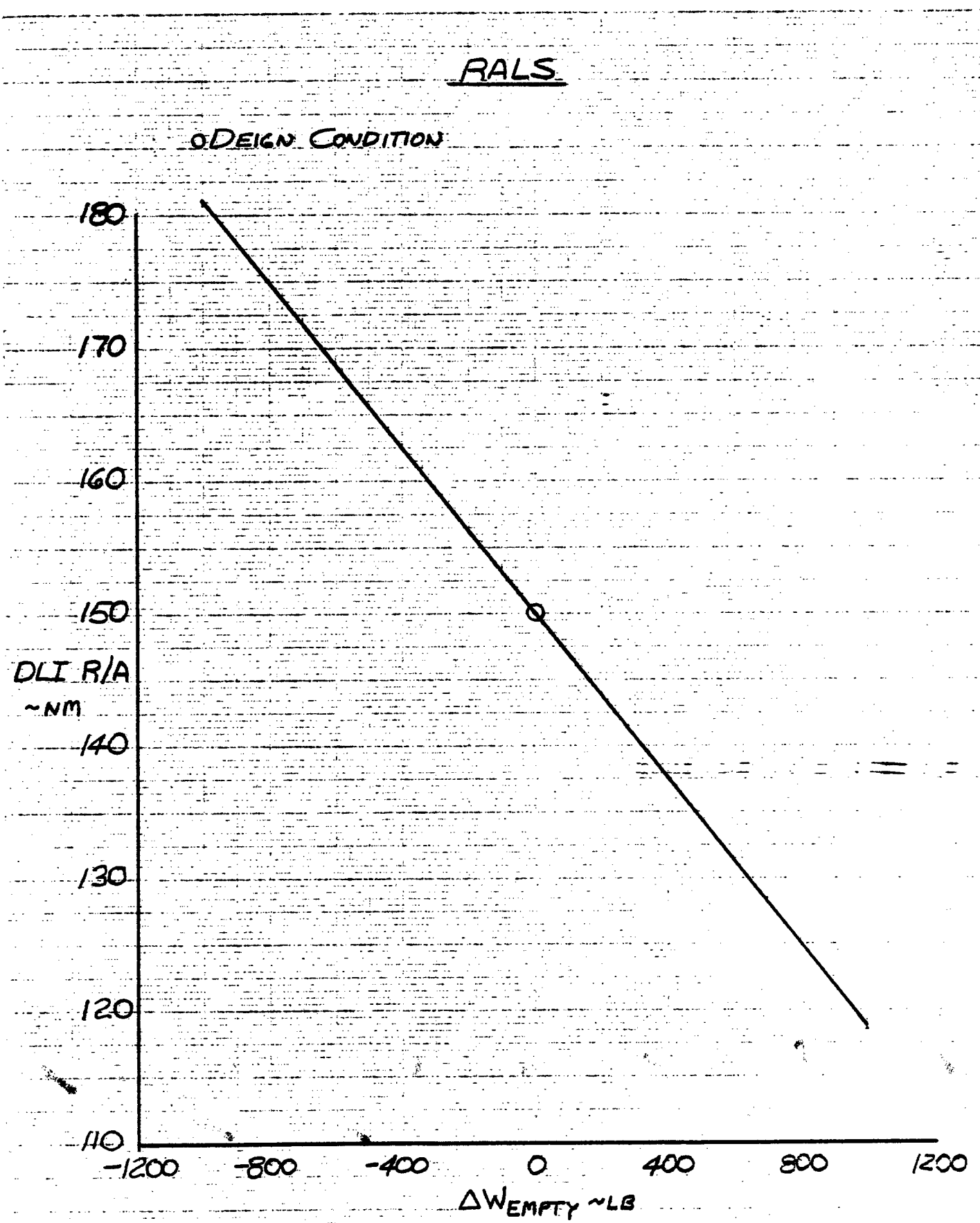


Figure 51. RALS DLI Radius of Action Sensitivity to Empty Weight